Faculdade de Engenharia da Universidade do Porto

FEUP

Modelling the gait of healthy and post-stroke individuals

Morgana Pires Afonso

Master's degree in Bioengineering

Supervisor:
Prof. João Manuel R.S. Tavares
Mechanical Engineering Department, FEUP

Co-supervisor:
Prof. Andreia Sofia Pinheiro Sousa
Physiotherapy Department, ESTSP

September 2015

Resumo

A locomoção é uma tarefa de grande importância na vida das pessoas. Mesmo que todos os indivíduos saudáveis apresentem uma variabilidade natural nos padrões da marcha, é possível definir um padrão aceitável para "marcha normal". Contudo, algumas patologias podem induzir padrões de marcha anormais que podem limitar a vida de uma pessoa, tornando-a dependente de outros e, consequentemente, reduzindo a sua qualidade de vida.

O acidente vascular encefálico (AVE) afeta 15 milhões de pessoas em cada ano, das quais 50% sofrem alterações da marcha não permanentes, de acordo com a Organização Mundial de Saúde. A marcha na sequência de um AVE é uma combinação de várias anomalias que dependem do indivíduo, da severidade e da localização do dano e do tempo decorrido após a ocorrência. A aplicação de um tratamento adequado nestes pacientes pode melhorar com o conhecimento de como a patologia afeta os músculos e os controlos nervosos associados a eles, permitindo desenhar soluções específicas e personalizadas a cada paciente. A análise experimental da marcha é de grande utilidade na extração de parâmetros de marcha, todavia, apresenta algumas fragilidades. Simulações computacionais dinâmicas, por outro lado, têm um grande potencial neste tipo de investigação e, combinada com dados experimentais, permitem a realização de estudos causa-efeito, sobre como músculos específicos afetam o movimento, por exemplo, em indivíduos que tenham sofrido um AVE.

*Neste trabalho, duas simulações computacionais foram desenvolvidas usando o OpenSim, a partir de dados cinemáticos e cinéticos obtidos em ensaios de marcha realizados num indivíduo saudável e outro na sequência de um AVE. Os dados experimentais foram extraídos de um ficheiro com a extensão *.c3d e pré-processados. Cada simulação começou com um modelo musculosquelético, que foi adaptado de acordo com a massa e dimensões do individuo posteriormente foram determinados os ângulos e momentos nas articulações por cinemática e dinâmica inversa; as forças e momentos residuais foram reduzidos e finalmente foi usado o "Computed Muscle Control" para determinar a contribuição muscular dos principais flexores plantares (soleus e gastrocnémio medial), flexor dorsal (tibial anterior) e um músculo da coxa*

(semimembranoso). Os ângulos e momentos nas articulações relativos ao indivíduo saudável revelaram-se de acordo com a referência. No entanto, os músculos analisados mostraram diferenças nos padrões de ativação. Na simulação envolvendo ao indivíduo pós AVE, verificou-se alguma redução do ângulo e momento no tornozelo do membro afetado, mas a ativação e potência dos flexores plantares só foi reduzida no gastrocnémio medial. Por outro lado, verificou-se ativação prolongada do semimembranoso durante a fase de apoio do membro afetado.

Os atuadores musculares não foram capazes de gerar a cinemática pretendida sem recorrer a forças residuais e de reserva e ainda foi verificado um erro alto no ângulo do tornozelo direito.

Abstract

Locomotion is a task with great importance in the life of a person. Even though every healthy individual shows natural variability in gait patterns, it is possible to define an acceptable pattern for "normal gait". However, some pathologies can induce abnormal gait patterns that can limit the life of a person, making him/her dependent of others and consequently reducing his/hers quality of life. Treatments involving rehabilitation or surgical procedures can revert or diminished the impairments in gait, showing good improvements on the people's life.

Stroke or cerebrovascular accident (CVA) affects 15 million people each year, from which 50% suffer non-permanent gait impairments, according to the World Health Organization. Gait after stroke is a combination of several abnormalities that depend on the individual, the severity and the location of the injury and the time passed after its occurrence.

The application of an adequate treatment in these patients can be improved with the understanding of how the pathology affects the muscles, and the neural controls associated with it and allow to design specific solutions for each patient. Experimental gait analysis is useful in measuring important gait parameters, but it has limited capabilities. Computational dynamic simulations, on the other hand, have great potential in this type of investigation and, combined with the experimental data, allow performing cause-effect studies, about how specific muscles influence the movement, for example, in individuals affected in the sequence of a stroke.

*In the present work, two computational dynamic simulations were developed using OpenSim, using kinematic and kinetic data collected from a gait trail performed on a healthy and a post-stroke individual. The experimental data was extracted from a *.c3d file and processed. Each simulation started from a musculoskeletal model, scaled according to the mass and dimensions of each individual; followed the determination of the joint angles and moments by solving an inverse kinematics and dynamics problem; then the residual forces were reduced and finally Computed Muscle Control was used to determine the muscle contributions for the gait of the principal plantarflexors (soleus and medial gastrocnemius) and dorsiflexors (tibialis anterior)*

and one hamstring (semimembranosus). The joint angles and moments relative to the healthy individual showed to be in agreement with the reference values for normal gait. However, the muscles analysed showed differences in the activation patterns. In the simulation involving a post-stroke individual it was verified lower plantarflexor angle and moment but the activation and power of the plantarflexor muscles were only reduced in the medial gastrocnemius of the impaired limb. On the other hand it was verified early activation of the plantarflexors and prolonged activation of the semimembranosus from the impaired limb during its stance.
The muscular actuators were not able to track the kinematics without the use of residual and reserve forces and the right ankle had a high error associated.

Acknowledgments

I would like to thank to my supervisor and co-supervisor, Professor Dr. João Tavares and Dra. Andreia Sousa, for their attention, guidance and advice during the development of this work.

Also I would like to thank to the Eng. Pedro Fonseca from the LABIOMEP for the provision of the experimental data and for the attention in answering my questions and to Dra. Augusta Silva for her help analysing the results.

I would like to express my sincere gratitude to my family and friends, for their constant support and care.

Finally I want to thank to God for the opportunities and people that He put in my path.

"Strength does not come from winning. Your struggles develop your strengths. When you go through hardships and decide not to surrender, that is strength."

Arnold Schwarzenegger

Table of Contents

List of Figures

List of tables

Abbreviations and Symbols

BTK	Biomechanical ToolKit
CE	Contractile Element
CMC	Computed Muscle Control
COM	Centre of Mass
CONTRA	Contralateral
COP	Centre of Pressure
CPG	Central Pattern Generator
CVA	Cerebrovascular Accident
DOF	Degree of Freedom
EMG	Electromyography
GRF	Ground Reaction Force
ID	Inverse Dynamics
IK	Inverse Kinematics
IPSI	Ipsilateral
LED	Light Emitting Diode
MEDGAS	Medial gastrocnemius
PEE	Parallel Elastic Element
PWA	Point of Wrench Application
RRA	Residual Reduction Algorithm
SEE	Series Elastic Element
SEMEMB	Semimembranosus
SOL	Soleus
TA	Tibialis Anterior

Chapter 1

Introduction to the dissertation and its structure

1.1 - Introduction

Locomotion is present in almost every animal and it is learned in the beginning of life. Terrestrial locomotion in humans, or gait, is of great importance in their daily life, since it is the vehicle for many other tasks.

Biomechanical gait analysis can be based in experimental methods that allows the determination of important gait parameters (kinematic, kinetic and electromyographic). However, using uniquely this approach it is difficult to establish cause-effect relations between a specific muscle's action and its contribution for the overall movement. Dynamic simulations are able to fill this gap since it enables the access to the inputs that generate the outputs assessed experimentally: the forces that originated the motions measured. This is due to the fact that the system (model) is known and is described mathematically. The description of the model is, however, complex and, as consequence, it is necessary to use computational tools to solve these equations. OpenSim is an example of a software designed for this purpose and allows performing dynamical simulations, using experimental data.

The application of gait analysis in the clinical field, for example, in the characterizations of the impact of a pathology in gait or even as a diagnostic tool is possible. Subjects with stroke present several gait impairments that are dependent of numerous factors: brain area affected, time after the injury, physical characteristics of the patient, etc. The study of the muscle forces in these individuals permits the identification of the source of the damages and allows the creation of suitable therapeutic and/or surgical solution for each patient. Moreover, taking into account studies performed in healthy individuals, it contributes to the increase of the knowledge about the outcomes of this pathology.

1.2 - Objectives

The main objectives of this monograph were the following:

1. Explore the fundamentals of the human gait, taking into account:
    a. The musculoskeletal system of the lower limb involved in the process: anatomical constitution (bones, joints and muscles) and function;
    b. Understand the process of gait as a coordinated movement as result of a complex system of neuromuscular control and study the gait cycle, by decomposing it in the respective phases and subphases in order to understand the sequence of events.
    c. Explore the concepts of gait abnormality and pathological gait and determine the consequences of a stroke in the task of walking, considering previous studies.
2. Elaborate a literature review addressing the following issues:
    a. Methodologies used currently in experimental gait analysis;
    b. Mathematical and mechanical models able to simulate the musculoskeletal system, the muscles and muscular control, developed to be used in computational simulations of gait;
3. Developed dynamic simulations of healthy and pathological gait in OpenSim, taking the following steps:
    a. Extract and process experimental data from a gait trial of a post stroke individual and prepare it to use as input in OpenSim;
    b. Execute the OpenSim workflow (choice of a musculoskeletal model, scaling, inverse kinematics, inverse dynamics, reduction of residuals and computed muscle control);
4. Compare the results obtained from the healthy and post stroke simulation and with the literature.

1.3 - Organizational Structure

This dissertation is divided in six chapters, each one containing the respective introduction and summary. Next, is presented a brief description of each remainder chapter.

Chapter 2 – Fundaments of Human Gait

In this chapter the anatomical structures composing the lower limb and the pelvis (bones, joints and muscles) are described with interest in understanding their role in the walking task. In a second part, it is described normal gait and from the neuromuscular control involved, following by the characteristic gait cycle and the respective phases and subphases.

Finally, are introduced the concepts of gait abnormality and pathological gait. A specific type of pathological gait, post-stroke gait, is explored. Considering experimental studies done with post-stroke individuals, the characteristics of this type of gait are enumerated and grouped according to their spacio-temporal, kinematic, kinetic and EMG nature.

Chapter 3 – Literature review

The state of art comprises the experimental and computational approaches of current gait analysis. In the first topic, the assessment of important gait parameters by visual gait analysis and the use of technological tools to extract kinematic and kinetic data, and the electrical activity of the muscles (EMG) is explained.

In the second topic, regarding the computational analysis of gait, the models designed to simulate mathematically and mechanically the musculoskeletal system, the muscle tension paths, the operation of the muscles and tendons as an actuator, the muscular activation and the neuromuscular control are described.

Chapter 4 – Methodology

In the first part of this chapter, the method used for extracting the kinetic and kinematic data from a *.c3d and the respective processing is presented. In the second part, the computational environment, OpenSim, and its capabilities are introduced. Then, each step of the implemented workflow is described: the choice of the musculoskeletal model, the scaling process, the inverse kinematics and dynamics step, the reduction of the residuals and, finally the computed muscle control.

Chapter 5 – Results and discussion

In this chapter, the experimental data extracted from the *.c3d file and processed is analysed and discussed, as well as the methods used. Following the errors and the results obtained from each step of the workflow are presented and discussed, comparing the simulations developed for the healthy and the post-stroke individual with the literature.

Chapter 6 - Final conclusions and future developments

Being this the final chapter, it presents the general conclusions of the present study, as well as the limitations of this study and possible future developments.

Annex

In the annex, the data that complement the understanding of the study is presented:

a. Annex 1 list of body markers used in the LABIOMEP and in OpenSim;

b. Annex 2: plots of the ground reaction moments filtered using different cut-off frequencies;

c. Annex 3: weights used for each marker in the scaling process;

d. Annex 4: weights attributed to each marker in the inverse kinematics process.

1.4 - Main Contributions

The present work increases the knowledge about the sequence of procedures necessary to model gait, using OpenSim, starting with the generation of the input files in the appropriate format from a *.c3d file, which is a standard format among the biomechanical community, until the study of the muscular behaviour. It also explores the influences in considering the horizontal moments as part of the external forces and moments in the simulations of gait, that usually are not taken into account in some gait studies.

Chapter 2

Fundaments of Human Gait

2.1 - Introduction

The understanding of anatomical organization of the lower limb and pelvis is fundamental in gait studies.

The bones are rigid structures able to support the body and move. The movement is only ensured because of the existence of joints connecting the bones. Each joint allows one or more degrees of freedom, depending on its conformation. The muscles involve the skeletal system, being linked to the bones in insertion points through tendons. Due to this configuration, muscular contraction is capable of generate movement of bones around the joints. When several muscles are contracting, coordinated by the neural controls, complex movements can be made, for example, walking.

Normal gait is difficult to define since there is some variability between healthy subjects, depending on the on the person sex, age, body geometry. Thus, the term “normal” has several definitions, according to the characteristics of the individual under study [1].

Gait is a complex task that involves nervous control to activate muscles and create a coordinated movement. The muscles are activated by electric impulses arriving through the neurons and sent from the mechanism controls.

The high controls of locomotion are located in the brain, consisting in the brain cortex, basal ganglia and the cerebellum, and are responsible for planned actions by the person. The spinal cord is also important and it is there were the rhythmic and “automatic” movements of walking are generated. Another important aspect is that the control of gait counts with feedback mechanisms that help modulating the muscle excitations, such as muscle spindles, Golgi organs and mechanoreceptors in the skin.

In order to study the gait cycle, it is necessary to focus our attention in one leg, since gait is symmetrical, and follows its movements through the cycle. Then it is possible to divide it in a

stance phase (when the foot contacts with the floor), a swing phase and the correspondent subphases.

Since human gait results from the action of the muscular system in conjunction with the neural controls, damages in one of these systems can lead to gait abnormalities that can reduce substantially the quality of life of the individual, once he may need a surgical intervention to correct the problem or to use of walking aids, and, in a worst case, he can become disable to walk (for example in a case of paraplegia).

Gait abnormalities can result from specific pathologies, for example, stroke. In this case, although the impairments vary from person to person and with the time after the accident, they frequently include weakness of the muscles of one side (hemiparesis) that can cause asymmetry in gait. Usually, the affected individuals walk slower and sometimes reveal spasticity.

In this chapter, an anatomical perspective with interest in studies of gait of the constitution of the lower limb and pelvis is provided. Firstly, the bones are presented, followed by the joints and ligaments and finally, by the most important muscles. Following that, an overview about the neuromuscular control involved in gait and a description considering its phases and subphases and the nomenclature associated is given. Also, the concepts of gait abnormality and pathological gait are analysed, as well as the most common gait impairments following stroke are discussed and studied in terms of spacio-temporal, kinematic (movement of the limbs) and EMG/kinetic (muscle actuation and resultant forces and moments) characteristics.

2.2 - Lower limb and pelvis anatomy

2.2.2 - Lower limb bones

It is considered that all the bones of the body take part in walking; however, in order to simplify the analysis, only the bones constituting the lower limb and the pelvic girdle can be taken into account. In terms of architecture, the lower limb (Figure 2.1) is very similar to the upper limb; nevertheless, the bones are generally more robust and longer in order to allow the support and motion of the body [1].

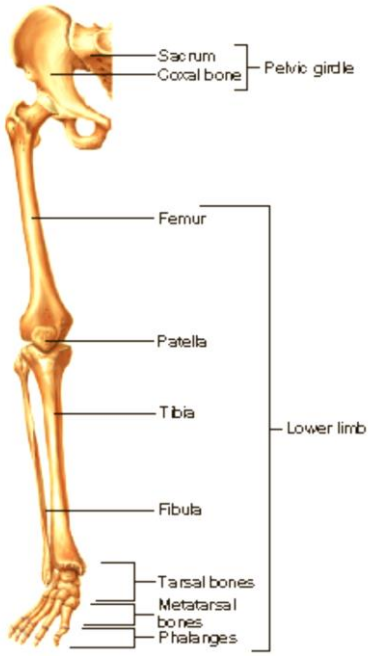

Figure 2.1. Anterior view of the lower limb bone constitution [2].

The pelvis is constituted by the pelvic girdle and the coccyx. The pelvic girdle includes the right and left coxal bones, articulating anteriorly with each other and posteriorly with the sacrum, which is the result of the union of five sacral vertebrae [2]. The coccyx is a vestigial tail, resultant from the fusion of three to five rudimentary vertebrae [1].

The femur is the longest bone in the human body and articulates with the pelvic girdle through the femoral head in the acetabulum, which is a surface located in the lateral part of each femur bone. In its proximal part, besides the head, it exhibits two projections situated laterally and inferiorly to the head and neck: the greater trochanter and the lesser trochanter, respectively, which are important sites for muscle attachment [2]. Downwards to the shaft of the femur, in its distal part, there are the medial e lateral condyles, which are smooth and rounded surfaces where the tibia articulates with the femur. Between them exists a groove that allows the articulation with the patella [2].

The patella (also known as kneecap) is a sesamoid bone embedded in the tendon which connects the quadriceps femoris muscle to the tibia (quadriceps tendon and patellar tendon to the portion between the patella and the tibia) [1]. It has an important mechanical function in reducing the muscle contraction necessary to move the tibia, by altering the angle between the quadriceps femoris muscle and the tibia [1, 2].

The leg is the term used to define the portion of the lower limb from the knee to the ankle and comprises the tibia and the fibula [2]. Between them, the tibia is the largest. In the proximal part, it has lateral and medial condyles that articulate with the femur and the tibial tuberosity

for the insertion of the patellar tendon anteriorly. The distal part present the medial malleolus, which participates in the upper and medial part of the ankle joint [2]. The fibula is located laterally to the tibia, and these two bones articulate between them in both extremities, forming tibiofibular joints. During their extension, there is a layer of fibrous tissue, the interosseous membrane. For these reasons, the relative movement between these two bones is very small and can be neglected in further studies [1].

The foot is a complex structure that is divided into three parts: hindfoot, midfoot and forefoot [1].

The hind foot is the most proximal part and is composed by the talus, the calcaneus, and the navicular: the talus articulates with the tibia, the fibula and the other bones of the hind foot; the calcaneus is placed inferiorly to the talus, and it has a protuberance covered with a thick layer of fat and fibrous skin (heelpad) that transmits the body weight to the ground [1, 2].

The midfoot includes three bones: the navicular, cuboid and cuneiform bones. The navicular is a boat-shaped bone located between the calcaneus and the cuneiform bones in the medial section of the foot. The cuboid has the shape of a cube and is placed laterally, articulating with the metatarsal bones and the calcaneus. The cuneiform bones are three: medial, intermediate and lateral, forming a row [2].

The forefoot is composed by the five metatarsal bones and the phalanges, the bones of the toes. There are two in the big toe and three in the other four toes [1]

2.2.3 - Lower limb joints and ligaments

Joints are regions of contact of two bones [1, 2]. They can be classified as fibrous, cartilaginous or synovial, based on the type o tissue that involves it and the presence or absence of synovial liquid. Our interest will be focused in the synovial joints since they are associated with larger movements [1].

Synovial joints are surrounded by a synovial capsule, where a lubricant synovial fluid is secreted and bone extremities are covered by a cartilaginous tissue. They can be classified as: plane, saddle, hinge, pivot, ball-and-socket and ellipsoid [1].

The **hip joint** is a true ball-and-socket joint, where the ball is the head of the femur and the socket is the acetabulum. The joint is protected by strong capsule surrounding it and reinforced by five ligaments, one of which connects to the centre of the acetabulum to the centre of the femoral head (ligamentum teres) [1, 2]. These factors allow the hip joint to be one of the most movable joints of the body, permitting movements of flexion, extension, abduction, adduction, internal and external rotations [1, 2].

The **knee joint** is an example of a hinge joint, where the medial and lateral condyles of the femur articulate with the corresponding condyles of the tibia, resulting in two separate joints, in each side. Since the femoral condyles are round shaped and the tibial ones are nearly flat,

it results in a gap around the contact points, which is filled by two menisci (articular disks of fibrocartilage), which helps to distribute the load [1, 2].

The main ligaments to achieve stability of the joint are the medial and posterior collateral ligaments and the anterior and posterior cruciate ligaments [1]. Other important features are the popliteal ligaments and tendons of the thigh muscles that spread around the knee, which contribute for the strength of the joint [2] and the synovial bursae (at least twelve) that help to reduce the friction between tendons and bones during the movements [3].

As a hinge joint, it allows movements of flexion and extension, but also these are combined with gliding and rolling and rotation around the vertical axis [3].

The **patellofemoral** joint happens between the posterior surface of the patella, where exists a superficial V-shaped ridge and the condyles of the femur in its anterior surface. The principal movement consists in the sliding of the patella up and down, during extension and flexion of the knee, respectively, and a slight medial-lateral movement [1].

The **ankle joint** or talocrural joint involves three bones: the tibia, the fibula and the talus and has three surfaces: upper, medial and lateral and it is classified as a modified hinge joint [2]. The medial and the lateral malleoli of the tibia and fibula form with the talus the medial and the lateral articular surfaces of this joint, while the upper surface is formed above by the tibia and bellow by the talus [1, 2].

Surrounding the ankle joint, there is a fibrous capsule that gets thicker in the medial and lateral parts, forming the collateral ligaments, keeping the contact between the bones [1, 2]. Also there are several ligaments between the tibia and the fibula, important to prevent the separation between these bones [1].

The movements associated with the ankle joint in a normal healthy individual are dorsiflexion, plantar flexion, limited hindfoot adduction and abduction and a slight rotation around the longitudinal axis of the leg [1, 2].

The joints existent in the foot include:

Subtalar or talocalcaneal joint: between the talus and the calcaneus. It allows the same movements of the ankle resulting in some difficulty in gait analysis when determining the origin of these movements [1];

Midtarsal joints: between the tarsal bones. The presence of ligaments does not allow large movements, but allow a flexible connection between the hindfoof and the forefoot [1];

Tarsometatalsal joints: flat joints between the cuboid and the cuneiform bones and the adjacent metatarsal bones, allowing small sliding movements [1];

Metatalsophalageal joints: between the metatarsal bones and the proximal phalanges, resulting in movements of flexion, extension, abduction and adduction [1];

Interphalangeal joints: between two phalanges and allowing movements of flexion and extension, being the maximum flexion angle greater [1].

The disposition of the bones, muscles and ligaments in the foot makes this structure to be flexible, but with restricted movements and to have three arches: the medial and longitudinal arches and the transverse arch, which have an important role in the distribution of the pressure (Figure 2.2). During standing and walking the body weight is transferred from the tibia and the fibula to the talus and then to the calcaneus. The system of arches allows the transmitting of the body weight through the lateral side to the ball of the foot (the head of the metatarsal bones) [2].

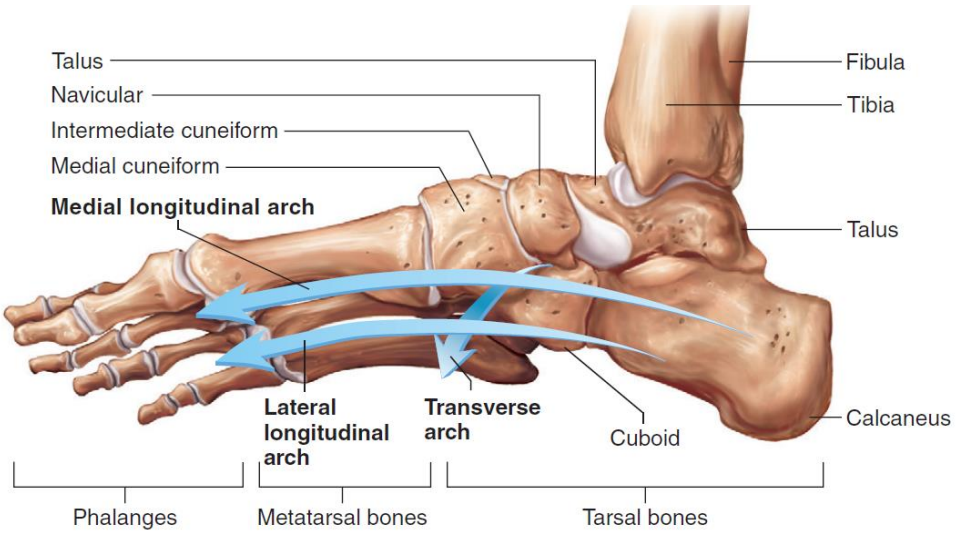

Figure 2.2. Medial inferior view of the foot with the representation of the medial and lateral longitudinal and transverse foot arches [2].

2.2.4 - Lower limb muscle

Muscles are positioned strategically in order to produce movements in the joints, being their extremities attached to bones and crossing one or more joints, which they will influence [1]. One extremity is the origin of the muscle, and the other is the insertion that narrows in the end, turning into a tendon [1].

The muscles of the lower limb (Figure 2.3) can be studied into three groups, regarding the articulation where they act: hip and thigh muscles, leg muscles and ankle, foot and toe muscles [2].

The muscles acting in hip and thigh can be divided as anterior, posterolateral and deep, according to their location [2]. The anterior muscles are the iliacus and the psoas, commonly mentioned together as iliopsoas, once their insertion tendons fuse together in the lesser trochanter of the femur. They are responsible for hip flexion [1, 2].

The posterior lateral group include the three gluteus (maximus, medius and minimus) with origin in the pelvis and insertion in the femur, being the first responsible for hip extension and

lateral rotation of the thigh and the latter two for hip abduction and medial rotation of the thigh [1, 2]. There is also the tensor fasciae latae that abducts the hip and also the knee [1]. The group of deep muscles is covered by part of the gluteus maximus and is composed by smaller muscles: piriformis, obturator internus and externus, superior and inferior gemelli and quadratus femoris. Their function is the lateral rotation of the thigh and also the stabilization of the hip joint, with the contribution of the ligaments [3].

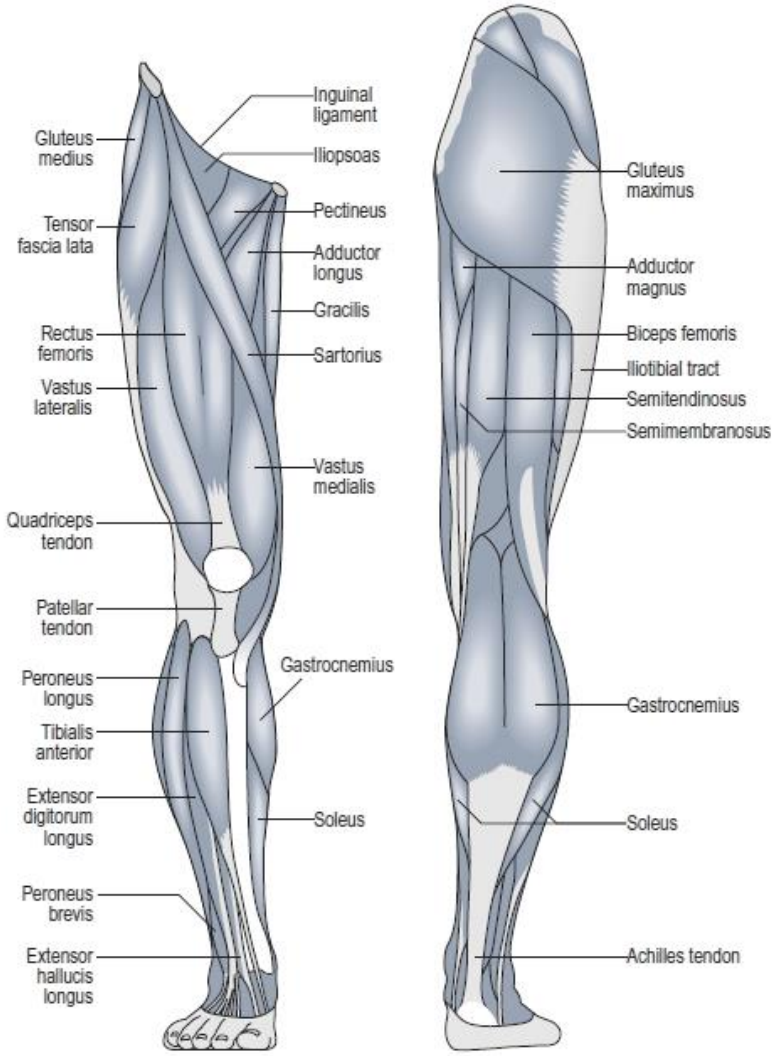

Figure 2.3. Anterior and posterior view of the lower limb muscle constitution [1].

The muscles of the leg have been organized in compartments: the anterior compartment, responsible for hip flexion and/or knee extension; the medial compartment that mainly adducts the thigh and the posterior compartment that extends the hip and/or flexes the knee, in opposition to the anterior one [2].

The anterior compartment is formed by the quadriceps femoris group of muscles that have insertion in the patellar tendon: rectus femoris, vastus lateralis, medialis and intermedius. The sartorius, the longest muscle of the body is also part of this compartment [2].
The medial compartment is formed by the adductor muscles (brevis, longus and magnus), the gracilis and the pectineus, while the posterior, also called hamstring muscles include the biceps femoris, the semimembranosus and the semitendinosus [2].
Lastly, the muscles located in the leg, responsible for the movements of the ankle, foot and toes are classified in extrinsic and intrinsic. The extrinsic are also divided into three groups [2], based on their location:
Anterior compartment: includes the extensor digitorum longus and hallucis longus, tibialis anterior and fibularis tertius and is responsible for dorsiflexion and eversion or inversion of the foot and extension of the toes;
Lateral compartment: formed by the fibularis brevis and longus and involved in eversion of the foot and also plantar flexion;
Posterior compartment: has superficial muscles, the gastrocnemius and soleus, which join the plantaris and form the calcaneal tendon (commonly known as Achilles tendon) and that are involved in plantar flexion of the foot. The deep muscles (flexor digitorum longus and hallucis longus, popliteus and tibialis posterior) act in flexion and inversion the toes.
The intrinsic muscles of the foot are located inside the foot, in a similar structure of the hand and are responsible for toe flexion, extension, adduction and abduction [2].

2.3 - Normal Gait

2.3.1 - Neuromuscular control

Skeletal muscles are well-organized complex structures, composed by hundreds of fascicles, which consist in hundreds of muscle fibbers [1]. These are, in turn, an arrangement of filaments actin and myosin, which cause muscular contraction when they slide relatively to each other [1].
A motor unit is considered to be the combination of a neuron, and the muscle fibbers enervated by it and its branches [1, 4]. The neuron transmits electrical signals (activation potential) to each muscle fibber, causing the release of calcium ions, which will trigger the muscle contraction and generate movement, with consumption of metabolic energy [1, 4]. Muscular contraction can be isometric, if the muscle generates tension, but does not change its length; isotonic if the length changes, but the tension generated does not; concentric if the contraction causes muscle shortening; and eccentric if it causes lengthening [1].

The walking movement was described as a complex interaction between supraspinal, spinal and afferent feedback mechanisms [5]. The supraspinal mechanisms are associated with the "fine control" of walking [6] and include [1, 7]:
Motor cortex, which generates voluntary movement;
Basal ganglia, responsible for planning and controlling parallel sequences of movements to produce complex movements;
Cerebellum, responsible for the timing of muscular activities, namely in the smooth and rapid transition from one movement to another, thus being involved in the equilibrium of the body. Also helps in the control of intensity of muscular contraction.
The spinal cord is responsible for the creation of reflexes that are fast reactions to a stimulus, detected by the afferent feedback mechanisms [1, 6]. The afferent feedback mechanisms include: muscle spindles, sensorial receptors located in the muscles responsible for muscle length and velocity feedback; Golgi organs, in charge for force feedback; and mechanoreceptors in the joints and skin, which give cutaneous feedback [5]. These mechanisms allow the adaptation of gait to the environment stimuli [8].
In the spinal cord, there are also Central Pattern Generators (CPG), which consist in networks of nervous cells [1, 8, 9]. Associated with the afferent feedback mechanism, the CPG produce rhythmic movements like walking, without conscious effort [6]. Even though the existence of these in quadruped animals was already proved, the evidence of those in human stills indirect [6, 10].

2.3.2 - Gait Cycle

Gait cycle is defined as the interval between two successive occurrences in the process of walking. For example, if it is considered the contact of the right foot with the ground ("initial contact") as the beginning of the cycle, then the cycle ends in the next contact between the right foot and the ground [1, 11]. This period is characterized by a stance phase, during which the foot is in contact with the ground, and a swing phase, where the limb swings in the air [1, 11]. When one leg is the stance phase, the opposite is in swing phase, excluding the moment of double contact, in which both are in stance phase (Figure 2.4).

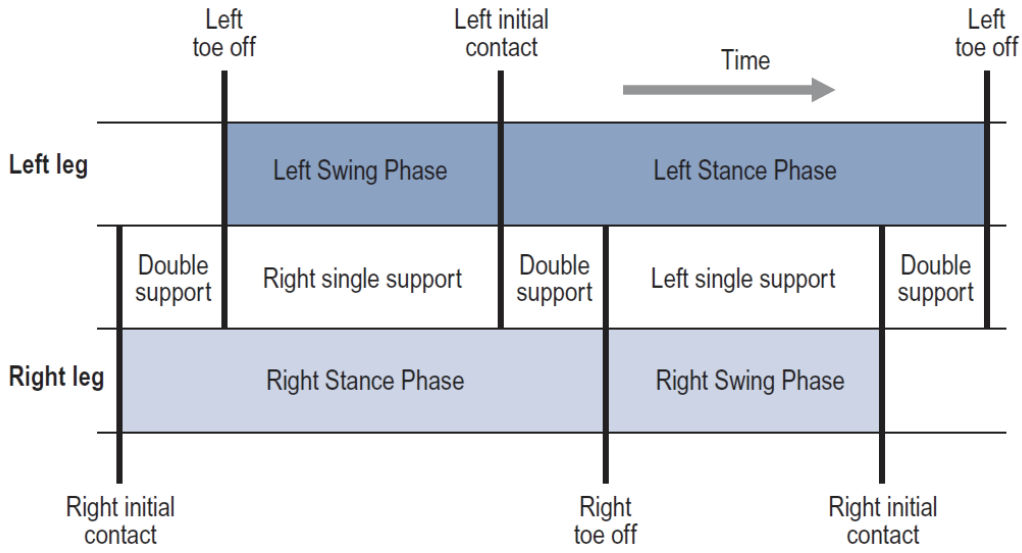

Figure 2.4. Diagram of the gait phases for left and right legs [1].

The stance phase lasts approximately 60% of the gait cycle [11] and begins with the initial contact and ends with the toe off of the same leg. It comprises four subphases (Figure 2.5) [1, 11]:

1. **Initial contact**: the initial stage of the loading response, when the heel of the right foot contacts with the ground. It is characterized by hip flexion, knee extension and neutral dorsiflexion of the ankle. The ground reaction force has upwards direction;
2. **Loading response:** occurs after the initial contact and before opposite toe-off, when both feet are in contact with the ground and the weight of the body is transferred from the left leg to the right one. In this phase the ankle presents plantarflexion and the ground reaction force increases its magnitude and direction from upwards to upwards and backwards;
3. **Mid-stance**: occurs after the opposite toe-off and before the heel rise. It corresponds to the moment when the left leg is in the swing phase and passes the right one. The hip increases the extension, which is achieved mainly because of the inertia and gravity, while the knee is reaches the highest flexion point of the stance phase before it starts to extend. The ankle, which was in plantarflexion changes to dorsiflexion. The ground reaction force moves forward along the foot, from the moment when the foot is in full contact with the ground [1];
4. **Terminal stance**: corresponds to the moment when the heel of right foot starts to leave the ground, before the left foot toe contacts with it [11]. The heel rise is characterized by peaks of hip and knee extension and ankle dorsiflexion. In opposite initial contact, the hip reaches the highest extension angle, while the knee starts flexing and the ankle moves into plantarflexion. During this phase, the ground reaction force moves forward [1];

5. **Pre-swing**: is characterized by double support, since the left foot contacts with the walking surface and the body weight is shared between the two legs and it lasts until the toe off moment, which separates the stance phase from the swing phase [1, 11].

The remaining 40% of the cycle consists in the swing phase (Figure 2.4), which is sub-divided in:

1. **Initial swing**: occurs when the right foot leaves the ground. The hip is flexed as well as the knee, and the ankle reaches the peak of plantarflexion immediately after the toe-off. The ground reaction force is positioned behind the knee and becomes zero when the foot leaves ground [1];
2. **Mid-swing**: starts with the feet adjacent, when the right and left legs are side by side and ends with the tibia vertical. In the first step, the hip continues to flex and the knee is also flexed, mostly as consequence of the hip flexion. The ankle moves to an attitude considered neutral or dorsiflexed. The ground reaction force is null, since the right foot is in the air [1];
3. **Terminal swing**: begins with tibia vertical, consisting on the tibia of the right leg being in a vertical position. The flexion of the hip ends, the knee is passively extended, and the ankle is between slight plantarflexion and dorsiflexion. This phase ends with the initial contact, which marks the beginning of a new cycle [1].

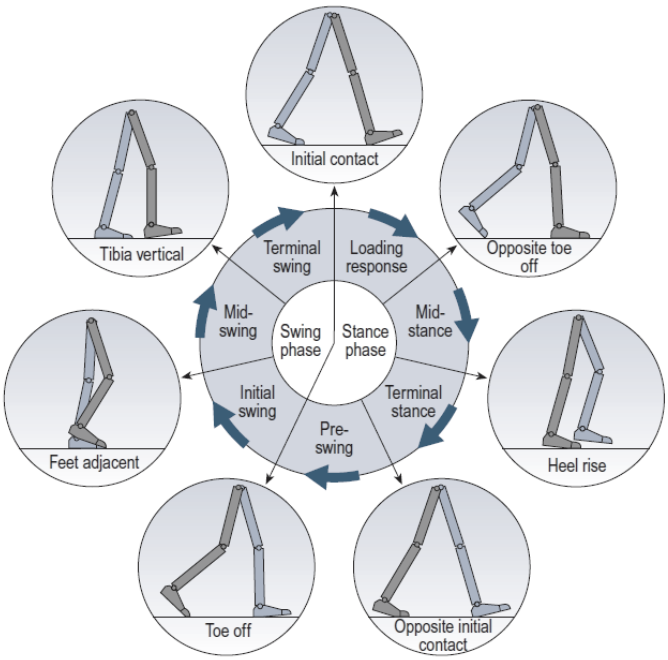

Figure 2.5. Stance and swing phases diagram and the respective subphases [1].

2.4 - Gait Disturbance

2.4.1 - Abnormal and pathological gait

Some gait characteristics vary from person to person; however, it is possible to quantify some variables that allow to define or acceptable range of values that characterize a normal gait pattern [1].

Gait is generally accomplished by four main tasks [1, 12]:

- Maintenance of the balance of the trunk, arms and head either statically or dynamically;
- The stance leg must be able to support the body weight;
- The swinging leg must advance to a position in order to accept the body weight transference;
- The energy supply must be enough to allow the forward movements.

It is considered that if at least one of these requirements is not fulfilled or the individual can perform all the tasks, but with extra energy consumption or with the need of walking aids (for example, canes), has a gait abnormality [1].

It is important to distinguish the term gait abnormality from pathological gait. Gait abnormality is the description of some gait characteristics that can be visually identified or by using experimental gait analysis methods (discussed in the chapter 3) and can include, for example: trunk bending, circumduction, hip hiking, vaulting, abnormal hip rotation, excessive knee extension/flexion, inadequate dorsiflexion control, abnormal foot contact, insufficient push-off, abnormal walking base, rhythmic disturbances, etc. [1] Pathological gait is related with a pathology, such as cerebral palsy, myelomeningocele, Parkinson's disease, stroke, etc. [1]. The gait patterns associated can include a single abnormality or a combination of several, which can interact between them and may change with time and therapy and vary from person to person [1, 13].

In pathological gait, an abnormality may result directly from any muscular or neural impairment such as muscle weakness, some deformity or spasticity, or be the consequence of a compensation of an impairment, being named in this case as adaptation [1, 12].

2.4.2 - Post-stroke gait

Cerebrovascular accident (CVA), commonly referred as stroke, is the death of brain tissue as consequence of a disturbance of the arterial blood supply [2, 12]. There are two types of stroke: haemorrhagic stroke that results from artery bleeding inside the brain and ischemic stroke that is consequence of the blockage of brain arteries by a thrombus, a blood clot, a fat globule or a gas bubble [2]. The outcomes of a stroke are dependent on the area of the brain which suffers

the temporary privation of blood and can include loss of communication and vision capabilities and abnormalities in the motor system. The most frequent case is the one in which one of the sides of the territory irrigated by the middle cerebral artery is affected and some motor functions are damaged, causing motor control disorders in the opposite side of the body [14]. In addition, motor function can also be impaired if the midbrain is injured because this can block nerve conduction the pathways between the brain and spinal cord, affecting the sensorial and motor systems and, consequently, abnormal gait [7].

Post-stroke patients suffer neurological and motor sequels, but more than 85% of stroke survivors are able to walk with or without assistance [15]. There is some variability of gait abnormalities between individuals following stroke, and they depend on the time after the injury, as well if the patient received rehabilitation therapy [12, 13].

Hemiparesis, one of the most common impairments [16], is the affection of one side of the body due to defective muscle activation [17]. In several studies, muscle activity was measured by electromyography (EMG), showing alterations in the magnitude and phase of the muscular activity patterns, comparing to health individuals and abnormalities on both the contralesional (CONTRA) and ipsilesional (IPSI) sides, leading to bilateral differences [18, 19].

Pronounced asymmetry in gait pattern, due to hemiparesis, may change some temporal, spacial, kinetic and kinematic gait variables [16]. Table 2.1 is presents a list of gait common impairments associated to post-stroke gait.

Table 2. 1. Common spacio-temporal, kinematic and kinetic/EMG abnormalities in gait of post-stroke patients.

	Gait modifications
Spacio-temporal [12, 13]	- Reduced walking velocity; - Shorter stride length; - Longer gait cycle duration; - Longer proportion of double-support phase and stance/swing phases of both legs.
Kinematics [19]	- General decrease of joint peak displacements at the hip, knee and ankle. **Sagittal plane** - Decreased hip extension during stance and decreased hip flexion during swing; - Higher ankle plantarflexion at initial contact [13]; - Knee hyperextension during weight acceptance;

	- Decrease of knee flexion and absence of dorsiflexion at swing phase. **Horizontal plane** - Larger external rotation of the paretic hip and knee; **Frontal plane** - Larger abduction of the hip and large inversion of the ankle in the paretic side; - Larger pelvic hiking and lateral displacement.

EMG/Kinetics	- Weakness of the paretic muscles, suggested by the overall decrease of EMG levels in the paretic side [12, 19];
	- Reduction of the plantarflexion moment in both sides in the correspondent late stance phases [17]:
	  - Paretic side: attributed to the early and reduced EMG activity of the paretic plantarflexors (namely medial gastrocnemius);
	  - Ipsilesional side: related with excessive antagonist co-activation as an adaptation for postural instability caused by impaired gait;
	- Prolonged stance co-activation of hamstrings and the quadriceps muscles in both sides (acting as compensatory mechanism for the weakness of the plantarflexors, which have been found to have the largest contribution to support during the single leg stance phase [16, 20, 21] ;
	- Hyperactive stretch reflexes that may cause knee hyperextension and hinder dorsiflexion in late stance phase, interfering with push-off [17]. Besides, plantarflexors generate large part of the energy to move the limbs forward during the push-off phase. This group of muscles, specifically the soleus and the gastrocnemius, showed insufficient power generation in the contralesional side [22];
	- Reduction of the dorsiflexion moment in the swing phase, in the contralesional side caused by weakness of ankle dorsiflexors, namely tibilalis anterior, combined with increased plantarflexor passive stiffness [15, 17];

- Dynamic spasticity of the plantarflexors and weakness of the dorsiflexors during loading response are responsible for the increasing of the step length [15, 17, 23].

- Concerning the power it is verified differences between slow and fast walkers[17]:

  - **Slow walkers:** Lower late stance ankle pull-off (A2: second ankle power burst) and early swing hip pull-off (H3: third hip power burst) propulsive power bursts on both sides;
  - **Fast walkers:** Larger positive work by both hip extensors in early stance (H1: first hip power burst) and, in the contralesional side, by the H3 propulsive power burst.

Spasticity is verified in 20-30% of the post-stroke patients [5, 12]. It is defined as a "motor disorder by velocity-dependent increase in tonic stretch reflexes (muscle tone) with exaggerated tendon jerks, resulting from hyper excitability of the tendon reflex" [5]. However, there is controversy between the authors about the contribution of the spasticity in post-stroke gait impairments [15, 21].

These impairments lead to a higher energetic cost, at the biological (metabolic) and mechanic levels [12, 13, 16]. The metabolic cost in hemiplegic gait was found to be 50% to 97% higher than in healthy subjects [18]. Lamontagne et al. [17] reported that this general higher energetic cost may be related to the excessive co-activation of antagonistic muscles.

2.5 -Summary

The lower limb is composed by several bones, joint and muscles, organized similarly to the upper limb in some aspects.

The localization of the muscles as well as their insertion in the bones is directly linked with the movement they generate. Considering their action, muscles can also be grouped, for example, the group of the hip flexors, which are involved in flexion of the hip.

The fact that the joints in lower limb (and also the upper limb) system are synovial is important considering that the relative movement of the limbs and the simultaneous task of supporting

the body weight lead to a high friction between the bones that could increase the wear if the joint was not equipped with cartilage, synovial lubricant and other mechanisms.

The hip, knee and ankle joints and associated bones and muscles must receive special attention since considerable amount of movement are generated there. On the other hand, the joints in the pelvis and in the foot are very restrictive of the motion, when compared to these joints.

Human gait involves control by supraspinal and spinal mechanisms that transmit electric signals to the muscles in order to generate the desired movement. In the particular case of locomotion, there are indirect evidences of a control center in the spinal cord, responsible for the generation of unconscious stepping. The gait cycle is divided in the stance and swing phases, which in turn are divided into five and three subphases, respectively. This method allows the study of the sequential events in terms of moments of the segments, ground reaction forces and muscles involved to achieve the task of locomotion.

Gait abnormalities following stroke are mostly the consequence of the weakness of the muscles of one side of the body. Spasticity, however, has a neural origin, but there is still disagreement between the studies performed, about the influence of it in post-stroke gait.

In the sequence of these disabilities, the affected individual develops mechanisms of compensation, with the objective of allowing his locomotion. Nevertheless, these are also classified as gait abnormalities.

In the sequence of a stroke, patients must receive rehabilitation therapy in order to minimize or eliminate its outcomes and improve their quality of life.

Chapter 3

Related Work

3.1 - Introduction

Human gait can be studied using an experimental approach by measuring several parameters that characterize gait, with the aid of the latest technologies available for this purpose. Many research laboratories and specialized clinics can perform this studies for purposes of research or to help in the process of rehabilitation.

With the development of new complex models simulating the human body and the development of the computers, it became possible to combine the data collected experimentally with computational models and make dynamic simulations, able to estimate, for example, the individual muscle contributions for the movement. Studies aiming to test hypothesis ("what if" studies), such as see what happens when a muscular excitation pattern is modified [24] are also possible using computational simulations, which is hard to implement experimentally.

In this chapter, the experimental methodologies to assess kinematic, kinetic measurements and muscle activity are reviewed. Afterwards, the mathematical models currently used with the aim to represent the biological structures (muscles, bones, ligaments) and the respective control are analysed. Finally, an overview of OpenSim, the software to be used, is given.

3.2 - Experimental methods for gait analysis

Gait analysis is defined as "the systematic measurement, description, and assessment of those quantities though to characterize human locomotion" [25]. The study of human locomotion has been increasingly used in the last decades in the fields of sports, rehabilitation [26] and in research [17].

Roy B. et al [25], in 1991, defined clinical gait analysis as the use of gait analysis in which the clinician quantitatively examines the outcomes of a certain disease or injury suffered for the

patient. However, in 1981, Brand et al. [27] had already enumerated four reasons that extend the applications of clinical gait analysis:

1. Diagnosis: identification of the disease;
2. Assessment of the state of the disease or injury and its severity;
3. Monitoring the progress of a patient in cases with and without intervention;
4. Prediction of the effects of the intervention or the absence of it.

Experimental gait analysis is performed by using technological tools to extract information from gait. Centres executing this type of analysis could beneficiate from the latest technological development to obtain more accurate data with more sophisticated techniques. Experimental gait analysis aims the obtaining information as the general parameters of gait, kinematic and kinetic data and muscle activity. In some cases, data related to the metabolic activity, for example, oxygen consumption and heart rate during gait is also assessed [14]. The main components of experimental gait analysis currently used are presented in the next sections.

3.2.1 - Visual gait analysis

The visual gait analysis consists on the unaided observation of the patient walking on a pre-determined path by one or more specialists. This approach is considered as semi-subjective, since it is highly dependent on the evaluation of the specialists [27].

The visual assessment of walking is frequently recorded from both sides and from the front and the back of the patient, so the clinicians can reproduce the visualization and analysing it using slow motion, freeze-frame and other tools [28].

This method allows the identification of some gait abnormalities, for example: abnormal rotation, extension and flexion in the joints, trunk bending, circumduction, hip hiking, problems in foot contact and rotation, insufficient push-off, etc. [1].

3.2.2 - General gait parameters

The general gait parameters, also called temporal and spatial parameters, are: cadence (the number of steps in each time unit) or the cycle time (the time that the patient takes in one step), stride length and the speed [1, 28].

These parameters usually are modified in most locomotor disabilities; however, they are not able to provide specific information about them, making necessary the assessment of other gait variables.

The cadence and time cycle can be assessed by counting the number of steps in 10 or 15 seconds and extrapolating the value for one minute; speed is calculated dividing the distance walked by the time the individual took; and the step length can be determined by direct measurement, by using methods to mark the places where the feet touch the ground, or indirect measurement, by using the cadence or de cycle of time [1]:

Stride length (m) = speed (m) x cycle time (s);
Stride length (m) = speed (m/s) x 2 x 60/cadence (steps/minute).

3.2.3 - Kinematics

Kinematic data include the position and orientation of the body segments, the angles of the joints and the corresponding velocities and accelerations (linear and angular) [1]. The collection of this type of data improved considerably because of the latest technological advances [29].

The basic principles rely on the use of a system of two or more high-speed cameras, placed in different viewpoints, in order to obtain a three-dimensional analysis. The individual under study wears clothes that expose the major part of the lower limbs and reflexive makers are placed in his/her skin, in specific points, which will allow to track the limb segments, the pelvis and the trunk as well as their orientation [1, 28].Near to the lens of the camera, there is a source of light directed to the individual, either visible or infrared, so that the markers become bright and therefore, easy to track in the recording. Usually, the cameras are connected to a computer that stores each frame as a two-dimensional image. These images are processed in a suitable software in order to determine the centroid of each marker and after to extract the kinematic data [1]. Currently, it is common to have clinical systems using 8, 10 or more cameras, operating at a frequency of over 100 Hz, able to detect many tens of markers having 9 to 25 mm diameter [29].

In order to obtain more accurate measurements, a previous calibration of the system is necessary. This is accomplished by using the cameras to view a calibration object that contain markers placed in known positions and processing the data acquired in the computer, to relate the images from the cameras with the real position of the markers [1, 25, 28, 29].

Another option consists in the use of active markers, namely LED (light-emitting diodes), and an optoelectronic camera able to determine the position of each marker by analysing the light that comes from it. Each LED is set to emit light in a way that there is no more than one active marker at the same time. That way each one can be easily identified and followed [1].

The current available systems are considered accurate in measuring marker positions and consequently, the limb positions and orientations [1, 29]; however, is necessary to mathematically differentiate the position data to obtain the linear and angular velocity and differentiate it two times to obtain the acceleration, leading to a significant amplification of measurement errors [1]. The use of inertial sensors, such as accelerometers and gyroscopes can solve this problem. Accelerometers are devices able to measure the linear acceleration, while gyroscopes measure the orientation, angular velocity and acceleration [1, 27]. The

miniaturization of these devices allowed its integration in IMUs (Inertial Measurement Units), currently one of the most used types of sensors in gait analysis [27]. They can be integrated on instrumented insoles for gait analysis, for example, the case of Veristride instrumented insoles developed by Bamberg et al. [30], which include an inertial sensor, a Bluetooth communication module and a pressure sensor, and the power is generated by an inductive charging system [27]. An image of this insole is shown in Figure 3.1.

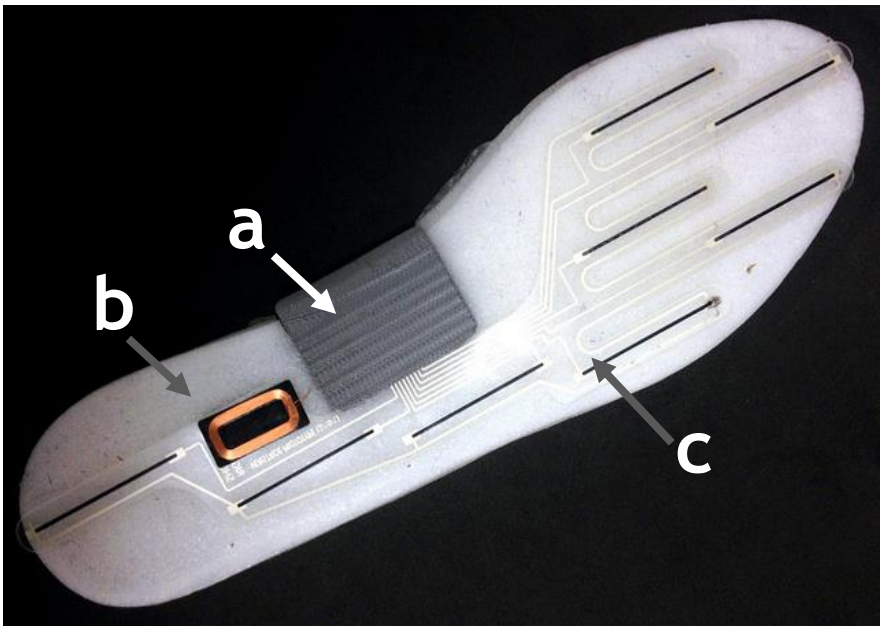

Figure 3.1. Veristride instrumented insole: a - inertial sensor, Bluetooth, microcontroller and battery module; b - coil allowing inductive recharging, and c - pressure sensors [31].

Other devices widely used are electrogoniometers, which are devices used to determine the angles in the joints, allowing the obtaining of plots of angle vs. time or angle vs. angle, when the measurements are made in two joints [1, 27]. According to their principle, they can be rotary potentiometers or flexible strain gauges. In rotary potentiometers, the rotation of the central spindle causes an alteration in the electrical resistance, which can give the information about the angle. In order to obtain the angles in three dimensions, it must be placed three goniometers in each joint, connected by wires to the computer. However, these devices are considered not very accurate, and they are more used in the clinical context more than in research centres [1]. Flexible strain gauges consist in flexible metal strains, placed along the joint to be studied, with each end in a different segment that constitutes the joint [1]. The material of the strain increases its resistance to conduct current when it is flexed, proportionally to the flexion angle. They can be used to determine the angles in the ankles, knees, hips and metatarsals, being frequently used in instrumented insoles [27].

3.2.4 - Kinetics

Kinetic data consists in information about the joint forces, moments and powers, which are defined as the measure of the rate of work generated by a muscle or group of muscles [1]. Knowledge about the power generation in joints is very useful, since it gives information if the muscles are contracting concentrically (power generation) or eccentrically (power absorption) [1, 28].

The Ground Reaction Force (GRF) is the force that opposes the one applied by the foot on the floor, having the same magnitude and opposite direction (3rd Newton's Law). The determination of it can be done by using sensor placed in the floor, like force platforms (or forceplates) or wearable sensor placed beneath the shoe [1, 27].

Force platforms are rectangular plates having an upper rigid surface made of a metal or of a lightweight honeycomb arrangement. Inside there are transducers that measure the small displacements of the upper surface, in the three axis, caused by the patient's foot while he walks. The electrical signal is sent to a computer, usually through an analog-to-digital converter [1].

Data obtained from the force platform are usually displayed as: individual components of the force vs. time; "butterfly diagram", which represent the vector of the GRF in sequential intervals of time; and diagrams displaying the location of the centre of pressure (the point where the force resultant acts) in each foot [1].

The wearable sensors are often used in instrumented shoes, for example, the one presented in Figure 3.1 [27]. There are three varieties of sensors used for this purpose: resistive, piezoelectric and capacitive. Howell et al. performed a study using insoles having 12 capacitive sensors and the results showed high correlation with the ones obtained in a laboratory, performing the same experiment [32].

The data obtained by measuring the GRF is more useful when combined with the kinematic data and the knowledge of the body mass, moment of inertia of each body segment and the location of the centre of gravity, in order to determine the joint forces, moments and powers, by inverse dynamics [28].

3.2.5 - Electromyography

The electromyography (EMG) is the measurement of the electrical activity of the muscles and is usually performed while the kinematic and kinetic parameters are obtained, so that the data can be complemented [1, 27, 28]. Indeed, electromyographic data do not allow to identify the

type of contraction of the muscle (concentric, eccentric or isometric) nor it can assess the force generated [28].

The acquisition of the EMG signal is obtained by using surface electrodes (non-invasive method) or by inserting fine wire electrodes into specific muscles, using a hypodermic needle (invasive method) [1, 28].

In the first case, only the activity of surface muscles can be measured. Two electrodes are placed in the skin, over the muscle or group of muscles and the voltage difference between them is measured. The resultant signal is very small and suffers the interference of adjacent muscles, which makes necessary the amplification and conditioning prior to the analysis [1, 27].

The use of fine wire electromyography tends to be very painful to the patient, so this type of analysis is only performed in some cases, when there is the need to study a particular muscle [1, 28]. Besides that, the signal obtained tends to have higher amplitude than the one obtained with surface electrodes, and the interference is lower [1].

3.3 - Computational modelling and simulation of the human gait

Experimental techniques for the quantitative assessment of gait are very useful to give information about the kinematic and kinetic characteristics of gait and the muscle activity, but alone they cannot provide information about how muscles act to originate the movement measured. In the last years, biomechanical computer simulations, were favored by the technological development of the computers, able to perform complex mathematically complex simulations and increasingly faster.

Human body is a complex structure, with several components from bones, tendons, ligaments to muscles activated by complexly generated neural signals. Therefore, simulation of a specific motor task can be accomplished with the creation of a simplistic model, modeled by mathematical equations.

The first models created for this purpose consist on mathematical/mechanical models composed by a multi-segment body and without muscle modeling [33]. The inverted pendulum model is the simplest behavioral model of walking [34]. The leg is modeled as a rigid beam connected, in the top, to a point having a mass equal to the body mass, and in the bottom is fixed. During the stance phase of gait, the mass point moves as the rigid beam rotated around the fixed point and reaches the highest point a mid-stance [34]. As in a normal pendulum, potential energy is 180º out of phase with the kinetic energy. The model is, therefore, suitable for studies about the transference of potential and kinetic energies [35]. Other simplistic models are the “ballistic walking”, which is a mathematical model developed by Mochon and McMahon in 1980 [36]. It represents the swing phase leg by two segments and the stance phase leg by one segment, and the muscles are admitted to act only in the beginning of the swing

phase to establish the initial configuration of the position and velocity of the limbs [36]. "Passive walking" model was introduced by McGeer [37] and is based in the idea that periodic stable walking can be reached without any muscular force when descending a slight slope, because the loss of kinetic energy during heel-strike is compensated by gravity force [33, 37].
The models mentioned above, although are useful to provide the basic understanding of walking, namely relations between mass, anthropometrics of the body, velocity and general mechanical energetics, do not allow studies concerning muscle coordination and sometimes can lead to erroneous conclusions [33].
Complex dynamical multi-segmented models have been developed and include the musculoskeletal geometry, a model of the muscle-tendon actuators and the motor control, including the excitation contraction dynamics [33].

3.3.1 - Musculoskeletal model

The musculoskeletal system is usually modeled as two or three dimensional composition of articulated (joints) rigid-body segments (bones) [35, 38]. The system is governed by the mechanical equations o the movement. For each segment, the acceleration $\ddot{q}$ can be written, according to:

$$I(q)\ddot{q} = M^{joint} + G(q)g + V(q,\dot{q}) + F^{ext}(q,\dot{q}) \quad (3.1)$$

where $q,\ \dot{q}\ and\ \ddot{q}$ are the vectors of the generalized coordinates, velocities and accelerations, respectively; $I(q)$ is the system mass matrix; M^{joint} is the vector of joint moments, given by $M^{joint} = R(q)\,F^{mus}$, $R(q)$ representing the moment arm matrix and F^{mus} the muscle forces; $G(q)g$, $V(q,\dot{q})$, $F^{non}(q,\dot{q})$ are the moments associated with the Gravity force, centripetal and Coriolis forces and external forces, respectively.

If the degrees of freedom of the musculoskeletal model are greater than four, it is necessary to use a computer to solve the equation above [35]. There are currently available some commercial packages designed for this purpose, for example: SD/FAST by Symbolic Dynamics Inc., DADS by CADSI, ADAMS by Mechanical Dynamics Inc., AUTOLEV by On-Line Dynamics Inc. and OpenSim by Stanford University, which will be used in this work [35, 38, 39].

3.3.2 - Muscle paths

The muscles and tendons are assumed to be inserted in a single point in the bones and muscles which insert in the bone through a large area are modeled using more than one portion with only two insertion extremities [35].
The forces generated by each muscle are applied to the segments through a tensile path [39]. This path can be considered as a simple straight line, though this method can lead to errors when the muscle wraps around another component like a bone or another muscle [35]. Another possibility is to represent the muscle's path through its cross-sectional centroids. However, this method presents several problems because it is hard to determine these points for every joint configuration [40]. An alternative method consists in establishing specific points along the cross-sectional centroid's path, which are fixed in the structures where the muscle wraps and are linked by straight lines or curved segments [35] (Figure 3.2).

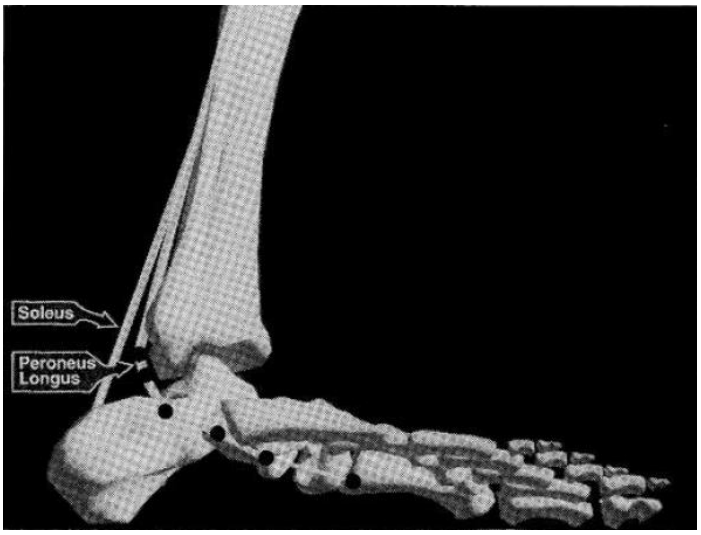

Figure 3.2. Three dimensional representation of the shank, foot and toes and the tensile path of the soleus muscle (single straight line) and of the peroneus longus, with a series of line segments and constrained "via points" [41].

Another option is the obstacle-set approach that allows does not constraint the muscle path in the contact with the other segments (bones and/or muscles), allowing it to move freely over the neighboring structures [40].

3.3.3 - Muscle-tendon actuator model

The Hill-type muscle-tendon actuator model was widely adopted in computational dynamical simulations since it is considered efficient and usable in several movements and has computational reduced cost [4, 20, 22, 38]. Originally, the model was developed by A. V. Hill and it was only composed by two elements [4], but since then it was improved and the version currently used is composed by a muscle with three elements and a tendon, as shown in Figure

3.3. The CE is a contractile element, where the force is generated and able to model the force-length-velocity property, and the SEE and the PEE are elastic elements (springs) positioned, respectively, in series and in parallel [38]. The first one is responsible for modelling the muscle active stiffness and the latter one models muscle passive stiffness [35]. In this model, the tendon is assumed to be an elastic element. However, it is known that the force associated varies non-linearly as the length of the tendon changes and that this simplification does not affect significantly the overall behavior [35].

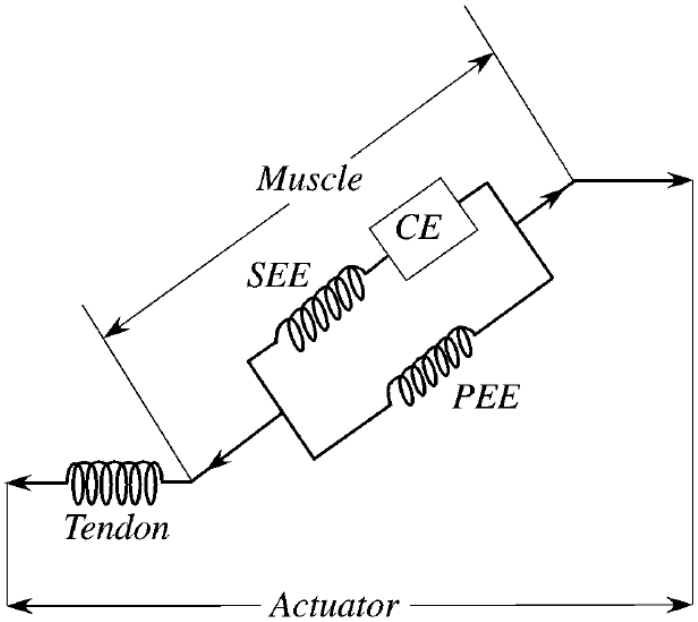

Figure 3.3. Hill-type muscle-tendon actuator, composed by a tendon in series with the muscle. The muscle is modeled by a contractile element (CE) in series with an elastic element (SEE) and in parallel with another elastic element (PEE) [38].

The muscle-tendon dynamic behavior is governed by a single non-linear differential equation [38]:

$$\dot{F}^{MT} = f(F^{MT}, l^{MT}, v^{MT}, a_m), 0 \leq a_m \leq 1 \quad (3.2)$$

where: F^{MT} is musculo-tendon force; $\dot{F}^{MT}$ is the rate of change of the muscle-tendon force; l^{MT} is the musculo-tendon length; v^{MT} is the musculo-tendon shortening velocity and a_m is the muscle activation.

3.3.4 - Muscle activation model

The excitation-contraction coupling has two steps (Figure 3.4): activation dynamics, consisting in the transduction of the neural stimulus into activation of the contractile element, and contraction dynamics, the transformation of activation into muscle contraction [39].

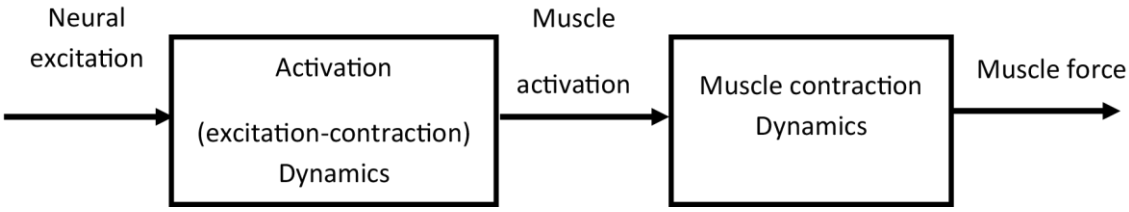

Figure 3.4. Musculo-tendon actuator dynamics [38].

There is a delay in time between the neural signal (excitation) and the consequent muscle activation (activation), due to the kinetics of chemical processes involving the calcium molecules [35, 39]. Consequently, several studies concerning gait analysis take in consideration this process [39], which is modeled by first-order differential equation:

$$\dot{a}^m = \left(\frac{1}{\tau_{rise}}\right)(u^2 - ua^m) + \left(\frac{1}{\tau_{fall}}\right)(u - a^m); u = u(t);\ a^m = a^m(t) \quad (3.3)$$

where: a^m and $\dot{a}^m$ are the muscular activation and the rate of muscular activation, respectively; u is the muscle excitation; τ_{rise} and τ_{fall} are the time constants for rise and fall, respectively.

3.3.5 - Neuromuscular control model

Having a musculoskeletal model built, it is necessary to define the control of the muscle excitation, so that realistic movements are produced [38]. There are admitted two basic approaches to do this: a dynamic optimization and a tracking solution problem [33, 35, 38].
Using dynamic optimization, it is necessary to define clearly an objective task/function in order to find the muscle controls that permit to achieve that objective [33, 38]. In the sports field, this method could be applied in studies where the objective task was, for example, the maximum height jumping [42], maximum speed pedaling [43] and maximum distance throwing [44].
In walking, Anderson and Pandy assumed that the objective function is the minimization of the metabolic energy consumed per distance unit, and the results of their study showed that the muscle function can be well described by assuming this objective function [45]. However, when we are dealing with the human gait, the objective task can be ambiguous in some cases [35].
An alternative method consists in solving the optimal tracking problem, by guiding the muscular controls in order to obtain the minimal difference between the simulation data and the

experimental data, by means of a least-squares approach [33, 38]. This solution is considered to be the suitable in simulations concerning subject-specific gait and pathological gait and to quantify the muscle contributions, identify joint loading and injuries [33, 38].

3.3.6 - Assessment of the muscle forces

The determination of muscle forces and the understanding of how a muscle affects the movement of the joints, and the segments can be done by using a musculoskeletal model as described in Figure 3.5, applying a forward or inverse dynamics strategy [35, 38].

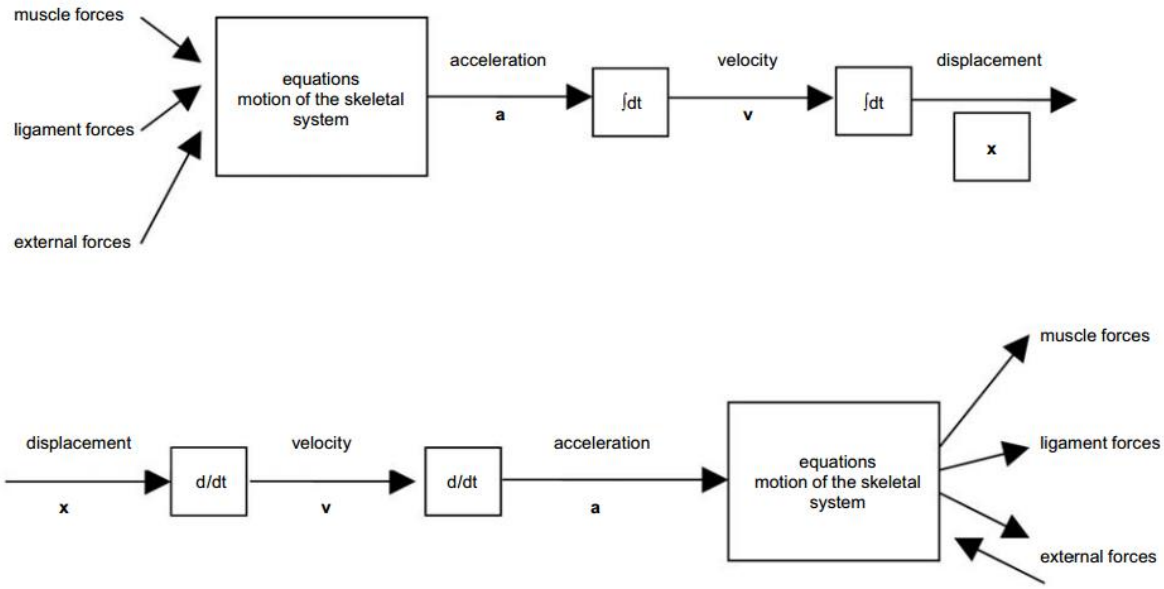

Figure 3.5. Diagram of the forward dynamics (top) and the inverse dynamics (bottom) methods [46].

Inverse dynamics (Figure 3.5) uses as input the body motions, which are differentiated and used to compute the muscle forces, by using the ground reaction forces and the joint moments in the classical Newton-Euler equations of motion [47]:

$$\vec{F} = m\vec{a} \tag{3.4}$$

$$\vec{M} = I\vec{\alpha} \tag{3.5}$$

where $\vec{F}$ is the force; $\vec{a}$ is the acceleration; $\vec{M}$ is the moment and is the angular acceleration.

The other approach is forward dynamics, in which the inputs of the system are the muscle excitations and when applied in the muscle-tendon model (taking into account the coupling

excitation-activation) it is possible to obtain the muscle forces (Figure 3.5). Using these forces and the other elements (musculoskeletal model and skeletal dynamics) it is possible to obtain the movements generated by the input excitations [35].

The number of muscles acting in one joint is greater than its number of DOF, consequently an optimization strategy is usually used when considering these two approaches. Using inverse dynamics, the muscle forces are determined using static optimization, which solves a different optimization problem at each instant of the movement, to determine the muscle forces from the joint kinematics. On the other hand, in the case of forward dynamics, if a goal or motor task is defined, it is possible to use dynamic optimization, in which a single optimization problem is solved for the complete cycle of the movement, being this approach more expensive computationally [35]. Therefore, dynamic optimization is used, for example, in studies related to sport performance, in which the objective or task desired is defined and the muscle activations are known [35].

3.4 - Summary

Experimental gait analysis techniques give useful information about the quantifiable characteristics of gait, but the use of this data in computational simulations is showing good results in assessing quantities not measurable experimentally. These simulations use mathematical/mechanical models, described by complex equations, which need to be treated and analyzed using computers.

Chapter 4

Methodology

4.1 - Introduction

Biomechanical laboratories around the world use different 3-D motion capture systems and software to collect their data, making more complicated sharing the data between users due to problems of software compatibility [48]. The situation has changed with the introduction of the *.c3d file format, that began in 1987 and since then it has been gradually adopted by the community, becoming a standard. *.c3d is a public domain type of binary file format to record and store synchronized 3D, analog and EMG raw data, processed data (for example gait events) and general information about the trial (instrumentation and software used and characteristics of the subject) [48].

Computational simulations are useful to study human motion, which involves complex mechanisms of control and actuation and frequently start from experimental data. OpenSim is a relatively new software that can be used to perform this type of simulations since it permits the understanding of how muscle actuates to reproduce a specific movement [39, 49, 50]. Thanks to its versatility (it allows to create and change the models and add components), has been used not only to study healthy movements of the human body, but as well pathological motion [51, 52]. Typically, a simulation starts from choosing a model and the data, conveniently treated and stored in the appropriate file format, serves as input. An OpenSim simulation consists in a sequence of steps, where the outputs from the previous step are used as inputs in the following, making necessary to reduce the errors as possible to avoid its accumulation.

OpenSim requires, however, that the experimental data used as input to be in a specific format: for the kinematic data uses the format *.trc (Track Row Column), created by Motion Analysis Corporation and for the kinetic data the format *.mot (Motion), created by the developers of SIMM (Software for Interactive Musculoskeletal Modelling) [50]. If the experimental data is stored in a *.c3d file, is possible to extract it using, for example, the Biomechanical Toolkit

(BTK), which is an open-source and cross-platform library of functions to read, write and modify acquisition files. These operations can be performed in Matlab, by using the Matlab wrapper [53] and writing the files in the adequate format to use as input.
The experimental data relative to a post-stroke individual was collected in the LABIOMEP and saved in *.c3d format. Matlab was used to extract and process the data and to extract the gait events, necessary to obtain one gait cycle to perform the biomechanical simulation that will be described in the Chapter 4.
In the second part of this chapter, it will be described the each step of the workflow of biomechanical simulation using OpenSim. A model of the head, torso and lower limbs was used to reproduce the data recorded from a post-stroke patient and a healthy individual. The kinematics and joint moments were determined, as well as the muscular activations and powers.

4.2 - Experimental data treatment and analysis

4.2.1 - Kinematic and kinetic data

The kinematic and kinetic data relative to a post-stroke subject was previously collected in the LABIOMEP, performing a gait trail with a male subject of 55 years old, 1,75 m height and 96Kg. The patient has suffered a CVA and he was mainly affected in the upper limbs. Consequently, the lower limb performance in gait was not substantially impaired. The patient pathology historical was not detailed known, the only information available was that his treatment included the application of botulin toxin only in the upper limbs.
The kinematic data was acquired using a motion capture system 3D Qualisys™ Oqus Camera Series system, operating at 200 Hz with 12 cameras retroreflectors of infrared light and 32 reflector (passive) body markers. The marker data was acquired using the native software, Qualisys Track Manager. The configuration of the markers of the torso and lower limbs is shown in the Figure 4.1.

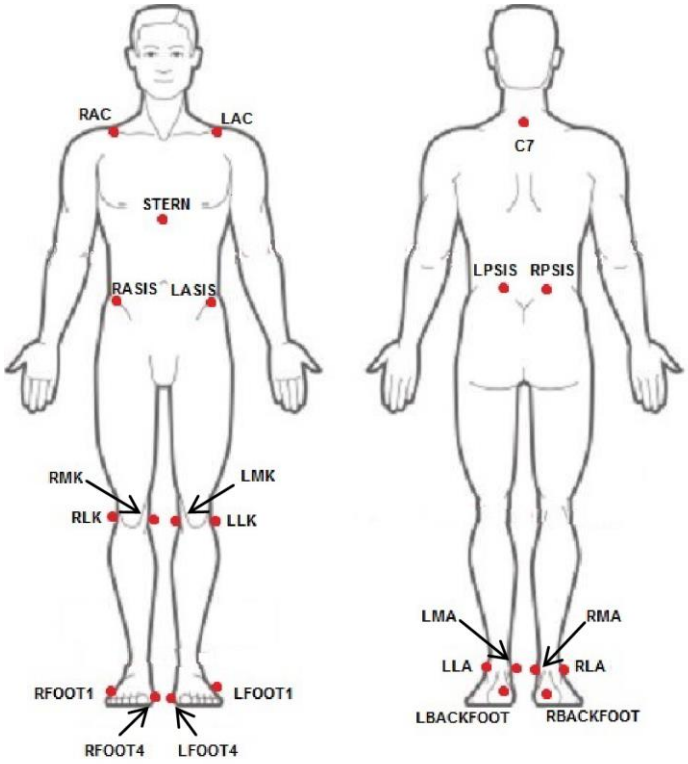

Figure 4.1. Location of the markers used in the gait trial performed in the LABIOMEP in a post-stroke patient: RAC – right acromion; LAC – left acromion; C7 – vertebra C7; STERN – sternum; RASIS – right superior iliac spine; LASIS – left superior iliac spine; RPSIS – right posterior superior iliac spine; LPSIS – left posterior iliac spine; RMK – right medial knee; LMK – left medial knee; RLK – right lateral knee; LLK – left lateral knee; RMA – right medial ankle; LMA – left lateral ankle; RLA – right lateral ankle; LLA – left medial ankle; RFOOT1 – right foot proximal phalange 5; LFOOT1 – left foot proximal phalange 5; RFOOT4 – right foot proximal phalange 5; LFOOT4 – left foot proximal phalange 5; RBACKFOOT – right back foot; LBACKFOOT – left back foot. (Only the markers of the torso and lower limbs, used in this study, are represented. The 10 markers used in the lower limbs are not shown).

During the trial, the subject walked over a set of six force platforms disposed as shown in the Figure 4.2, allowing the temporal synchronization between the kinematic and kinetic data. The platforms 1, 2 and 6 (Bertec FP4060) and 3, 4 (Bertec FP6090) were type 2 extensiometric. The platform 5 was piezoelectric, type 3 (Kistler 9281E). The subject stepped in the platforms 2, 3, 4 and 6 and the data was collected with a sampling frequency of 2000 Hz.

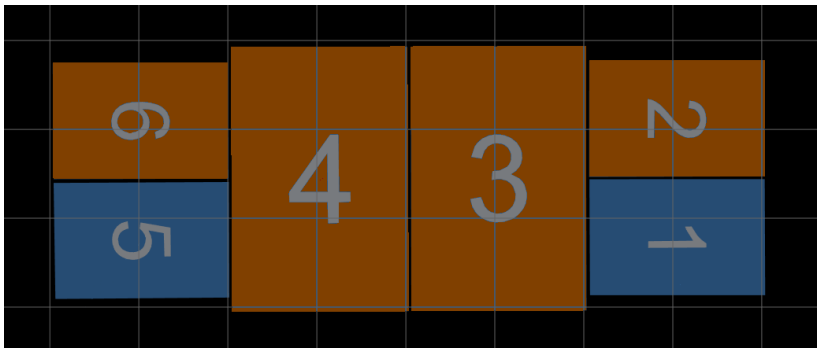

Figure 4.2. Force platform disposition in the floor during the gait trial in the LABIOMEP. The force platforms in which the subject stepped are shown in orange (2, 3, 4 and 6). Image obtained using the software Mokka.

4.2.2 - Data extracting and pre-processing

The data resulting from the trial described above was stored in *.c3d format and, posteriorly, it was extracted and processed using Matlab ®.

There are already available functions developed by the OpenSim community, developed for this purpose [54]. In this work, the toolbox "**c3d2OpenSim**" developed by James Dunne in 2015 was used and adapted to the data. This toolbox uses as basis the functions of the Biomechanical ToolKit (BTK).

In the Figure 0.3 is shown the sequence of actions performed prepare to use as input in OpenSim.

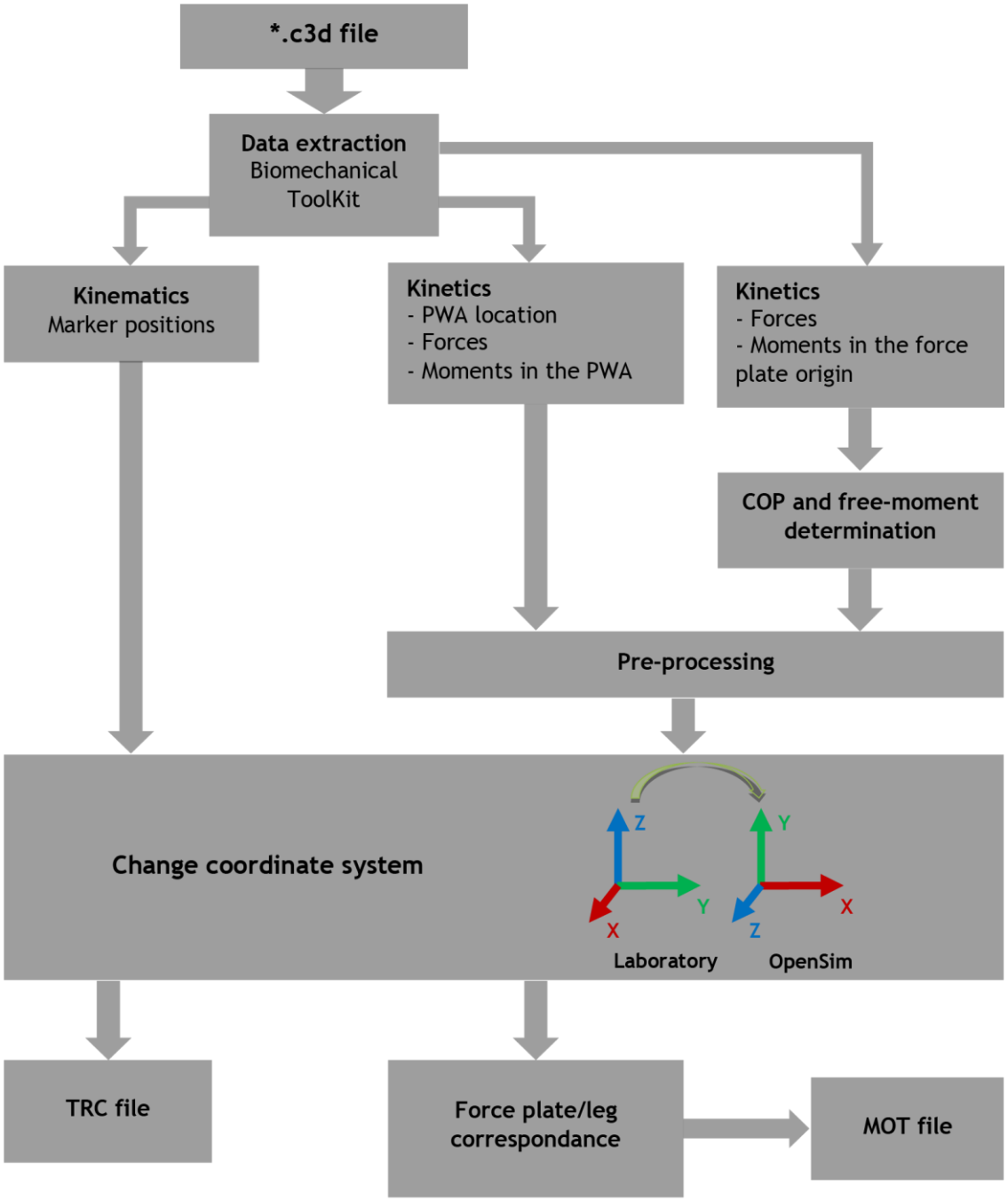

Figure 4.3. Sequence of steps taken to obtain the OpenSim input files containing the kinematic and kinetic data (*.trc and *.mot files, respectively) relative to the post-stroke individual.

The information contained in the *.c3d file was extracted and stored inside a Matlab *struct* using a sequence of functions from the BTK. The function *btkGetMarkers* extracts the positions of the makers, defined in the laboratory coordinate system. Then, this values were converted to the OpenSim coordinate system and finally, a *.trc file was printed with this information. Regarding the force platform data, there are two methods for extracting the data: the function

btkGetForcePlatformWrenches extracts the values of the forces, the location of the origin of the force platform and the moments acting on it, while the function btkGetGroundReactionWrenches extracts the forces, the PWA (Point of Wrench Application) location and the moments on the PWA. In gait analysis, even in pathological gait analysis is commonly used the COP, defined as the point where the vertical component of the force intersects the surface and where the moments in the horizontal plane are zero [55]. The PWA is considered the point where the wrench vector intersects the surface of contact between the foot and the ground (Figure 4.4) [55]. The two methods were used, however, when using *btkGetForcePlatformWrenches* it was necessary to determine the location of the COP and, additionally, to compute the free moment (the vertical moment) acting on it, as described in the equations 4.3 and 4.6, respectively. The values of the COP and PWA and the moments defined in the respective points were assumed as zero for the instants were the vertical force was zero.

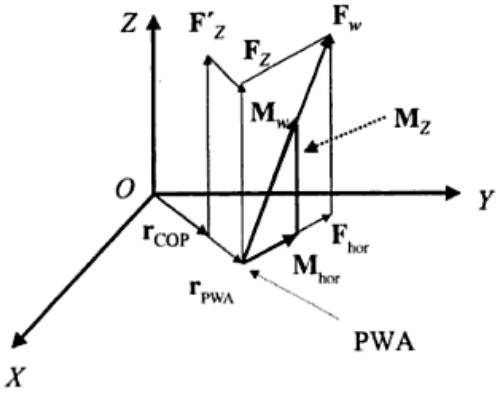

Figure 4. 4. Difference between the COP and the PWA. $\boldsymbol{F_W}$ and $\boldsymbol{M_W}$ represent the resultant force and moment of the wrench; $\boldsymbol{F_Z}$ and $\boldsymbol{M_Z}$ are the vertical components of the resultant force and moment and $\boldsymbol{F_{hor}}$ and $\boldsymbol{M_{hor}}$ are the corresponding the horizontal components. $\boldsymbol{r_{COP}}$ and $\boldsymbol{r_{PWA}}$ represent the position vector of the COP and the PWA [55].

The horizontal moment in the origin $\vec{M}_{hor}^{0}$ is caused by the vertical force acting in the COP $\overrightarrow{F_Z}$[55]:

$$\vec{M}_{hor}^{0} = \vec{M}_{hor}^{COP} + (\vec{r}_{COP} - \vec{r}_0) \times \overrightarrow{F_Z} \tag{4.1}$$

$$\begin{bmatrix} M_x^0 \\ M_y^0 \\ 0 \end{bmatrix} = \begin{bmatrix} 0 \\ 0 \\ 0 \end{bmatrix} + \begin{bmatrix} r_x^{COP} - r_x^0 \\ r_y^{COP} - r_y^0 \\ r_z^{COP} - r_z^0 \end{bmatrix} \times \begin{bmatrix} 0 \\ 0 \\ F_z \end{bmatrix} \tag{4.2}$$

$$\begin{cases} r_x^{COP} = \frac{-M_y^0 + r_x^0 F_z}{F_z} \\ r_y^{COP} = \frac{M_x^0 + r_y^0 F_z}{F_z} \end{cases} \tag{4.3}$$

Having the forces and the three dimensional location of the COP it is possible to determine the free-moment (T_z), knowing that $T_z = M_z^{COP}$:

$$\vec{M}^0 = \vec{M}^{COP} + (\vec{r}_{COP} - \vec{r}_0) \times \vec{F} \tag{4.4}$$

$$\begin{bmatrix} M_x^0 \\ M_y^0 \\ M_z^0 \end{bmatrix} = \begin{bmatrix} 0 \\ 0 \\ M_z^{COP} \end{bmatrix} + \begin{bmatrix} r_x^{COP} - r_x^0 \\ r_y^{COP} - r_y^0 \\ r_z^{COP} - r_z^0 \end{bmatrix} \times \begin{bmatrix} F_x \\ F_y \\ F_z \end{bmatrix} \tag{4.5}$$

$$M_z^{COP} = M_z^0 - (r_x^{COP} - r_x^0)F_y + \left(r_y^{COP} - r_y^0\right)F_x \tag{4.6}$$

The force and moment data was low-pass filtered using a fourth-order Butterworth filter with zero-lag. The cut-off frequency was 8Hz, similarly to the study [14]. A higher cut-off frequency of 20Hz, used in other works [22, 56] was tested and a lower value of 6 Hz as well. It was verified that using high frequencies (20Hz), the moment data shows noise and high peaks at the end of the beginning of the stance phase, while using the low frequency (6Hz) some features of the signal are changed (see annex 2). The data relative to the location of the COP and PWA showed high peaks in the beginning and end of the contact phase that were eliminated using a median filter followed by a low pass-filter (4th Butterworth zero-lag with cut-off frequency of 20Hz).

After this, the data was defined in the OpenSim coordinate system and it was made the correspondence between the force platform data to the foot stepping in it. Only the data of force platforms 2, 3 and 4 were used, since the subject did not step into force platforms 1 and 5 and the data from 6 was not consistent. Finally the information was exported into to a *.mot file.

The *.c3d file of the trial did not include the location in time of the events necessary to divide the gait cycle, so, it was created a Matlab routine cable of making that division by identify the basic phases of the cycle: single and double contact phases, and initial contact and toe-off for each leg. The contact frames/time for the right and left leg were considered the ones where the vertical ground reaction force (*Fy*) was higher than 1% of the subject's body weight and the double contact as the intersection of the two cases. However, since for the right leg it was only available the force data corresponding to one stance phase, to extract one complete gait cycle, it was necessary to determine the first left toe-off. The procedure to determine the point of the first left toe-off consisted in obtaining the value of the vertical force component of the right leg (Right *Fy*) while the second left toe-off was happening. Then it was searched one frame where the Right *Fy* took a similar value, located during the first right leg stance

phase, before the first *Fy* peak, as described in the Figure 0.5.This frame was assumed as the left toe-off.

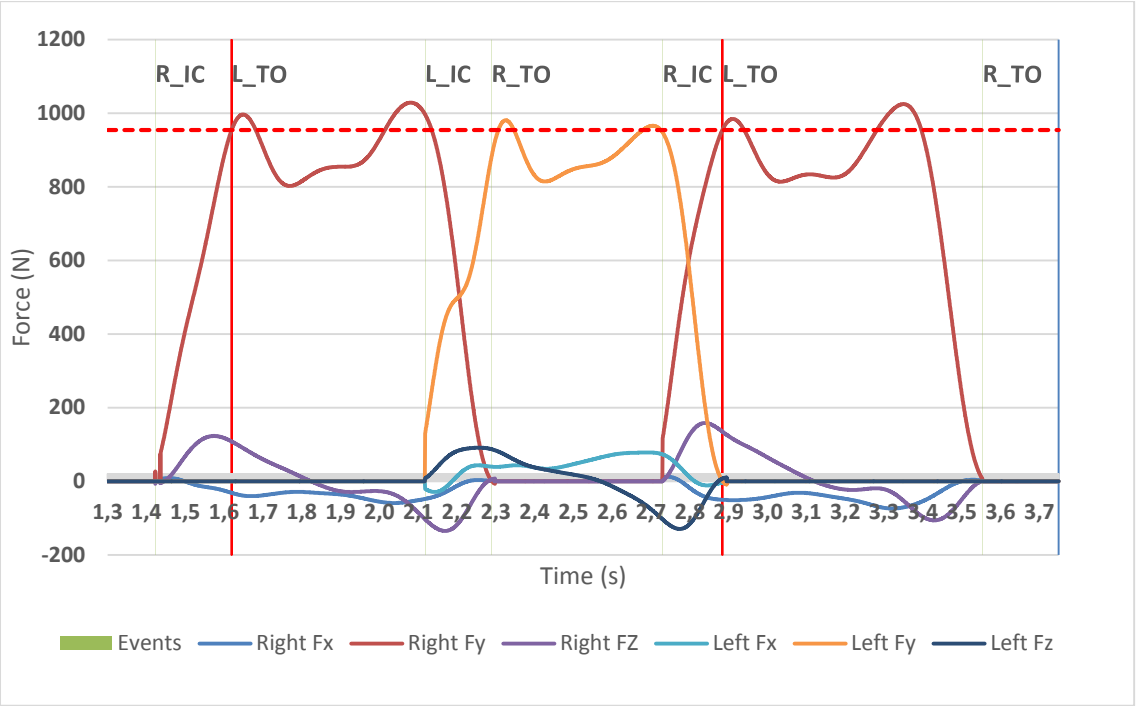

Figure 4.5. Plot of the three components of the GRF acting in the right and left leg of the post-stroke individual. It was calculated the value of right Fy during the second left toe-off in the second right stance phase and it was used to determine the occurrence of the first left toe-off, by locating a close value in right Fy, during the first right leg stance phase. R_IC and L_IC are the events for right and left initial contact; and R_TO and L_TO are the events for right and left toe-off.

The final gait cycle was then obtained and it is shown in the Figure 4.6. It consists in a sequence of a complete swing and stance phases for the left leg, while for the right leg the stance phase is divided.

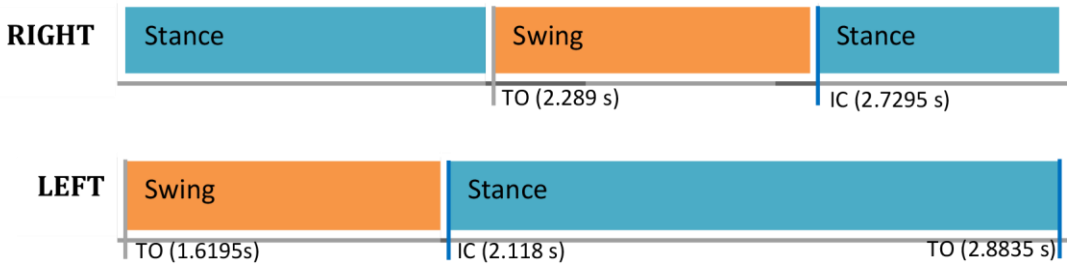

Figure 4.6. Gait cycle of the post-stroke individual, starting with the toe-off of the left leg (1,6195 s) and ending with the consecutive toe-off of the same leg, at 2,8835 s.

4.3 - Computational Simulation

4.3.1 - Software: OpenSim

OpenSim is an open-source software system developed by NCSRR (National Center for Simulation in Rehabilitation Research), Stanford University, USA, that allows modeling, simulating and analysing the neuromusculoskeletal system [49]. The first version of OpenSim was released in 2007 and in 2014 OpenSim 3.2, the 15th version was available [50].

OpenSim was developed aiming to encourage the sharing of the advances in dynamic simulations, since it is free, the source code is obtainable and the users can create models and share them online with the other members of the community. As a result, there is available online a library of musculoskeletal models of the whole bone or isolated parts and analysis, which the users can obtain, adapt and improve [57].

The capabilities of this software include [39]:

- Scaling of the models to match with subject specific anthropometry;
- Inverse kinematics, to associate the experimental maker positions to the correspondent in the model;
- Inverse dynamics, to define the forces resultant from known accelerations;
- Static optimization and computed muscle control, to determine the individual muscle force from net generalized forces;
- Forward dynamics, to calculate the trajectories resultant from the input controls and external forces;

OpenSim models include bones (rigid bodies); joints (mobilizers, constrains and forces), contact elements (rigid constrains and compliant forces), ligaments and muscles (modeled as Hill-type actuators) and control algorithms [39, 57].

Using OpenSim, two independent simulations were performed, as described below:

Study 1) Healthy gait: kinematic and kinetic data available in the online OpenSim community [57]. The experimental data was collected as part of the study [58] and corresponds to a healthy subject with 72,6 Kg. This trial was performed at self-selected velocity;

Study 2) Pathological gait: kinematic and kinetic data from the gait evaluation performed in the LABIOMEP with a post-stroke subject (96 Kg body mass), affected in the left side of the body. The trial was also performed at self-selected velocity.

The design of each study followed the typical OpenSim workflow, as described in the Figure 4.7. The first step consisted in choosing a model, adapting it to the dimensions and weight of the subject, by scaling with the Scale Tool, then determine the joint angles, using the Inverse Kinematics Tool, following by the process of reducing the residual forces (RRA Tool) and finally, computing the muscle forces, excitations and activations (CMC Tool). Each step will be described in the following points.

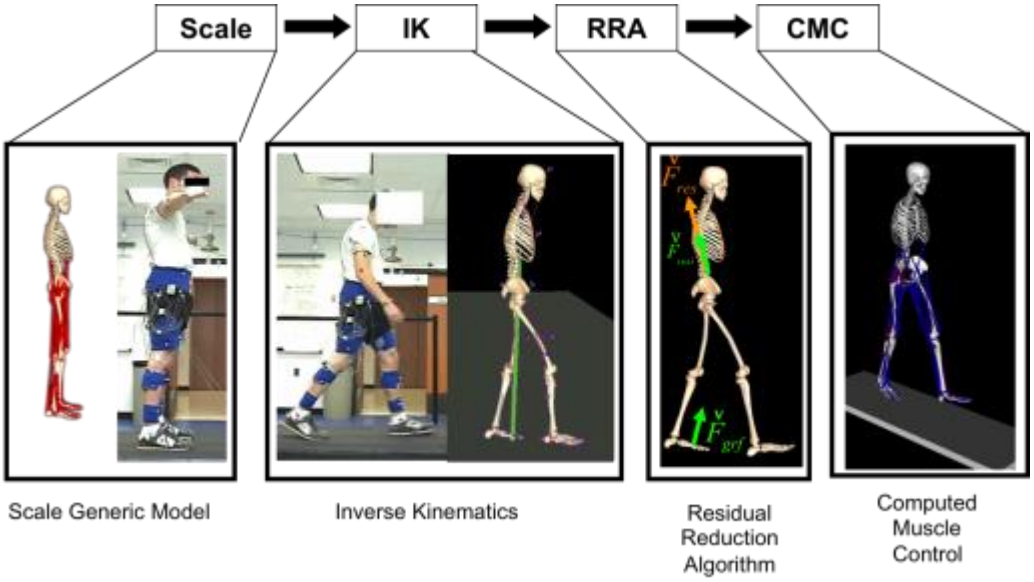

Figure 4.7. OpenSim workflow [50].

4.3.2 - Musculoskeletal model

The OpenSim musculoskeletal model "Gait2392", downloadable in the library of models available online [57], was used in both simulations. This model is composed by the head, torso and lower limbs, having 92 musculotendon actuators and 23-degrees-of-freedom (DOFs) (Figure 4.8). The DOFs included in the model consist in: pelvis position (3 DOFs), pelvis orientation (3 degrees of DOFs), lumbar joint (3 DOFs), and for each leg, hip flexion–extension, abduction–adduction, and internal–external rotation, knee flexion–extension, ankle plantarflexion–dorsiflexion, inversion-eversion and toes flexion-extension [50].

Figure 4. 8. Model "Gait2392" used in the simulations.

4.3.3 - Scaling of the model

With the purpose of making the model match the subject's anthropometry and weight, the model was scaled using the OpenSim Scaling Tool.

The scaling tool allows to change manually the dimensions of each body. However, the scaling based in the measurements was used. Using this option, the distance (*m1*) between each pair of virtual markers (the markers placed in the model Gait_2392) and the corresponding marker pair used in the experimental trial (*e1)* is calculated. Considering this two distances, it is determined a scale factor (*s1* = *e1*/*m1*) which is used to change the dimensions of the body associated with the markers pair.

Regarding the **Study 2**, in which the data collected in the LABIOMEP was used, the marker configuration used was different from the default used in OpenSim. Hence, some model markers were excluded and others were created or had their designation changed, using the *Marker Editor*. The marker lists of the Study 2 and Study 1 is shown in the annex 1.

With the aim of calculating the distance between the pairs, the Scale Tool usually uses a static trial, in which the marker data is recorded while the subject stands still in a neutral position for a few seconds. Since the experimental data for the **Study 2** did not include a static trial, the dynamic trial was used and it was only considered a time instant of the trial (4,5 s), which corresponds to a double support phase. This position was chosen because is the one most similar to the neutral position, during the gait cycle.

It was necessary to associate to each body one or more maker pair, so that the corresponding scale factor was applied to that body. In the case of using more than one marker pair, the scale factor is computed as the average between the factors computed for each one. In the Figure 4.9 it is shown the *Marker Set* of the *Scaling Tool* for the **Study 2**, showing each body and the corresponding marker pairs associated.

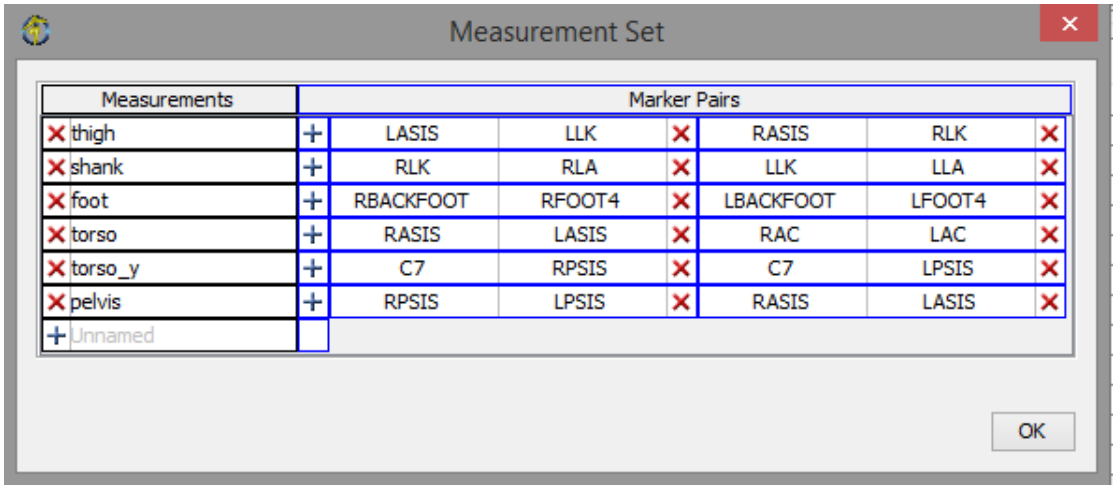

Figure 4.9. Display of the Measurement Set of the Scaling Tool (Study 2). At the left is presented a list of the measurements, associated with the scale factors are computed using the marker pairs shown at the right.

The torso and the pelvis are recommended to be scaled non-uniformly [50], this is, with different scale factors in the three directions. For that reason, *x* and *z* direction of the torso was associated with the marker pairs RAC/LAC and RASIS/LASIS and for the *y* direction (vertical) with C7/RPSIS and C7/LPSIS (Figure 4.10). Although the markers chosen to scale the vertical direction are not aligned in the vertical direction, they are better indicators of the torso's vertical length. A sacral marker would be more suitable for this purpose.

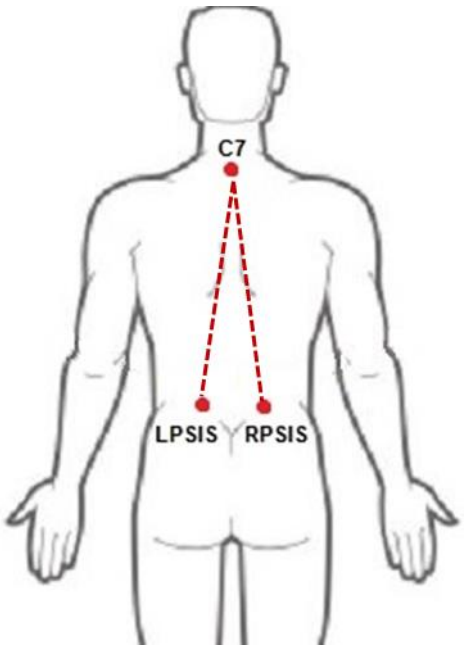

Figure 4.10. Markers used to calculate the vertical scale factor of the torso. The dashed line represents the distances between the pairs C7/LPSIS and C7/RPSIS.

Concerning the weight, the Scaling Tool offers has two possible approaches: preserve the total mass of the subject of the experiment, maintaining the relative masses of the bodies in the model, or scaling each segment mass taking into account only the scale factors computed before. In the last approach the total mass might not match the subject's real mass. The first alternative was chosen, since mass modifications could lead to errors in the next steps, when the ground reaction forces measured are considered. It important to note that the Scaling tool adapts the mass distribution (inertia matrix) of each body, when changing its mass and dimensions and, using his option, the scale factors computed using the measurement set (Figure 4.9) are not used for the mass scaling [50].

It is also necessary to weight each marker relatively to the others. Larger weights mean that the marker is tracked more tightly and the tracking errors are more penalized. For this reason the markers representing bone landmarks and functional joint centres should have larger weights [50], which is the case of the markers at the hip, knee and ankle joint .The coordinates representing the subtalar and metatarsophalangeal joints were locked in the neutral position (angle set to zero) and weighted heavily, so that they remain in that position during the simulations. In the OpenSim guide this step is recommended [50] and the reason why this recommended is because the model does not possess enough muscles to control these joints.

In the case of the **Study 1**, there was no need to change the default marker configuration of the OpenSim. It was used a static trial file for scaling and the *Measurement Set* was already

defined in a file that came with the data. The weighting process was done by attributing larger weights the markers located in functional joint centres and bone landmarks, similarly to the Study 2. The relative weights used in both studies can be found in annex.

After defining the parameters described above in both studies, the position of the experimental markers was manually adjusted to match the virtual markers, making several iterations until the RMS and the maximum error were minimized.

4.3.4 - Inverse kinematic (IK)

The Inverse Kinematics Tool allows to determine the joint angles and translations that best reproduce the experimental position of the markers. For each frame, it is solved a least-squares problem, in order to minimize the weighted error for each coordinate [49]:

$$Squared\ Error = \sum_{i=1}^{markers} w_i \left(\vec{x}_i^{subject} - \vec{x}_i^{model}\right)^2 + \sum_{j=1}^{joint\ angle} w_j \left(\vec{\theta}_j^{subject} - \vec{\theta}_j^{model}\right)^2 \qquad (4.6)$$

Where $\vec{x}_i^{subject}$ and $\vec{x}_i^{model}$ are the three-dimensional positions of the i^{th} marker, for the subject and the model; $\vec{\theta}_j^{subject}$ and $\vec{\theta}_j^{model}$ are the angles of the j^{th} joint, for the subject and the model; and w_i and w_j are the corresponding weights of the markers and the joints.
This tool uses as input the makers positions stored in the *.trc file. The weighting of the markers was done by attributing larger weights to markers less susceptible to movements due to skin and soft tissue during gait [50]. The weights used in both simulations can be consulted in the annex 3.

4.3.5 - Inverse dynamics (ID)

The Inverse Dynamics Tool calculates the joint moments necessary to make the model perform the desired kinematics, according to the basic equations of motion (Equations 3.4 and 3.5). Although, the following steps are not dependent on the ID results, this step was done to analyse the joint moments and the forces acting in the pelvis, before the reduction of the residuals.
The output *.mot file of the Inverse Kinematics step was used as input, as well as the *.mot file containing the ground reaction forces, moments and the PWA/COP. The Inverse Dynamics Tool allows the possibility to consider the interaction with the ground as a *body force*, which acts in the centre of mass of a body or as a *point force* that acts in the PWA/COP and produces a torque. The second option was used in both simulations. During this and the following steps, the subtalar and the metatarsophalangeal joint were locked in the *Coordinates Editor*, so that the model was consistent with the kinematics obtained through the Inverse Kinematics step

4.3.6 - Residual reduction algorithm (RRA)

With the purpose of reducing the residual forces and moments acting in the model, which are assumed to solve the dynamic inconsistency between the experimental data and the model, the Residual Reduction Algorithm Tool was used. The residual forces are determined as described in the Equation 4.7, and the errors associated are obtained by the Equation 4.8.

$$\vec{F}_{external} = \sum_{i=1}^{segments} m_i \vec{a}_i - \vec{F}_{residual} \quad (4.7)$$

Where $\vec{F}_{external}$ is the external force acting on the model; m_i and $\vec{a}_i$ are the masse and acceleration of the i^{th} segment and $\vec{F}_{residual}$ is the residual force.

$$Squared\ Error = \sum_{j=1}^{joints} \Omega_i \left(\ddot{q}_j^{desired} - \ddot{q}_j^{model}\right)^2 \quad (4.8)$$

Where $\ddot{q}_j^{desired}$ and $\ddot{q}_j^{model}$ are, respectively, the desired and the effective acceleration of the j^{th} joint and Ω_i is the weight associated to that joint.

This algorithm replaces the muscles of the model by ideal actuators acting in each coordinate, and each one has an optimal force and an excitation control associated. The force produced by the ideal actuator is then given by the Equation 4.9.

$$Force_{ideal\ actuator} = Optimal\ Force \times Excitation \quad (4.9)$$

The tool uses as inputs the files containing the kinematics and the ground reaction forces and two XML files:

- Actuators file, where are described the ideal actuators and their properties: optimal force, point of application (for point actuators), bodies (in the case of torque actuators) and the minimum and maximum excitation;
- Tasks file, which specifies the relative weight attributed to each joint.

Initially it was done an initial pass to verify if the model was strong enough to reproduce the kinematics. Actuators that require lower controls to generate force are less expensive for the algorithm and, consequently, it relies in these actuators. Thus, in the initial pass, high optimal forces were attributed to residual point actuators (*Fx, Fy* and *Fz*) and to residual torque actuators (*Mx, My* and *Mz*) and the weights were the same to each actuator. The results were analysed and the optimal forces of residual actuators were decreased to force the algorithm to use the coordinate actuators (joint actuators) instead of the residual ones. For each iteration

the error associated to each coordinate was verified and the weights of the coordinates with high error were increased to improve their tracking. This was done until an optimal solution was found, in which the RMS and the maximum values of the residuals and the errors were considered acceptable, according to [50]. It is important to refer that, since the subtalar and the metatarsophalangeal joints were kept locked, there were not include in the tasks file, because they were not tracked. And the actuators acting in these joints were removed.
At the end of the process, OpenSim automatically adjusts the COM (Centre of Mass) of the torso and suggests mass adjustments to each one of the bodies, in order to reduce the residual forces, which were applied to the model before the next step.

4.3.7 - Computed muscle control (CMC)

Computed Muscle Control Tool was used to determine how the muscles of the model actuates to produce the movement. This algorithm uses a combination of a proportional-derivative (PD) control and static optimization, as shown in the scheme of the Figure 4.11.

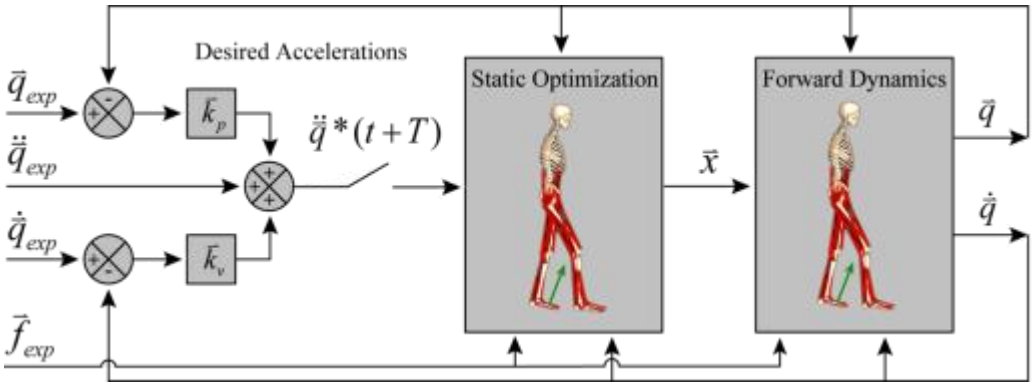

Figure 4. 11. Scheme of the CMC algorithm used in gait [59].

Static optimization distributes the load to the muscles, which are synergistic actuators, for each time instant. This process uses a performance criterion that is intended to be minimized, with two possible formulations: slow and fast target (Equation 4.10). The fast target approach, generally recommended by producing better tracking [50], was used in both simulations.

$$J = \sum_{i=1}^{nx} x_i^2 \, ; C_j = \ddot{q}_j^* - \ddot{q}_j \forall j \tag{4.10}$$

Where J is the performance criterion; x_i is the excitation of the i[th] actuator; $\ddot{q}_j^*$ and $\ddot{q}_j$ are the desired and the obtained accelerations of the j[th] joint; and C_j is the equality constraint (C=0), that requires the difference between the desired and obtained acceleration to be within the tolerance value, in this case was used 0,00001.

The file inputs of CMC are:

- *.mot file describing the kinematics, obtained with the RRA;
- *.mot file with ground reaction forces (the same used in ID);
- *.xml files containing:
    - model actuators: muscles, the reserve and residual actuators and their properties. The reserve actuators are ideal actuators that
    - control constraints, where are specified the maximum and minimum excitation for the actuators described in the model actuators file;
    - tasks which contains the relative weights for each coordinate, similarly to the tasks file from RRA.

Similarly to the RRA step, it was made an initial pass with large optimal forces for residual and reserve actuators and the same weights for each coordinate. In the following iterations the optimal forces for reserves and residuals were reduced and the controls constrains increased, so that the controller choose to rely on muscles instead of residual and reserve forces. The iterations were stopped when the residuals, reserves and errors associated were reduced enough to acceptable values.

4.4 - Summary

The data from a gait trial performed with post-stroke individual was extracted from a *.c3d file and processed using the BTK in Matlab and a *.trc and a *.mot file were obtained. The first one stores the marker trajectory data (kinematic) and the second one stores the ground reaction force data (kinetic). These two files were used as inputs in the OpenSim simulation described in the next chapter.

Two gait simulations were performed using OpenSim, one with a subject considered healthy and the other with a post-stroke individual. From the correspondent experimental data, it was determined the joint angles and torques, using inverse kinematics and inverse dynamics, respectively, the residual forces and moments acting in the model were reduced (through RRA) and finally, the muscular behaviour was determined using CMC.

Chapter 5

Results and discussion

5.1 - Introduction

In this chapter the results are presented and discussed. In the first part, the results from the extraction from a *.c3d file and the processing of the experimental data used in the **Study 2** are presented. Secondly, the results obtained in each step of the workflow of the OpenSim are shown and analysed. In the case of the **Study 1**, since it consists in a simulation of a healthy individual, the values of the joint angles and moments and the muscle activations and powers were compared with the available reference values in the literature. For the **Study 2**, these parameters were also compared with the literature about post-stroke gait.
In both cases, an analysis of the muscular activation and powers of the principal plantarflexor muscles (soleus and medial gastrocnemius), the main dorsiflexor (tibialis anterior) and one hamstring (semimembranosus) was done and analysed together with the results of the kinematics.

5.2 -Experimental data

The data representing the 3D position of the markers was not subjected to processing, since it was not corrupted with noise. The software used in the data collection (Qualisys Track Manager) includes post-processing of the marker data, eliminating the need of filtering to remove the noise [60]. Using the software MLSViewer, a Motion Lab Systems Software © to display the

contents stored in a *.c3d file [61], it is possible to visualize the recorded trajectory of the markers. In the **Figure 5.1** it is shown the trajectory of the marker placed in the heel of left foot (LBACKFOOT) in the three directions (x, y and z of the laboratory coordinate system), using MLSViewer, where is possible to see that the data is clean. Besides, this data was automatically filtered in OpenSim when using the IK, ID and RRA Tools, as recommended in the OpenSim guide [50].

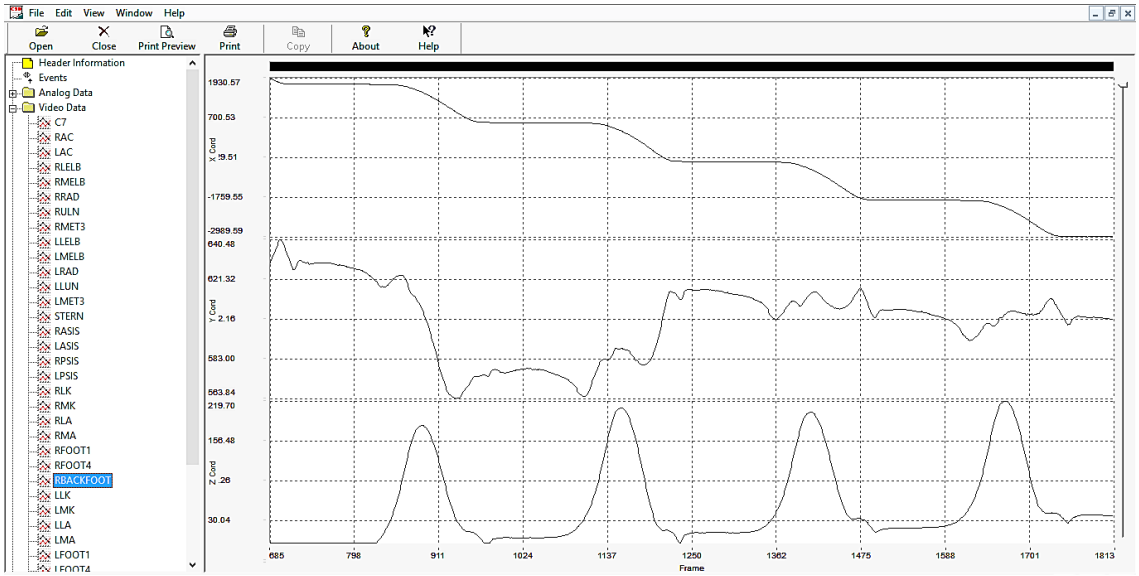

Figure 5.1. Visualization of the position, in the three directions x, y and z (laboratory coordinate system) of the marker RBACKFOOT of the post-stroke individual, in MLSViewer.

The force platforms used in the experimental trial and considered in this study were of type 2, meaning that each one has six output channels for analog data of the three components of the force and of the moments acting in the origin of the force platform [48]. This data was stored in a *.c3d, which contained also the scale factors and the calibration matrixes necessary to convert the raw data (electric output) into force data. This operation has been done by using the BTK, which has two distinct functions, both used in this work. Since the code of the functions is not available, it is not possible to analyse the each step of the operations performed. The output of the function *btkGetForcePlatformWrenches* is the value of the forces and moments in the origin of the force platform, consequently this function only needs to transform the electrical signal of the force plate, using the scale and calibration information, into force and moment data. On the other hand, according to the informative webpage of the BTK [62], the function *btkGetGroundReactionWrenches*, which gives the forces, location of the PWA and the moments defined in that point, in addition to this transformation, determines the PWA and the moments on it, by using the formula developed by Shimba [63] which also was described in Zatsiorsky [55].

Regarding the location of the COP and the PWA, all three components of the position did not show considerable differences, suggesting that the distance between this two points is not relevant.

It was verified that the values of the forces obtained with the two functions were the same, as expected. The vertical moments showed small dissimilarities which mean once more that the location of the PWA and the COP is very small. In fact, these difference of positions is explained by the horizontal moments about the PWA that, in this case, are very small (Figure 5.2).

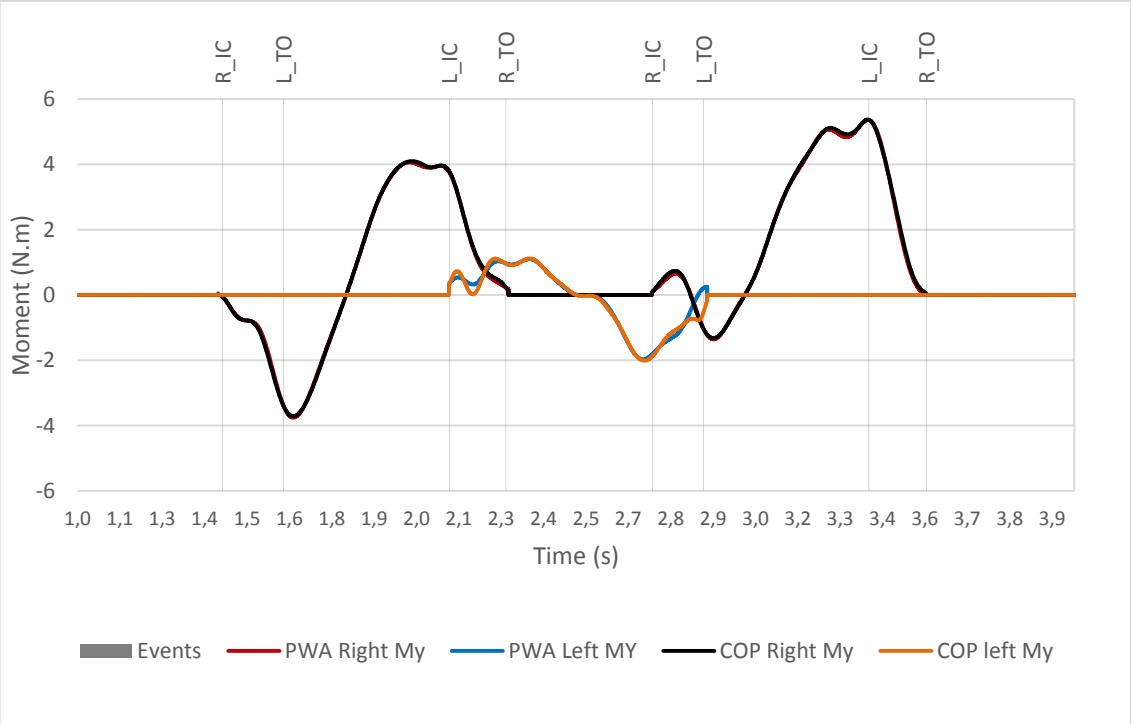

Figure 5.2. Ground reaction moment in the vertical direction (My, considering the OpenSim coordinate system) in the PWA, obtained using the function *btkGetGroundReactionWrenches* (PWA Right My and PWA Left My) and the free-moment acting in the COP, for the right and left legs of the post-stroke individual.

Regarding the horizontal moments in the PWA (Figure 5.3), it were verified abnormal peaks in the beginning and the end of the contact phases. By analysing directly the data of the horizontal moments obtained with the function *btkGetGroundReactionWrenches*, it was noticed that the time of the beginning and of the end of the contact, assumed to be where the vertical force is higher than zero, it does not coincide with the delimitation of the contact in the horizontal moments.

The found peaks could be smoothed by interpolating the data at the initial and final moments of contact. However, it is important to notice that the value of the horizontal moments is very

small, comparatively to the vertical moment and, consequently, the most part of the studies concerning gait analysis, including pathological gait analysis [1, 55], do not take into account this moments. Indeed, the studies of gait generally use only the ground reaction forces and neglect the moments [16, 22, 56, 64].

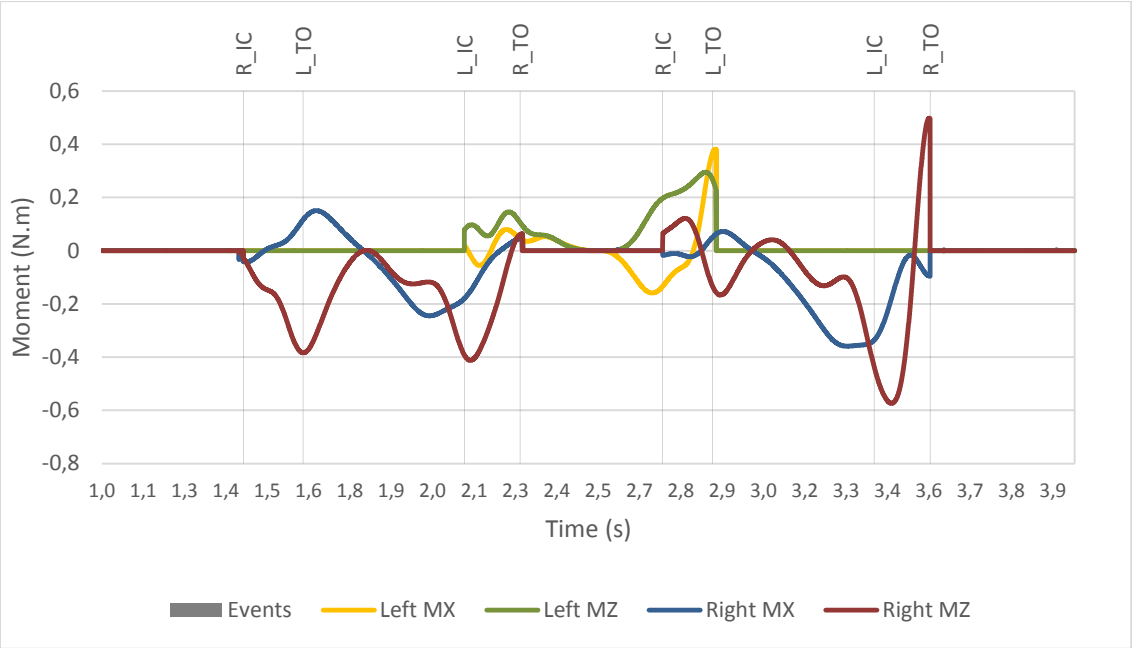

Figure 5.3. Horizontal ground reaction moments acting on the right and left side (Mx and Mz, considering the OpenSim coordinate system) of the post-stroke individual.

5.2.1- General spacio-temporal gait parameters

Table 5.1. General gait parameters obtained for the Study 2 and Study 1.

	Study 1	**Study 2**
Velocity (m/s)	1.30	0.92
Cadence (steps/min)	97.6	95.2
Left step length (m)	0.563	0.588
Right step length (m)	0.552	0.593
Gait cycle time (s)	1.23	1.26
Double support (%)	33.3	26.0
Right stance (%)	67	65
Left stance (%)	66	60

General spacio-temporal gait parameters (Table 5.1) were determined because they help characterizing gait and detecting abnormalities, like asymmetry. Since in both gait trials the subject walked with self-selected speed, it is possible to analyse this parameter. Gait velocity was higher in the **Study 1** (1.30 m/s) comparing to **Study 2** (0.92 m/s). However, the velocity obtained for the post-stroke individual was not inside the range reported in [13] for post-stroke individuals, from 0.10 m/s to 0.76 m/s. The time of duration of one gait cycle was higher in the **Study 2** (1.26 s), and consequently, the cadence was lower (95.2 steps/minute), comparing to the **Study 1** (1.23 s of gait cycle time and 97.6 steps/minute). The literature reports these characteristics for post-stroke individuals with slow gait slow gait [12, 19]. These studies also refer that the stride length is shorter in post-stroke gait, but this was not verified. Comparing the step length between the two limbs, in both **Study 1** and **Study 2** the right and left legs showed similar step length. However, according to the studies, it is common that the stride length verified in the CONTRA limb is higher, even though it exists considerable variability between the individuals [13, 19].

Also post-stroke gait is associated with higher double support percentage in the gait cycle [65], which was not verified in the **Study 2** (26.0%), comparing to a healthy individual (33.3%). In a typical gait cycle, the double support phase occupies about 20% in one complete gait cycle[1]. Relatively to the single limb stance, in the **Study 2** it was verified higher time percentage of stance for the IPSI limb, which is in accordance with the study [19]. However it was predicted that the single stance for a post-stroke individual was higher, comparing to a healthy one, which was not verified and for the **Study 1** this percentage was even higher than the reference value for healthy people (60%) [1].

5.3 - OpenSim Simulation

5.3.1- Scaling of the model

According to the OpenSim guide [50], the RMS value and the maximum marker error should be inferior to 1 cm and 2 cm, respectively. In both studies the recommended error limits were not achieved and the **Study 1** showed higher RMS and maximum marker error (**Table 5.2**). Similar values of these errors were obtained in [66], where the model Gait2354 (musculoskeletal model with 23 DOFs and 54 musculotendon actuators) and the same static trial data was used: 3,4 cm (RMS) and 6 cm (max error). The maximum marker error in the scaling of the **Study 1** is relative to the marker *Top.Head*, which did not correspond to a functional joint centre or a bony landmark, while in the scaling of the **Study 2** the maximum error was associated with a marker that represented a bony landmark, but not a functional joint centre.

Table 5. 2 Marker error (RMS) and maximum error associated with the scaling process for the models in the Study 2 and Study 1 and the respective limit values recommended in [50].

	Study 2	**Study 1**	**Recommended limits**
Marker error: RMS (cm)	1.49	3.02	< 1
Max error (cm)	2.05 (LPSIS)	6.14 (Top.Head)	< 2

The errors associated with scaling could be decreased if during the collection of the experimental data it were taken pictures of the individuals with the markers placed, in order to analyse the exact position of them. Also recording the trial would be valued since it would allow to associate the visual evaluation of gait with the results, to identify less reliable markers (not viable for inverse kinematics) and to verify if the assumption that the subtalar and metatarsophalangeal joints remain in the supposed neutral position (0º) was consistent. To verify if the locking of subtalar and metatarsophalangeal joints in the neutral position could influence the errors, scaling was done with this joints unlocked and the resulting errors did not vary. So, since in the next steps they were locked, it was more coherent to lock them in scaling. Additional measurements of the length of the body segments and its mass distribution (using a DXA - Dual-energy X-ray absorptiometry) would contribute for a scaling more accurate [50]. In the case of the **Study 2**, a static trial could also be performed, since it is the most recommended for scaling.

Since the process was done choosing the option to preserve the total mass of the subject, when scaling each segment it was used a constant scale factor, independent from the computed with

the marker measurements, so that the mass distribution of each one was the same as the model. However, is important to notice that the mass distribution varies considerably from on individual to other, especially in the torso. However this option was chosen so that the final total mass matched the measured mass of each individual and it wouldn't affect the simulation when the ground reaction data was taken into account.

The total mass of the subjects include the mass of the arms and since the model does not possess the superior limbs, their mass was distributed for the other segments. This could influence the scaling process, since the process maintains the mass distribution of each segment, when scaling is done, and a higher mass could lead to augmented volume of the segments, interfering with the marker placement. Also, it might increase the magnitude of the moments, once the segments will have higher mass then the real.

5.3.2- Inverse kinematics

Solving an inverse kinematics problem, it was possible to obtain the joint angles and compare them with the literature. In the Figure 5.5 the plots of hip, knee and ankle angles obtained for the **Study 1** and **Study 2** are presented and the Figure 5.4 shows the curves of reference [1] for these joints, considering a healthy gait cycle. It is important to take into account that in the curves obtained in simulation the gait cycle starts with the left toe-off (L_TO), while the reference curves only show the gait cycle for one leg and it starts with the respective initial contact (L_IC).

Analysing the hip angles, the results from **Study 1** (healthy subject) show similar curves in both sides and, comparing with the reference curve, shows lower maximum hip flexion angle (22º in the left leg and 24º in the right leg), which is approximately 30º in the reference.

The knee angle curve of the healthy subject appears to match the reference, having a maximum flexion of 70º, that is inside the expected (60º to 70º[1]).

Relatively to the ankle angle, the results from the simulation of the healthy individual show some differences from the reference, which might be related to the characteristic gait pattern of the individual that is being studied. The maximum plantarflexion of the ankle that happens during toe-off registered a lower value (approximately -8º) in both sides and in the reference the corresponding value is approximately -25º. Also the maximum dorsiflexion value in both legs, before the respective toe-off, was 15º in the **Study 1** while the reference value is near to 5º.

In post-stroke gait, the authors frequently report decrease of hip extension during stance and increase hip extension during swing in the CONTRA limb [19]. In the results of the inverse kinematics from the **Study 2** only the first characteristic was observed in the CONTRA limb (left

limb, in the **Study 2**) and during swing it was verified a decrease of hip extension prior toe-off, comparing to the IPSI limb (right limb, in the **Study 2**).

Also the results for the knee angle are not in agreement with the characteristic post-stroke gait, reported in [19]. It was expected an increase of knee extension during initial contact in the CONTRA limb, but it was verified lower knee extension during the left toe-off (-11°), in comparison with the IPSI limb (-4.5°).

The CONTRA limb, presents also some differences in relation to the IPSI in the ankle angle: higher dorsiflexion in the swing phase and prior to the respective toe-off and decrease maximum plantarflexion in the left toe-off (-3.6°), comparing to the IPSI limb (-8.6°). The decrease of plantarflexion is a common in post-stroke gait, usually as consequence of plantarflexors weakness [12, 13, 19], however, this type of gait is also characterized by decrease of dorsiflexion during swing and, in this case, the results of the inverse kinematics show the contrary.

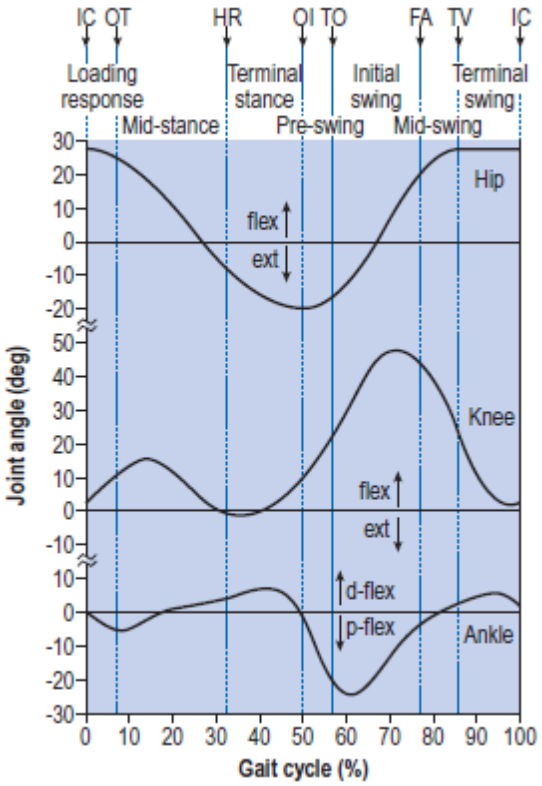

Figure 5.4. Reference hip, knee and ankle joint angles for healthy gait [1]. The gait events are represented as: IC – initial contact; OT – opposite toe-off; HR – heel rise; OI – opposite initial contact; TO – toe-off; FA – feet-adjacent; TV – tibia vertical.

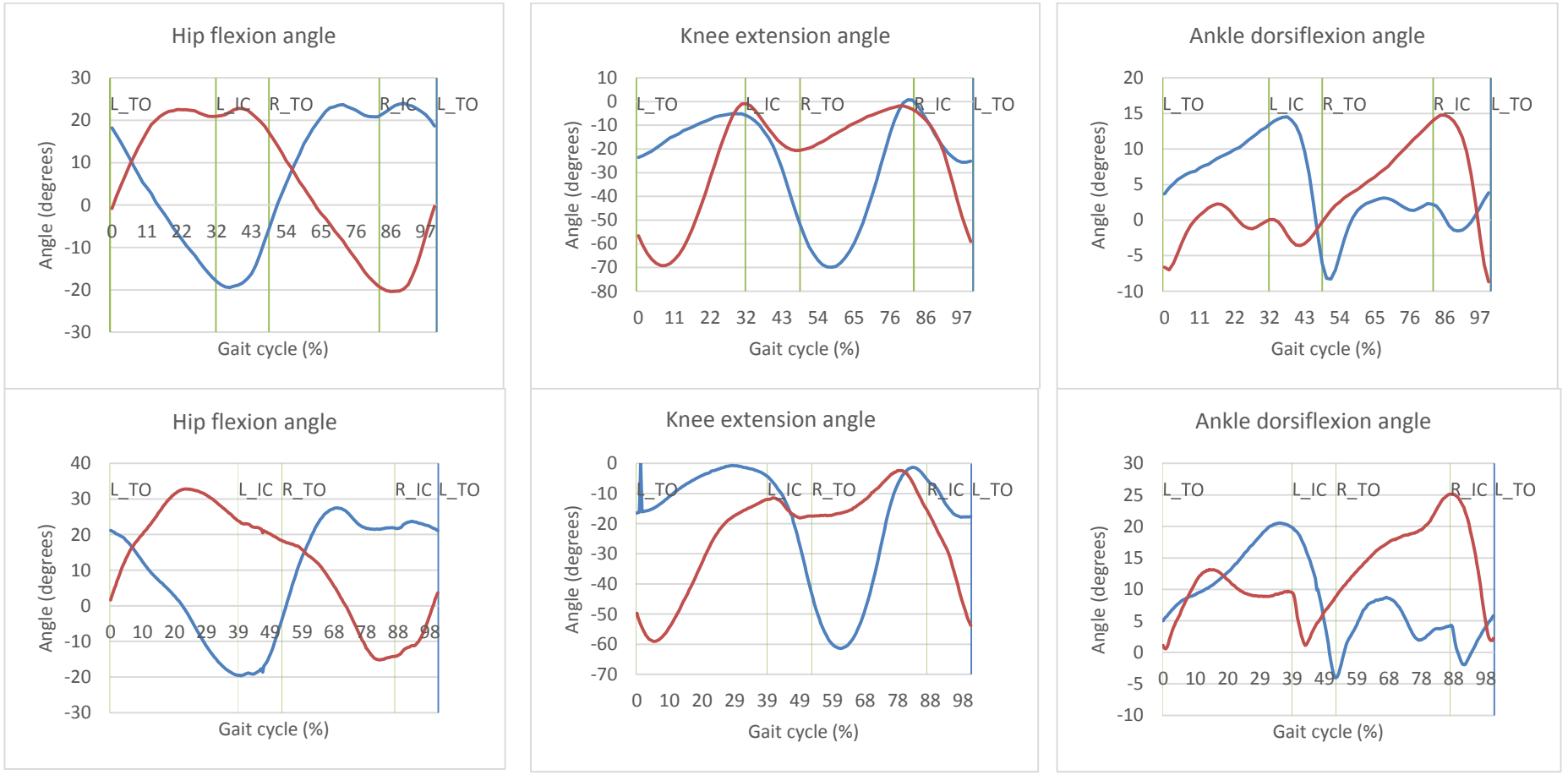

Figure 5. 5. Hip, knee and ankle kinematics obtained with inverse kinematics, for the Study 1 (first row) and the Study 2 (second row). The blue line refers to the right limb (IPSI limb in the Study 2) and the red line to the left limb (CONTRA limb in the Study 2).

The errors associated with the tracking of the markers during the inverse kinematics process were satisfactory for the **Study 2**, but exceeded the recommended limits in the **Study 1** (Table 5.3). The maximum error registered in this study is associated with the marker R.Acromium, which had associated a lower tracking weight.
The IK process is very dependent of the scaling process [50] and consequently, the high errors registered in the IK for the **Study 1** might be related with the errors obtained in the corresponding scaling process.

Table 5. 3 Marker error (RMS) and maximum error associated with the scaling process for the models in the Study 2 and Study 1 and the respective limit values recommended in [50].

	Study 1	**Study 2**	**Recommended limits**
Marker error: RMS (cm)	2.25	1.19	< 2
Max error (cm)	8.56 (R.Acromium)	3.98 (RMK)	< 2-4

5.3.3- Inverse dynamics

Using inverse dynamics, the model tried to reproduce the movement determined by inverse kinematics in the previous step while subjected to the external forces and moments contained in the *.mot files created.
Making a first analysis of the force that acts in the pelvis, higher peaks in the vertical force (Fy) are observed in the instants of initial contact of the two limbs (Figure 5.6). If the vertical ground reaction forces are plotted in the same graph as the forces acting in the pelvis, from ID, (Figure 5.7) there is a coincidence with decrease of the peaks and the beginning of the contact. Indeed, the vertical force acting in the pelvis appears to be compensating the inexistence of a force in the instants before Fy becomes different from zero. This force is the major force component and accounts for the vertical acceleration of the centre of mass and the characteristic curve of this force includes a quick increase after heel strike [67]. However the vertical force obtained has an abrupt increase, verified in these instants, which rise from zero to 130 N (in the left initial contact) and 125 N (right initial contact) in a small interval of time. To minimize the errors originated from this, smoothing the data could be done in the processing step.

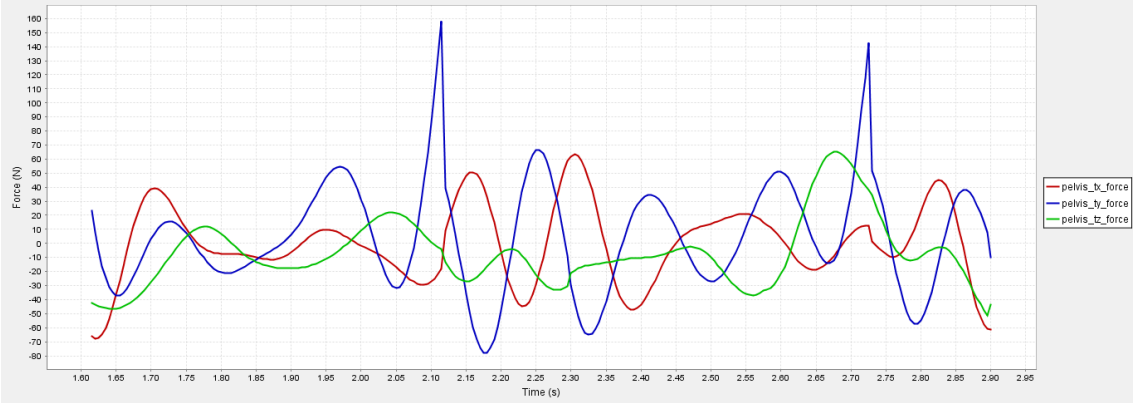

Figure 5. 6. Forces acting in the pelvis, obtained using ID, before reducing the residuals. The blue line represent the vertical residual force, the red and the green represent the horizontal residual forces (Fx and Fy).

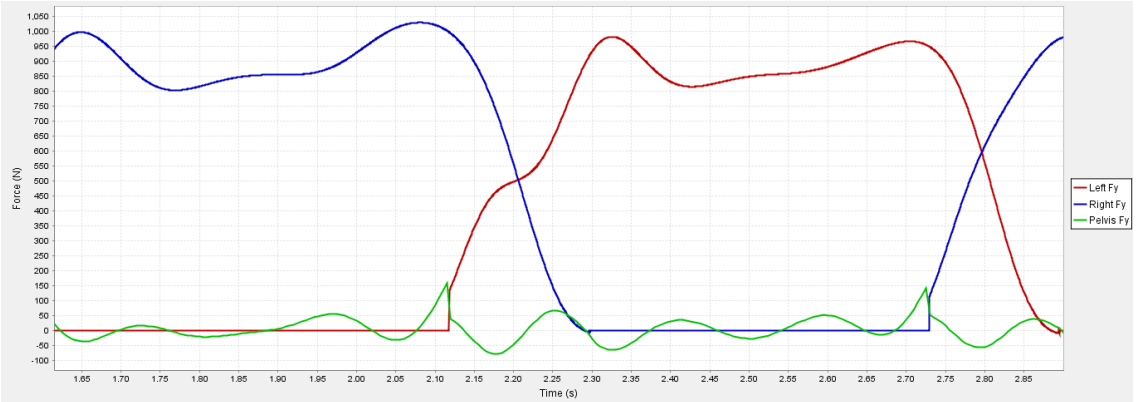

Figure 5. 7. Plot of the vertical GRF acting on the left (red) and right (blue) legs and the force acting in the pelvis (green).

Considering the differences between individuals in the size and weight of the segments, in order to compare the joint moments with the literature is necessary to scale these values in newton-meters per kilogram body mass.

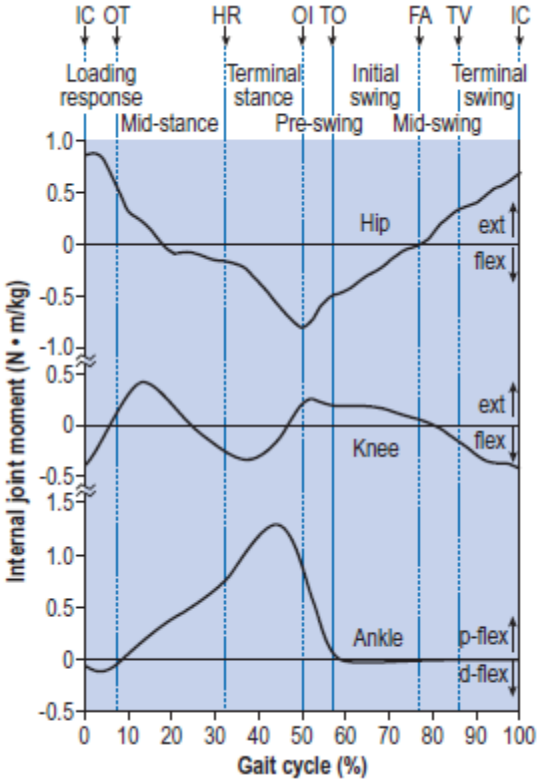

Figure 5. 8. Reference internal joint moments for the hip, knee and ankle according to [1], in N.m/Kg, for one gait cycle. The gait events are represented as: IC – initial contact; OT – opposite toe-off; HR – heel rise; OI – opposite initial contact; TO – toe-off; FA – feet-adjacent; TV – tibia vertical

Comparing the results of hip joint moments obtained in the healthy subject from the Study 1 (Figure 5.9) with the values found in the literature (Figure 5.8), the moment curve has a similar shape, however, the two legs show different range values: -0.8/ 0.5 N.m/Kg for the right leg and -0.6/0.6 N.m/Kg for the left leg. Also the knee moment obtained in this simulation is in agreement with the reference, though there were found differences between the two legs in the maximum hip flexion, at initial contact: the right leg reached a moment of -0.7 N.m/Kg and the left -0.6 N.m/Kg.

Relatively to the ankle, the maximum plantarflexor moment it was higher than the reference values (approximately -1 N.m/Kg) in both limbs and the right leg registered a higher value (-1.77 N.m/Kg) than the left (1.50 N.m/Kg).

Normal gait is assumed to be symmetric, even though it is accepted a small degree of asymmetry, which is negligible in healthy subjects [68]. The results do not show considerable differences between both sides.

Relatively to the **Study 2,** ID was performed using the external force data considering the COP and the PWA. Analysing the results obtained, there was not found considerable differences between them. The curves show the similar shape and maximum and minimum moment values. In the Figure 5.9 the joint moments obtained using the PWA are shown. The maximum hip flexion moment was higher for the IPSI limb (0.52 N.m/Kg) comparing to the CONTRA limb (0.45

N.m/Kg), while the maximum hip extension moment for the IPSI limb was -0.80 N.m/Kg and for the CONTRA limb -0.70 N.m/Kg.

Regarding the knee moment, it was found a lower knee flexor moment in the CONTRA limb (-0.16 N.m/Kg) before the initial contact, comparing to the IPSI limb in the correspondent initial contact (-0.32 N.m/Kg). However, it is observed high abnormal peaks happening during the initial contact, in both sides, that also occur in the hip moment data, higher than the ones that appear in the inverse dynamics results from the **Study 1**.

The ankle plantarflexor maximum moment differ slightly from one limb to the other (-1.47 N.m/Kg in the IPSI limb and -1.40 N.m/Kg in the CONTRA limb). In both limbs it was not found the dorsiflexor moment after initial contact as expected, by looking at the curve found in the literature. An abnormal peak appeared in the IPSI limb during its initial contact.

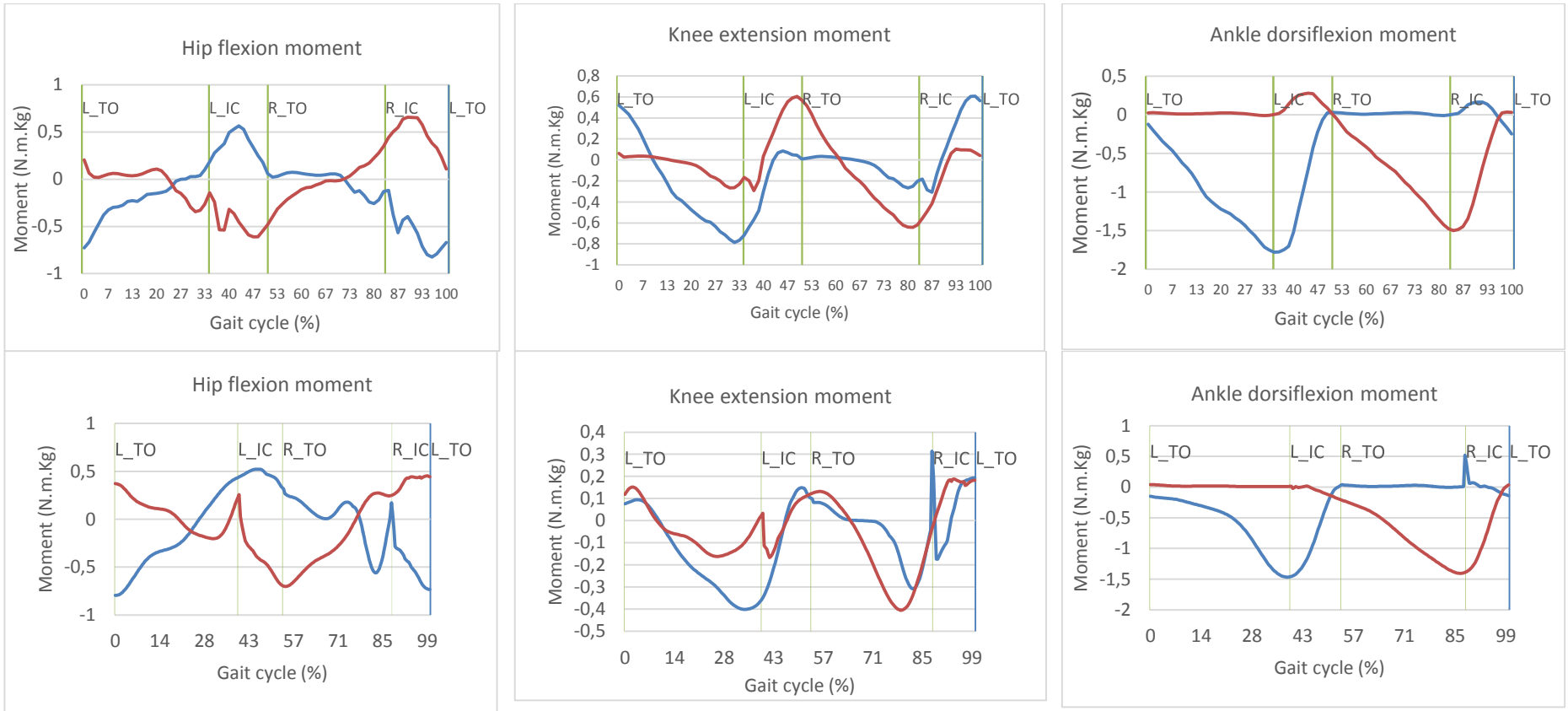

Figure 5. 9. Hip, knee and ankle joint moments obtained with inverse kinematics, for the Study 1 (first row) and the Study 2 (second row). The blue line refers to the right limb (IPSI limb in the Study 2) and the red line to the left limb (CONTRA limb in the Study 2).

5.3.4- Residual reduction algorithm

The reduction of the residuals was successfully accomplished in both studies 1 and 2, according to the recommended in the OpenSim guide [50], as it is possible to verify by analysing the Table 5.4 . The best results were obtained for the **Study 1**, in which the values of maximum and RMS residuals and errors were inside the optimal limit. In the **Study 2**, the residuals overpassed the optimal threshold, however, decreasing residuals would increase the errors associated with the kinematics beyond the acceptable values. Analysing the plot of the residual forces in the **Study 2** (considering the PWA), it is possible to see peaks in the vertical force (Fy), in the point of the right and left initial contact, also verified in the internal moments from ID. However, it is verified a decrease of the magnitude of these peaks, after the reduction of the residuals (Figure 5.10).

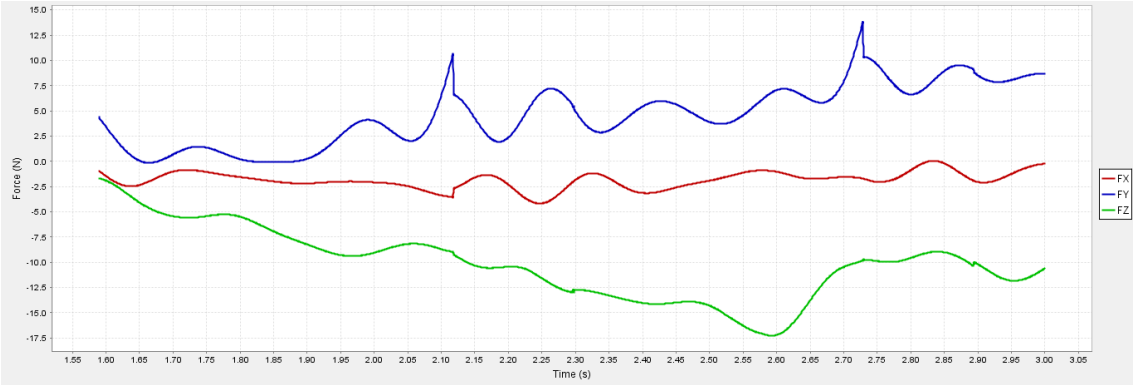

Figure 5. 10. Residuals forces obtained in RRA for the Study 1, using PWA. The blue line represent the vertical residual force, the red and the green represent the horizontal residual forces (Fx and Fy).

In ID, the action of external forces (GRF) is balanced only with the body forces, while in RRA the residuals that are the forces and moments acting in the pelvis are reduced and, consequently, this reduction is compensated by changes in the actuation of the other joint actuators.

There are no reference values to evaluate the dimension of the total mass adjustment recommended by after the RRA step. In both cases it was less than 1%, being lower for the healthy model (**Study 1**). This might not be related with the pathology, but with the experimental data itself, since the RRA intends to compensate for dynamic inconsistencies.

Table 5. 4 Maximum and RMS values of the residual forces and moments and rotational errors obtained for the RRA of the Study 2 and Study 1 and the recommended [50] optimal and maximum thresholds.

	Study 1	Study 2		Absolute optimal threshold	Absolute max threshold
		COP	PWA		
Max Residual Forces (N)	-7,21 (Fx)	-19,00 (Fz)	-17,27 (Fz)	< 10	< 25
RMS Residual Forces (N)	3,26	6,98	7,10	< 5	< 10
Max Residual moments (Nm)	-22,80 (Mz)	-62,13 (Mx)	-58,66 (Mx)	< 50	< 75
RMS Residual Moments (Nm)	9,08	15,17	16,32	< 30	< 50
Max translational error (cm)	-1,09 (Pelvis x)	-2,89 (Pelvis z)	-2,83 (Pelvis z)	< 2	< 5
RMS translational error (cm)	0,61	1,31	1,35	< 2	< 4
Max rotational error (deg)	-0,40 (Right hip flexion)	-3,00 (Right ankle angle)	-1,57 (Right ankle angle)	< 2	< 5
RMS rotational error (deg)	0,16	0,64	0.58	< 2	< 5
Total mass adjustment (Kg)	-0,05	-0,43	-0,56	-	-
Total mass adjustment (%)	-0,07%	-0,45%	-0,58%	-	-

Relatively to the **Study 2**, the RRA was also performed having the GRF considering the COP and the PWA, to verify the influence mainly the influence of the horizontal moments in the simulation. In both cases it was used the same settings for the actuators and tasks. Small differences were detected in what concerns to the internal joint moments an the residuals obtained. The highest difference verified between the two analysis was found in the maximum rotational error associated with the right ankle, which was 1,57º when the PWA is considered and -3,00º for the analysis using the COP. The weight associated with the right ankle was increased to attempt to diminish the error in tracking this joint, however, the error was not diminished. This means that the model cannot track the motion completely without the action

of the residual forces and its decrease, particularly in the instants were the peaks exist, caused errors in tracking the kinematics.

In the next step (CMC) it was used the PWA approach for the external forces, since the maximum error associated was lower and it will decrease the accumulation of errors in kinematics in the final result.

5.3.5- Computer muscle control

The results of the kinematics computed in the previous step were used as the motion to track during CMC. For both studies it was performed several iterations in order to try to find the optimal solution, in which the residuals, reserves and errors were inside the optimal, or at least, the acceptable limits. In the Table 5.5 are shown the results for these parameters. The results relative to the **Study 1** are satisfactory since all the parameters are inside the optimal threshold. In the case of the **Study 2,** the maximum values of residual moments, rotational error and reserve force surpassed this optimal limit, but still acceptable. However, it was obtained a peak of 130,60N of residual vertical force (*Fz*) in the simulation using the PWA, in the right initial contact (Figure5.11).

Table 5. 5 Maximum and RMS values of the residual forces and moments, reserve forces and translational and rotational errors obtained for the CMC of the Study 2 and Study 1 and the recommended [50] optimal and maximum thresholds.

	Study 1	**Study 2 (PWA)**	**Optimal threshold**	**Max threshold**
Max Residual Forces (N)	-8,83 (Fx)	130,66 (Fz)	< 10	< 25
RMS Residual Forces (N)	3,37	12,85	< 10	< 25
Max Residual moments (Nm)	-22,39 (Mz)	59,31 (Mx)	< 50	< 75
RMS Residual Moments (Nm)	9,43	15,76	< 30	< 50
Max translational error (cm)	-0,01 (Pelvis z)	0,10 (Pelvis z)	< 1	< 2
RMS translational error (cm)	5,31E-3	0,02	< 1	< 2
Max rotational error (deg)	-0,38 (Left knee angle)	-6,54 (Right ankle angle)	< 2	< 5

RMS rotational error (deg)	0,09	0,46	< 2	< 5
Max Reserve (N.m)	3.12 (Left ankle angle)	-64,61 (Right knee angle reserve)	< 25	< 50
RMS Reserve (N.m)	0,12	2,96	< 10	< 25

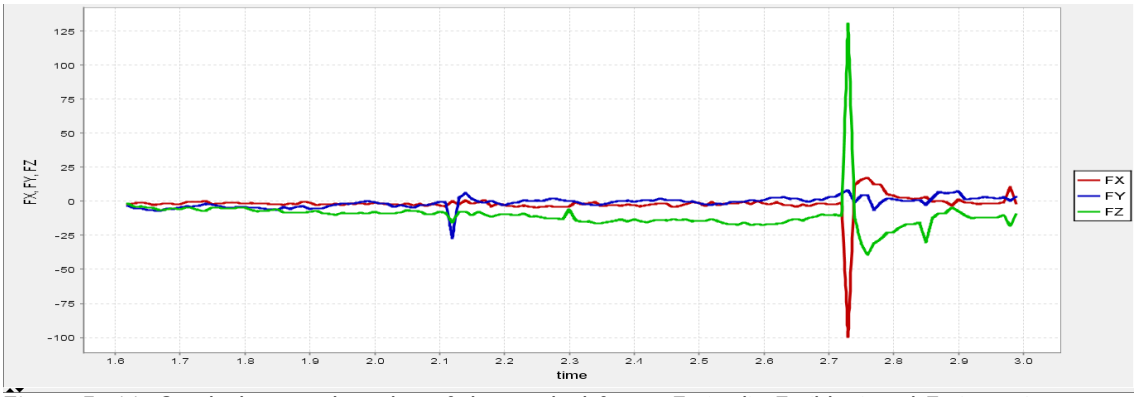

Figure 5. 11. Graph showing the value of the residual forces *Fx* (red), *Fy* (blue) and *Fz* (green) acting in the pelvis, resulting from CMC.

The right ankle had the highest tracking error associated (-6,54º). Looking at the curve of the right ankle kinematics after RRA and after CMC (Figure5.12, it is possible to see that the error starts from the right initial contact, the instant where the large residuals were obtained, suggesting a relation between this occurrences. Similarly, in the previous step (RRA) the largest tracking error was associated with the right ankle angle, even though was inside the acceptable limits. Also in the instant of right initial contact it were verified high reserve moments in the right side: the right knee reserve actuator reached the maximum reserve value (-64,61 N.m) and also the right ankle registered 50,20 N.m. Decreasing the optimal force of this reserve actuators, so that the model would not use them, leads to interruption of CMC process, meaning that the model needs the action of these actuators to follow the kinematics.

It could be hypothesized that the locking of the subtalar and metatarsophalangeal joints could influence the errors in tracking the ankle movement, but it was not verified the same problem in the left ankle, which was satisfactorily tracked in the CMC (0.69º), making this hypothesis less plausible.

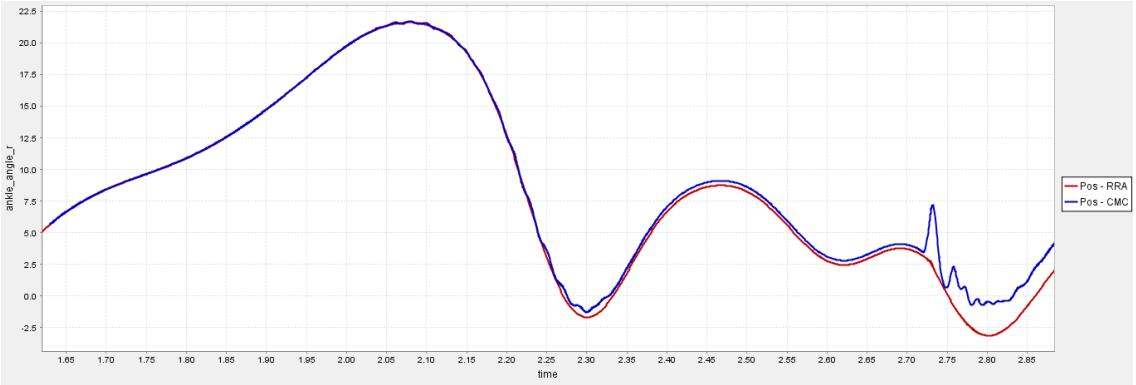

Figure 5. 12. Right ankle angle error. The red line corresponds to the right ankle angle obtained after RRA and the blue line represents the right ankle angle after CMC.

5.3.6- Muscle action

The output files of the CMC include:

- Joint kinematics (position and angular velocity and acceleration) and in the case of the pelvis also the linear velocity and acceleration;
- Tracking errors of the kinematics;
- Actuator (muscle and reserves) forces and powers;
- Actuator (muscle and reserves) powers;
- Controls: excitation patterns of each actuator;
- States: muscle activation and fibber length.

The activation pattern of each reserve and residual actuator is directly linked to the respective excitation, since the activation is the result of the product of the excitation by the optimal force [50]. In the case of the muscles, the activation is obtained through the excitation-activation dynamics (**Figure 3.4**), described by the differential equation 3.3, resulting in some time delay between excitation and activation.

The analysis of the muscle force through time is not enough to a better understanding of the behaviour of the muscles. Since a muscle can produce force isometrically (no fibber length changing), concentrically (produces force by contracting in the same direction of the movement) and eccentrically produces force by lengthening in the direction of the movement) and also can change its length and not exert force [1, 4]. Consequently, to do a more complete analysis is necessary to study the muscle activation together with the kinematics in the respective time, to verify the activation and the direction of the movement. When a muscle contracts concentrically, it produces energy, meaning that it generates positive power, while eccentric contraction leads to energy absorbing and, consequently negative power [1]. Since power is the variation of energy (joule) with time, its units are joule per second (J/s) watt (W).

Studies about the muscle impairments in post-stroke gait often report weakness of plantarflexors and also the dorsiflexors of the contralesional limb (CONTRA) and changes in the activation of the hamstring and quadriceps as a compensatory mechanism [16, 17, 19] in both limbs. The analysis of the muscle action will be focused in these group of muscles. The soleus (SOL) and medial gastrocnemius (MEDGAS) are the plantarflexors most studied in post stroke gait [69, 70]. For that reason these two muscles were chosen for analysis. The semimembranosus (SMEMB), from the hamstring group, was also analysed. This muscle was chosen because in the model it has higher maximum isometric force and, consequently, will be preferably used by the model to generate the necessary force, since it is considered a "cheaper" actuator, comparing to the others muscles in the same group with lower maximum isometric force and the same constrains in activation.

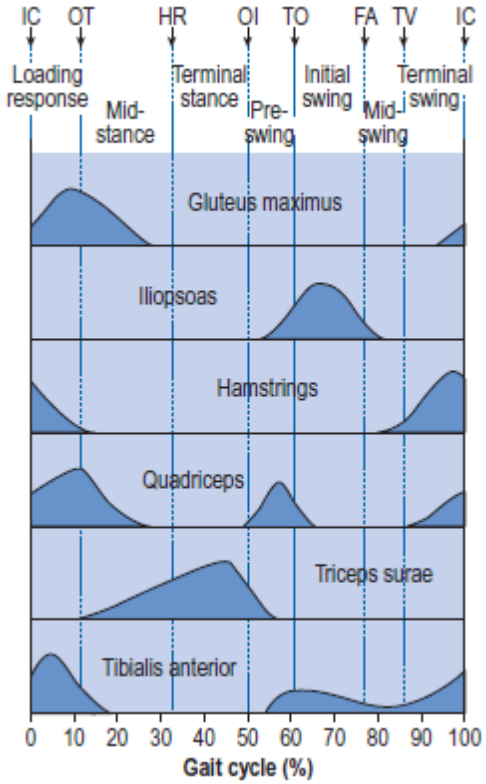

Figure 5. 13. Activation of the main muscle groups during the gait cycle [1].

Study 1 – healthy gait

According to the bibliography (Figure 5.13), the activation of the triceps surae muscles, which include SOL and MEDGAS, begins at opposite toe-off and lasts until the middle of terminal swing, reaching the maximum at terminal stance phase. The contraction of this muscles is concentric since while active the ankle moves to plantarflexion. Since concentric contraction is associated with energy generation, that results in positive power. During this phase it is verified the largest amount of power generated during the gait cycle, essential to accelerate the limb before its toe-off [1]. Looking at the graphs showing the powers of the SOL, MEDGAS

(Figure 5.14) it can be seen a large amount of positive power in this phase, even though in the case of the gastrocnemius muscles it is verified some oscillations. There were verified differences in the activation of the plantarflexor muscles comparing the two sides, not evident when looking at the maximum activation reached, but in the duration. The healthy right SOL and also the MEDGAS show longer activation before the maximum is reached.

After toe-off, the contraction of the triceps surae ceases and the dorsiflexors of the ankle are activated, namely the tibialis anterior (TA)[1]. In both sides, there is an increase of activity of TA after the respective toe-off, as expected. At this point the power of TA is positive in both sides (Figure 5.14). This muscle usually stays active until the next mid-stance, after the opposite toe-off happens [1]. The left TA presents an unusual high activation at the opposite initial contact (at 90% of the considered gait cycle). The right leg also shows unpredicted activation of the TA during the right stance and low activation after initial contact.

Relatively to the power associated, both right and left TA showed negative power before the respective toe-off, where they contract eccentrically and a positive power after toe-off, indicating concentric contraction. Both legs showed power oscillations during the cycle.

Since in the simulation referent to the healthy subject the kinematics of the hip did not show considerable asymmetries, it was expected that the muscular activation between the right and left legs would be also symmetric, which was verified. In the case of the healthy SMEMB, the pattern of activation did not match the reference. The hamstring muscles, which contribute for hip extension and knee flexion, are usually activated during terminal swing, before initial contact until opposite toe-off. In the results obtained, both right and left SMEMB are activated in during these part of the gait cycle, with negative power before initial contact, since the hip is moving to flexion, and positive work after initial contact because the hip starts to extend. However, both muscles are active after the initial contact of the opposite limb with positive power associated. Since the hamstrings also are responsible for knee flexion, this non expected activation might be related with the high knee flexion that happens in these instants (Figure 5.5).

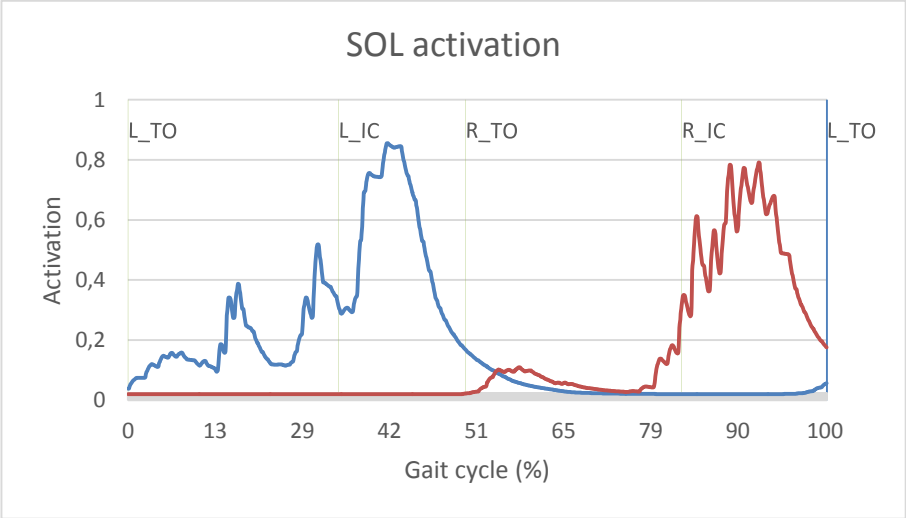
SOL activation
Activation
1
0,8
0,6
0,4
0,2
0
L_TO
L_IC
R_TO
R_IC
L_TO
0
13
29
42
51
65
79
90
100
Gait cycle (%)

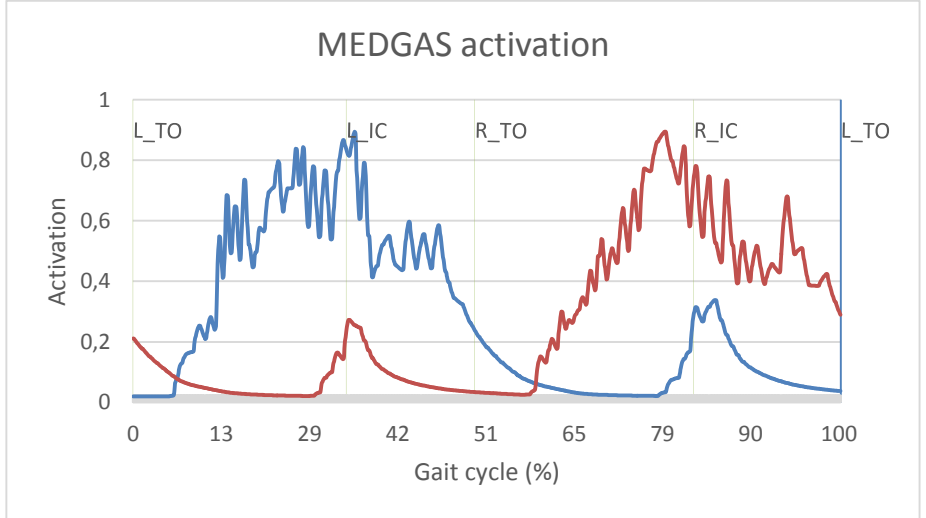
MEDGAS activation
Activation
1
0,8
0,6
0,4
0,2
0
L_TO
L_IC
R_TO
R_IC
L_TO
0
13
29
42
51
65
79
90
100
Gait cycle (%)

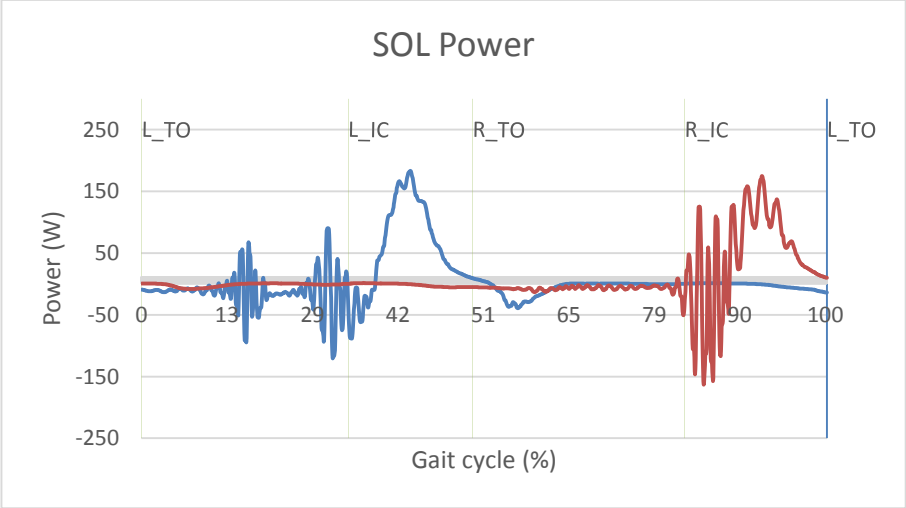
SOL Power
Power (W)
250
150
50
-50
-150
-250
L_TO
L_IC
R_TO
R_IC
L_TO
0
13
29
42
51
65
79
90
100
Gait cycle (%)

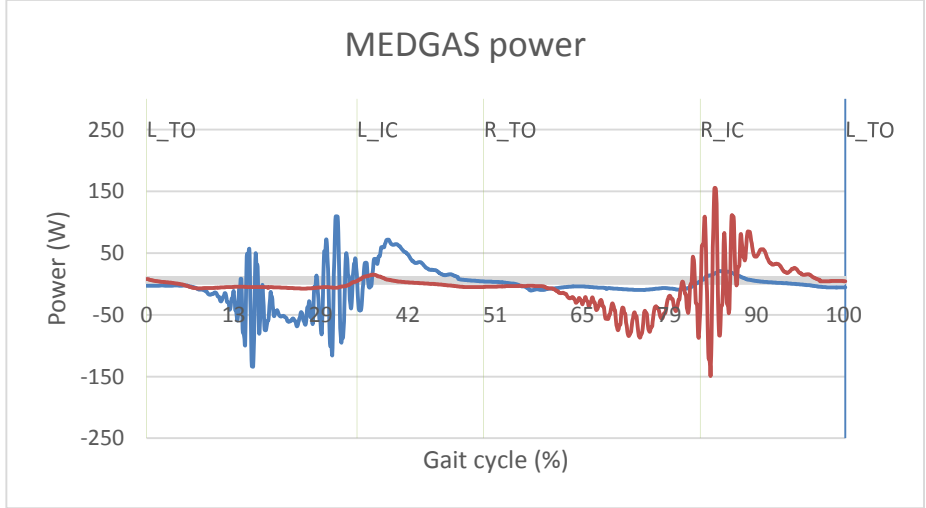
MEDGAS power
Power (W)
250
150
50
-50
-150
-250
L_TO
L_IC
R_TO
R_IC
L_TO
0
13
29
42
51
65
79
90
100
Gait cycle (%)

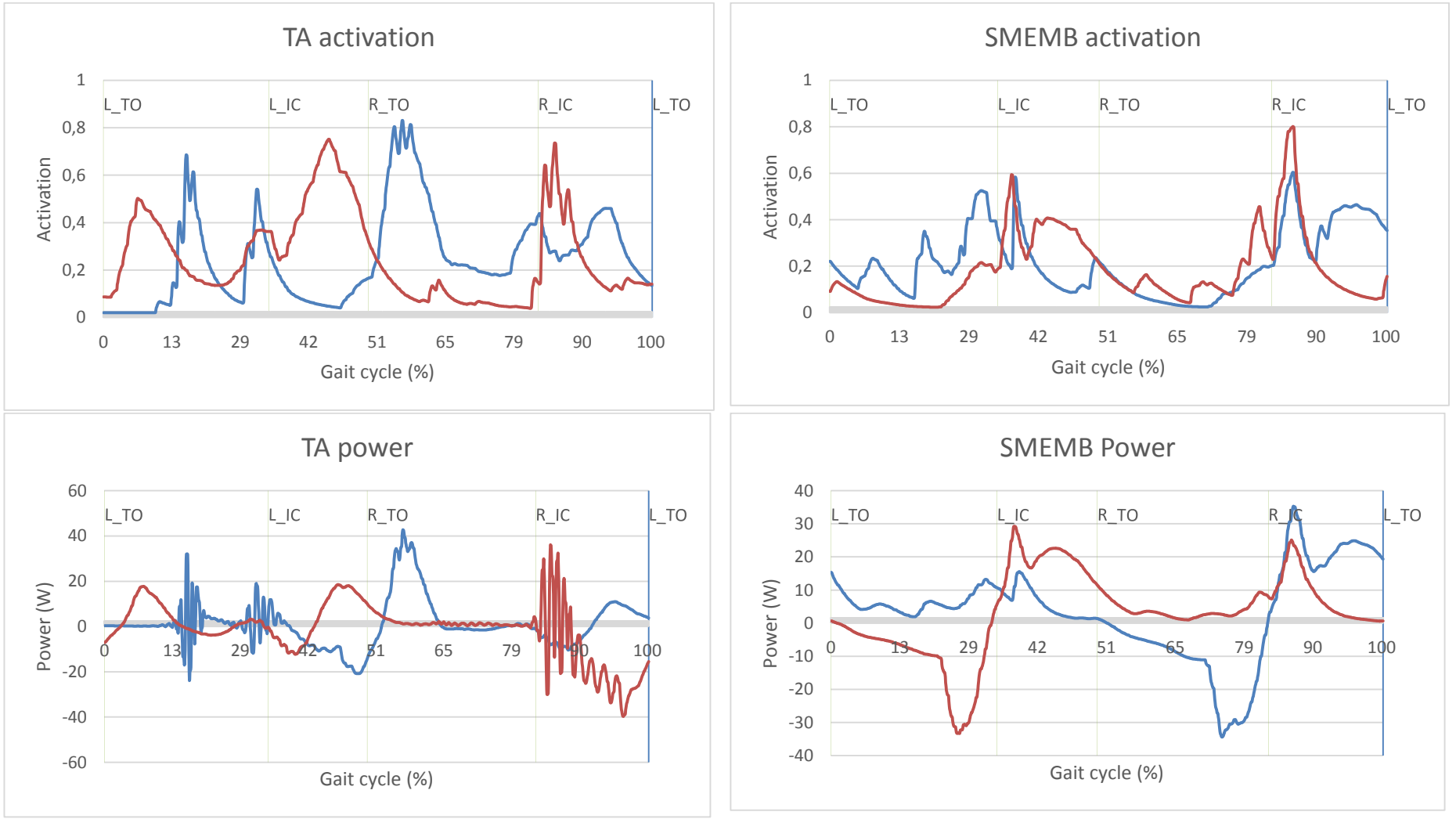

Figure 5. 14. Activation and power associated with the muscles SOL, MEDGAS, TA, SMEMB, obtained in CMC (Study 1). The red line refers to the CONTRA limb and the blue line refers to the IPSI limb.

Study 2 – Post-stroke gait

Usually stroke is associated with weakness of the CONTRA plantarflexors, specially the SOL and GAS [12, 13, 19], this means that lower activations of these muscles should be expected. Moreover, these studies reported early activation of these muscles before the instant when it reaches its maximum. The SOL of the CONTRA limb (left) (Figure 5.15) shows higher maximum activation before toe-off, comparing to the SOL of the IPSI limb. On the other hand, its activation starts earlier. The powers associated show coherence with the activation since both SOL have positive work prior to the respective toe-off and the CONTRA SOL have some oscillations (negative and positive values) of power before the full activation is reached. The MEDGAS, in contrast, registered less activation levels on the CONTRA limb and also earlier activation and the work associated follows a similar pattern as the SOL. There is, however, a peak at IPSI initial contact, which might be associated with the high values of residual forces verified in this instant. Both plantarflexors show activation on the corresponding initial contact, while the plantarflexors from the opposite side is active. According to the reference this does not happen in a healthy individual and also is not a characteristic of post-stroke gait. Looking at the activation of the MEDGAS of the **Study 1**, the curve also shows the same behaviour, but this activation is relatively small. Since high magnitude residuals were obtained in the initial contact in both studies and in both sides, it is possible that this activation could be linked to inconsistencies in those instants.

The TA activation on the IPSI limb had a behaviour similar to the reference, having high activation during the toe-off, with negative work, and prior to the opposite toe-off, with positive work. The CONTRA limb shows activation during the respective stance, which results in oscillations in power. The plantarflexor and dorsiflexor muscles from the IPSI limb appeared to be affected for the inconsistencies observed especially during the right initial contact (2.73s), where the ankle angle had registered a high error.

Regarding the muscles from the hip, in post-stroke gait is often reported co-activation of the muscles in both sides, as a compensation mechanism [16, 19, 20]. The hip extensor SMEMB from the CONTRA limb showed prolonged activation during the stance phase of the corresponding limb, associated with positive power. This might be associated with the gradual decrease of the hip flexion and of knee extension (Figure 5.5) verified in phase, after the maximum was reached at approximately 30% of the cycle.

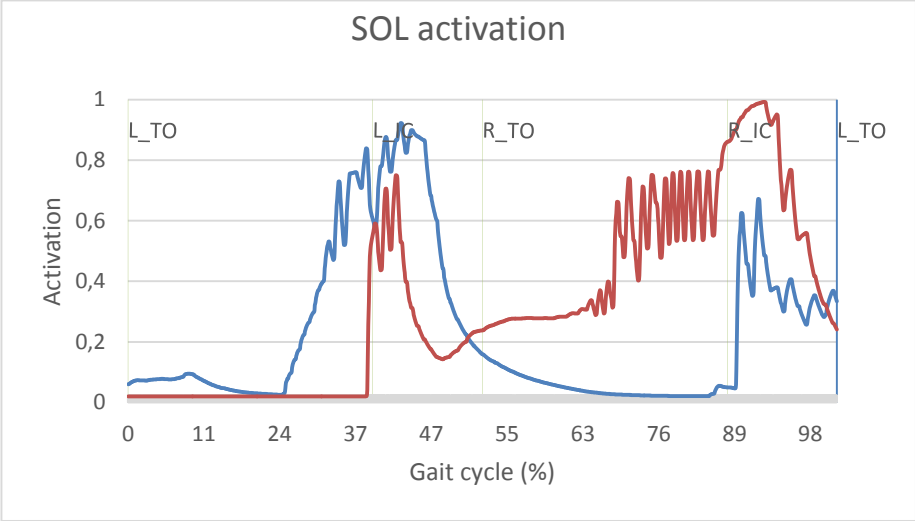
SOL activation
Activation
1
0,8
0,6
0,4
0,2
0
L_TO
L_IC
R_TO
R_IC
L_TO
0
11
24
37
47
55
63
76
89
98
Gait cycle (%)

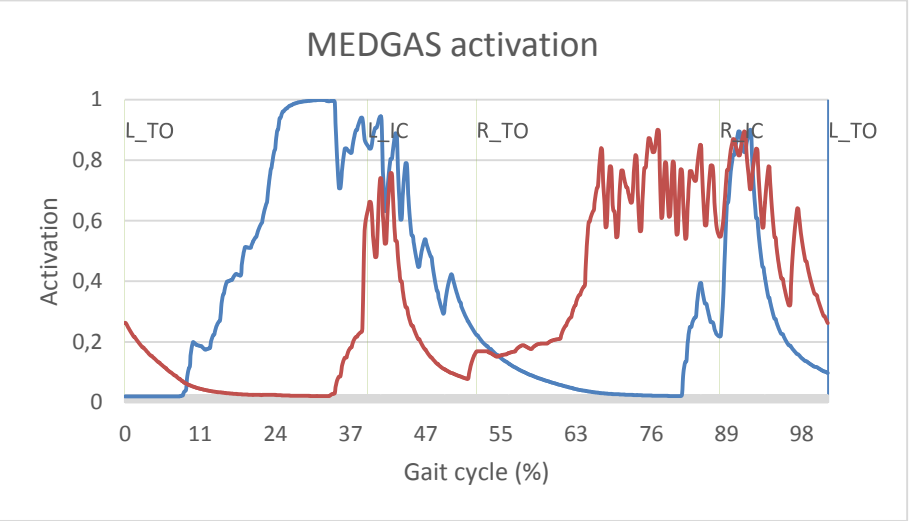
MEDGAS activation
Activation
1
0,8
0,6
0,4
0,2
0
L_TO
L_IC
R_TO
R_IC
L_TO
0
11
24
37
47
55
63
76
89
98
Gait cycle (%)

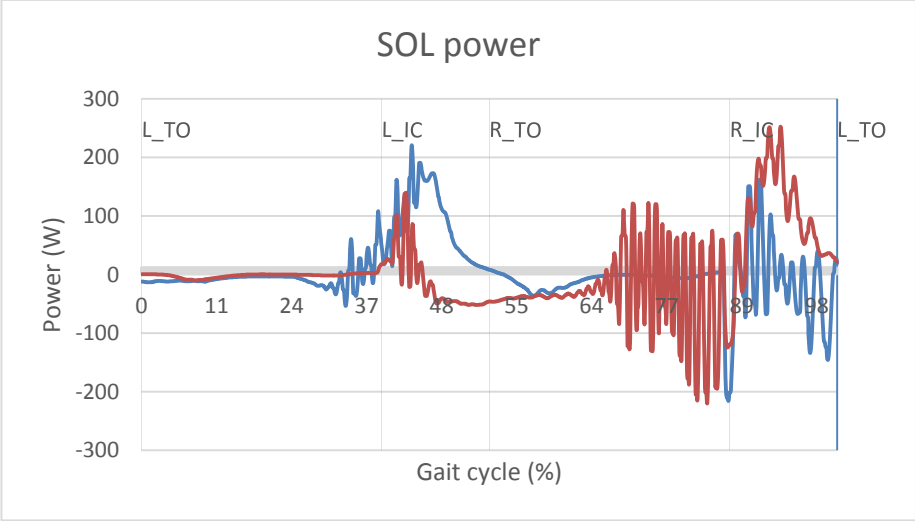
SOL power
Power (W)
300
200
100
0
-100
-200
-300
L_TO
L_IC
R_TO
R_IC
L_TO
0
11
24
37
48
55
64
77
89
98
Gait cycle (%)

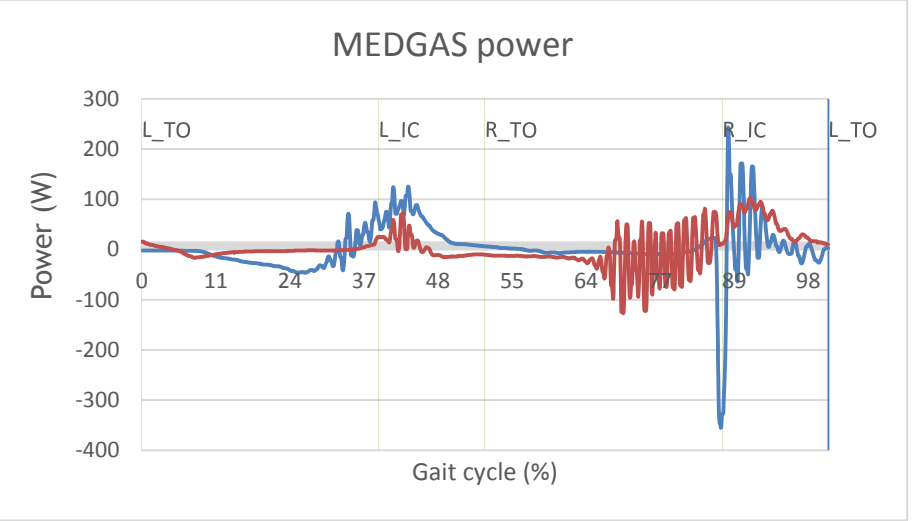
MEDGAS power
Power (W)
300
200
100
0
-100
-200
-300
-400
L_TO
L_IC
R_TO
R_IC
L_TO
0
11
24
37
48
55
64
77
89
98
Gait cycle (%)

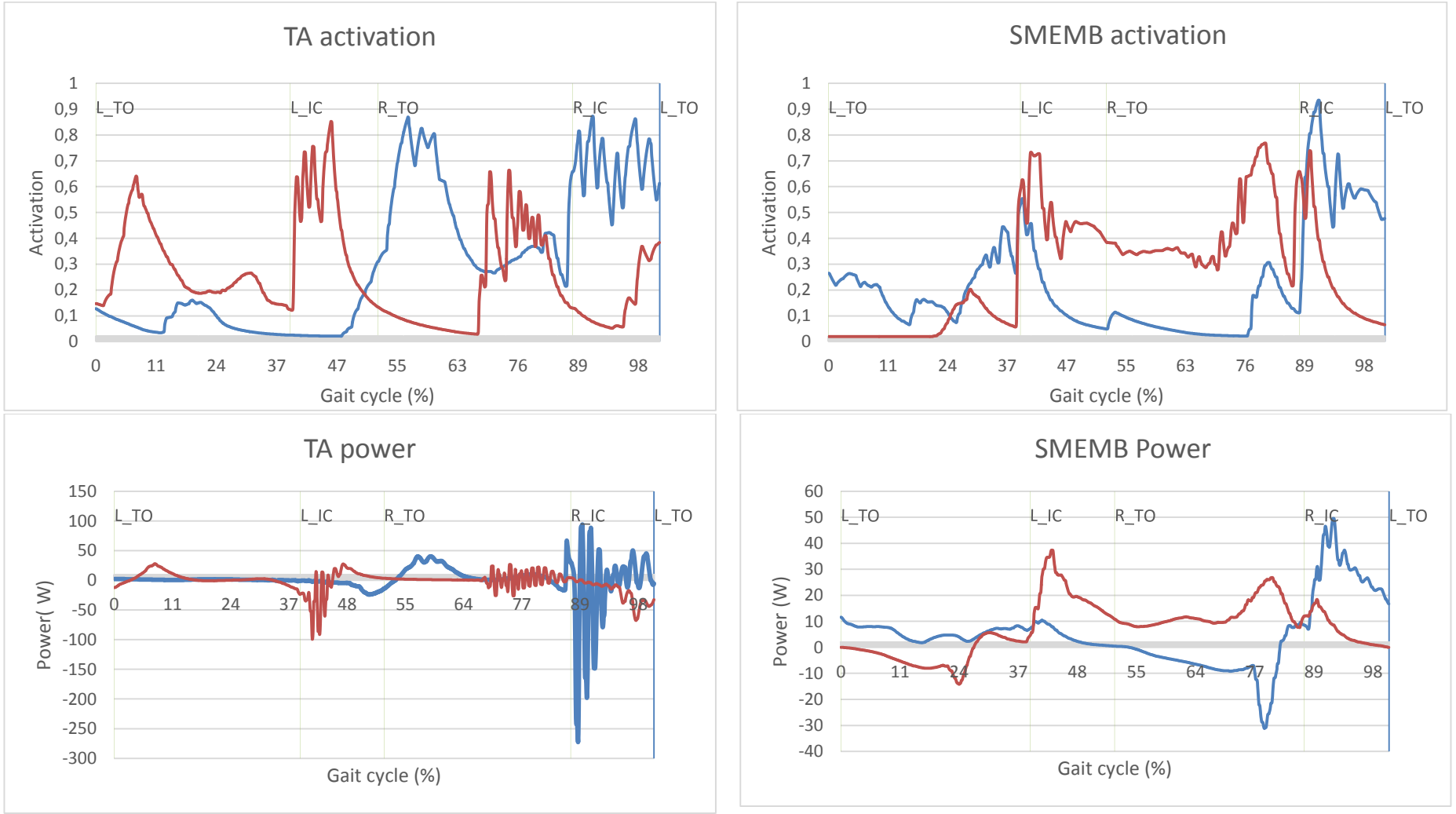

Figure 5. 15. Activation and power associated with the muscles SOL, MEDGAS, TA, SMEMB, obtained in CMC (Study 2). The red line refers to the CONTRA limb and the blue line refers to the IPSI limb.

5.4 - Summary

Two simulations of gait were developed, one using normal gait and other using post-stroke gait. The experimental data used to simulate post-stroke gait was extracted from a *.cd3 file and the respective force platform data was used to compute the forces and moments that act in the PWA and in the COP. The results showed not relevant differences between the location of these points and the moments in the horizontal plane were small comparing to the vertical moment.

The kinematics and joint moments obtained for the healthy model revealed to be in accordance with the reference. However, the muscular activations showed some asymmetry and, in the case of the TA and the SMEMB, these muscles were activated in instants of the cycle where it doesn't happen in the reference.

The kinematics of the post-stroke model, however, showed only low plantarflexion as the main impairment and the results from CMC for the plantarflexor muscles showed early activation, but not diminished in the paretic side. These muscles appeared to be able to generate the necessary power before propulsion. The hamstring muscle (SMEMB) from the CONTRA limb, showed prolonged activation during stance phase, which it is usually reported in the literature as a compensatory mechanism for plantarflexor weakness.

This model had associated high tracking error for the right ankle and high magnitude residuals and reserves at the instant of right initial contact, suggesting that it was not able to reproduce its kinematics relying mainly in the muscular actuators.

Chapter 6

Final conclusions and future developments

6.1- Final conclusions

The aim of this dissertation consisted in simulate healthy and a pathological gait, specifically post-stroke gait, using computational methods, starting from experimental data.

Firstly, the fundamentals of human gait were explored, regarding the anatomy and the neuromuscular controls involved. After that, gait impairments in the sequence of a stroke were studied and described. The experimental methodologies used to collect kinetic and kinematic data and the mathematical models that serve as fundamentals of the computational tools for biomechanical modelling were reviewed and described.

The procedure for obtain the experimental kinematic and kinetic data from a *.c3d file was described, as well as its processing and conversion into *.trc and *.mot files to use as input in OpenSim. Following, the implementation of the OpenSim workflow described for each step of both simulations.

The results obtained for the model of the healthy individual were in accordance with the literature, when the joint angles and moments were compared, despite small asymmetries, accepted in healthy subjects. The muscular actuators were activated according to the reference, however the TA and SMEMB actuators were also activated in other unpredicted instants.

Regarding the post-stroke model, the kinematics associated revealed low plantarflexion in the CONTRA limb, characteristic from the post-stroke gait. The hamstring muscle SMEMB also

showed prolonged activation during CONTRA limb stance, which might be associated with the gradual decrease of hip flexion. However, the muscle activations of the plantarflexors only showed diminished activation in the medial gastrocnemius and in both plantarflexors, SOL and MEDGAS, showed early activation, as it is described in post-stroke gait literature. It is important to consider that the model was not able to completely reproduce the kinematics and even though tracking errors were expected, the right ankle angle had associated an error that overpassed the acceptable limits. Indeed, it was verified that the model had to use the residual and reserve actuators, even though these actuators were more expensive for the controller.

6.1- Limitations

The limitations of the present work are mainly related with the experimental data used. Less was known about the individuals and the conditions of collection of experimental data. Concerning the post-stroke patient, important information about the pathology historical was unknown: severity and affected brain area, time past after the accident and if he had received physiotherapy. Also the post-stroke individual used in the present work did not show accentuated impairments in gait, since he was mainly affected in the upper limbs.

6.2- Future work

As future work it is proposed to perform gait evaluations of a healthy and a post-stroke individuals with similar age, body height and weight, in the same conditions (use of the same number of markers, perform a static trial for scaling, making measurements of body segments and total height and body mass) and use EMG to assess the muscular activation experimentally. Taking pictures of the individual and record in video the gait trial would help to find subject-specific characteristics and to identify sources of error related to it.
Using the two models could be performed an Induced Acceleration Analysis (IAA) in OpenSim, with the purpose of obtaining the muscle contributions for the acceleration of the centre of mass. An additional study could be done, by starting from a healthy model and diminishing the activation of specific muscles (for example the plantarflexors and the dorsiflexors) and analyse the muscle compensations used by the model to reproduce the healthy gait.

References

[1] M. Whittle, *Gait analysis : an introduction*. Edinburgh; New York: Butterworth-Heinemann, 2007.

[2] C. L. VanPutte and R. R. Seeley, *Seeley's anatomy & physiology*. New York, NY: McGraw-Hill, 2014.

[3] K. L. Moore and A. F. Dalley, "Clinically oriented anatomy," ed. Philadelphia, Pa.; London: Lippincott Williams & Wilkins, 2013.

[4] F. E. Zajac, "Muscle and tendon: properties, models, scaling, and application to biomechanics and motor control," *Critical reviews in biomedical engineering,* vol. 17, pp. 359-411, 1988.

[5] K. Jansen, F. De Groote, W. Aerts, J. De Schutter, J. Duysens, and I. Jonkers, "Altering length and velocity feedback during a neuro-musculoskeletal simulation of normal gait contributes to hemiparetic gait characteristics," *Journal of NeuroEngineering and Rehabilitation,* vol. 11, pp. 1-15, 2014/04/30 2014.

[6] R. Verma, K. N. Arya, P. Sharma, and R. K. Garg, "Understanding gait control in post-stroke: implications for management," *J Bodyw Mov Ther,* vol. 16, pp. 14-21, Jan 2012.

[7] A. C. Guyton and J. E. Hall, *Textbook of medical physiology*. Philadelphia: Elsevier Saunders, 2006.

[8] S. Rossignol, R. Dubuc, and J. P. Gossard, "Dynamic sensorimotor interactions in locomotion," *Physiol Rev,* vol. 86, pp. 89-154, Jan 2006.

[9] V. Dietz, "Spinal cord pattern generators for locomotion," *Clinical Neurophysiology,* vol. 114, pp. 1379-1389, 2003.

[10] A. Frigon and S. Rossignol, "Experiments and models of sensorimotor interactions during locomotion," *Biol Cybern,* vol. 95, pp. 607-27, Dec 2006.

[11] D. T. H. Lai, R. K. Begg, and M. Palaniswami, "Computational Intelligence in Gait Research: A Perspective on Current Applications and Future Challenges," *IEEE Trans. Inform. Technol. Biomed. IEEE Transactions on Information Technology in Biomedicine,* vol. 13, pp. 687-702, 2009.

[12] S. J. Olney and C. Richards, "Hemiparetic gait following stroke. Part I: Characteristics," *Gait & Posture Gait & Posture,* vol. 4, pp. 136-148, 1996.

[13] B. Balaban and F. Tok, "Gait disturbances in patients with stroke," *PM R,* vol. 6, pp. 635-42, Jul 2014.

[14] A. S. Sousa, A. Silva, and J. M. R. Tavares, "Interlimb relation during the double support phase of gait: An electromyographic, mechanical and energy-based analysis," *Proceedings of the Institution of Mechanical Engineers, Part H: Journal of Engineering in Medicine,* vol. 227, pp. 327-333, 2013.

[15] P. Y. Lin, Y. R. Yang, S. J. Cheng, and R. Y. Wang, "The relation between ankle impairments and gait velocity and symmetry in people with stroke," *Arch Phys Med Rehabil,* vol. 87, pp. 562-8, Apr 2006.

[16] G. Chen and C. Patten, "Joint moment work during the stance-to-swing transition in hemiparetic subjects," *J Biomech,* vol. 41, pp. 877-83, 2008.

[17] A. Lamontagne, F. Malouin, C. L. Richards, and F. Dumas, "Mechanisms of disturbed motor control in ankle weakness during gait after stroke," *Gait & Posture Gait & Posture,* vol. 15, pp. 244-255, 2002.

[18] S. M. Woolley, "Characteristics of gait in hemiplegia," *Topics in stroke rehabilitation,* vol. 7, pp. 1-18, 2001.

[19] A. Lamontagne, J. L. Stephenson, and J. Fung, "Physiological evaluation of gait disturbances post stroke," *Clin Neurophysiol,* vol. 118, pp. 717-29, Apr 2007.

[20] J. S. Higginson, F. E. Zajac, R. R. Neptune, S. A. Kautz, and S. L. Delp, "Muscle contributions to support during gait in an individual with post-stroke hemiparesis," *J Biomech,* vol. 39, pp. 1769-77, 2006.

[21] A. R. Den Otter, A. C. Geurts, T. Mulder, and J. Duysens, "Gait recovery is not associated with changes in the temporal patterning of muscle activity during treadmill walking in patients with post-stroke hemiparesis," *Clin Neurophysiol,* vol. 117, pp. 4-15, Jan 2006.

[22] C. L. Peterson, A. L. Hall, S. A. Kautz, and R. R. Neptune, "Pre-swing deficits in forward propulsion, swing initiation and power generation by individual muscles during hemiparetic walking," *J Biomech,* vol. 43, pp. 2348-55, Aug 26 2010.

[23] A. S. AHMED M., "Kinetics and Kinematics of Loading Response in Stroke Patients (A Review Article)," *ANNALS,* vol. 4, OCT.- DEC. 2008 2008.

[24] P. A. Goldie, T. A. Matyas, and O. M. Evans, "Gait after stroke: initial deficit and changes in temporal patterns for each gait phase," *Arch Phys Med Rehabil,* vol. 82, pp. 1057-65, Aug 2001.

[25] R. B. Davis Iii, S. Õunpuu, D. Tyburski, and J. R. Gage, "A gait analysis data collection and reduction technique," *Human Movement Science,* vol. 10, pp. 575-587, 10// 1991.

[26] T. S. Kuan, J. Y. Tsou, and F. C. Su, "Hemiplegic gait of stroke patients: the effect of using a cane," *Archives of physical medicine and rehabilitation,* vol. 80, pp. 777-84, 1999.

[27] A. Muro-de-la-Herran, B. Garcia-Zapirain, and A. Mendez-Zorrilla, "Gait analysis methods: an overview of wearable and non-wearable systems, highlighting clinical applications," *Sensors (Basel),* vol. 14, pp. 3362-94, 2014.

[28] M. W. Whittle, "Clinical gait analysis: A review," *Human Movement Science,* vol. 15, pp. 369-387, 6// 1996.

[29] R. Baker, "Gait analysis methods in rehabilitation," *J Neuroeng Rehabil,* vol. 3, p. 4, 2006.

[30] S. J. Bamberg, A. Y. Benbasat, D. M. Scarborough, D. E. Krebs, and J. A. Paradiso, "Gait analysis using a shoe-integrated wireless sensor system," *IEEE transactions on information technology in biomedicine : a publication of the IEEE Engineering in Medicine and Biology Society,* vol. 12, pp. 413-23, 2008.

[31] (2015, 17-02-15). *Veristride*. Available: http://www.veristride.com/

[32] A. M. K. Howell, T.; Hayes, H.A.; Foreman, K.B.; Bamberg, S.J.M., "Kinetic gait analysis using a low-cost insole," *IEEE Trans. Biomed. Eng.,* vol. 60, pp. 3284 - 3290, 2013.

[33] F. E. Zajac, R. R. Neptune, and S. A. Kautz, "Biomechanics and muscle coordination of human walking: Part II: Lessons from dynamical simulations and clinical implications," *Gait & Posture,* vol. 17, pp. 1-17, 2// 2003.

[34] C. T. Farley and D. P. Ferris, "Biomechanics of Walking and Running: Center of Mass Movements to Muscle Action," *Exercise and sport sciences reviews,* vol. 26, pp. 253-286, 1998.

[35] M. G. Pandy, "Computer modeling and simulation of human movement," *Annual review of biomedical engineering,* vol. 3, pp. 245-273, 2001.

[36] S. Mochon and T. A. McMahon, "Ballistic walking," *Journal of biomechanics,* vol. 13, pp. 49-57, 1980.

[37] T. McGeer, "Passive dynamic walking," *the international journal of robotics research,* vol. 9, pp. 62-82, 1990.

[38] R. R. Neptune, "Computer modeling and simulation of human movement," *Sci Princ Sports Rehabil,* vol. 11, pp. 417-434, 2000.

[39] A. Seth, M. Sherman, J. A. Reinbolt, and S. L. Delp, "OpenSim: a musculoskeletal modeling and simulation framework for in silico investigations and exchange," *Procedia IUTAM,* vol. 2, pp. 212-232, // 2011.

[40] B. A. Garner and M. G. Pandy, "The obstacle-set method for representing muscle paths in musculoskeletal models," *Computer methods in biomechanics and biomedical engineering,* vol. 3, pp. 1-30, 2000.
[41] S. L. Delp, J. P. Loan, M. G. Hoy, F. E. Zajac, E. L. Topp, and J. M. Rosen, "An interactive graphics-based model of the lower extremity to study orthopaedic surgical procedures," *Biomedical Engineering, IEEE Transactions on,* vol. 37, pp. 757-767, 1990.
[42] M. G. Pandy, F. E. Zajac, E. Sim, and W. S. Levine, "An optimal control model for maximum-height human jumping," *Journal of biomechanics,* vol. 23, pp. 1185-1198, 1990.
[43] C. C. Raasch, F. E. Zajac, B. Ma, and W. S. Levine, "Muscle coordination of maximum-speed pedaling," *Journal of biomechanics,* vol. 30, pp. 595-602, 1997.
[44] M. Hubbard and L. W. Alaways, "Rapid and accurate estimation of release conditions in the javelin throw," *Journal of Biomechanics,* vol. 22, pp. 583-595, 1989.
[45] F. C. Anderson and M. G. Pandy, "Dynamic Optimization of Human Walking," *Journal of Biomechanical Engineering,* vol. 123, p. 381, 2001.
[46] A. Wit and A. Czaplicki, "Inverse dynamics and artificial neural network applications in gait analysis of the disabled subjects," *Human Movement,* vol. 9, pp. 93-102, 2008.
[47] F. E. Zajac, R. R. Neptune, and S. A. Kautz, "Biomechanics and muscle coordination of human walking: Part I: Introduction to concepts, power transfer, dynamics and simulations," *Gait & posture,* vol. 16, pp. 215-232, 2002.
[48] E. Cramp. (1998, 25-08-15). *C3D.ORG - The biomechanics standard*. Available: https://www.c3d.org/
[49] S. L. Delp, F. C. Anderson, A. S. Arnold, P. Loan, A. Habib, C. T. John*, et al.*, "OpenSim: Open-Source Software to Create and Analyze Dynamic Simulations of Movement," *Biomedical Engineering, IEEE Transactions on,* vol. 54, pp. 1940-1950, 2007.
[50] J. Hicks. (2011, 18-08-15). *User's Guide - OpenSim Documentation*. Available: http://simtk-confluence.stanford.edu:8080/display/OpenSim/User%27s+Guide
[51] K. M. Steele, A. Seth, J. L. Hicks, M. S. Schwartz, and S. L. Delp, "Muscle contributions to support and progression during single-limb stance in crouch gait," *J Biomech,* vol. 43, pp. 2099-105, Aug 10 2010.
[52] C. Richards and J. Higginson, "Knee contact force in subjects with symmetrical OA grades: differences between OA severities," *Journal of biomechanics,* vol. 43, pp. 2595-2600, 2010.
[53] A. Barre and S. Armand, "Biomechanical ToolKit: Open-source framework to visualize and process biomechanical data," *Comput Methods Programs Biomed,* vol. 114, pp. 80-7, Apr 2014.
[54] J. Dunne. (2013, 28-08-15). *Tools for Preparing Motion Data - OpenSim Documentation* Available: http://simtk-confluence.stanford.edu:8080/display/OpenSim/Tools+for+Preparing+Motion+Data
[55] V. M. Zatsiorsky, *Kinematics of Human Motion*: Human Kinetics, 1998.
[56] J. L. Allen, S. A. Kautz, and R. R. Neptune, "The influence of merged muscle excitation modules on post-stroke hemiparetic walking performance," *Clin Biomech (Bristol, Avon),* vol. 28, pp. 697-704, Jul 2013.
[57] C. Au. (2012, 28-08-15). *Musculoskeletal Models - OpenSim Documentation* Available: http://simtk-confluence.stanford.edu:8080/display/OpenSim/Musculoskeletal+Models
[58] C. T. John, F. C. Anderson, J. S. Higginson, and S. L. Delp, "Stabilisation of walking by intrinsic muscle properties revealed in a three-dimensional muscle-driven simulation," *Computer methods in biomechanics and biomedical engineering,* vol. 16, pp. 451-462, 2013.
[59] D. G. Thelen and F. C. Anderson, "Using computed muscle control to generate forward dynamic simulations of human walking from experimental data," *J Biomech,* vol. 39, pp. 1107-15, 2006.
[60] Qualisys. (2013). *Qualisys Track Manager - QTM*. Available: http://www.qualisys.com/

[61] I. Motion Lab Systems. (2015, 12-09-15). *Motion Lab Systems Software*. Available: https://www.motion-labs.com/index_software.html

[62] Doxygen. (2014, 12-09-15). *Tutorial*. Available: https://b-tk.googlecode.com/svn/doc/Matlab/0.3/index.html

[63] T. Shimba, "An estimation of center of gravity from force platform data," *Journal of Biomechanics,* vol. 17, pp. 53-60, 1984.

[64] M. G. Bowden, C. K. Balasubramanian, R. R. Neptune, and S. A. Kautz, "Anterior-posterior ground reaction forces as a measure of paretic leg contribution in hemiparetic walking," *Stroke,* vol. 37, pp. 872-6, Mar 2006.

[65] G. Chen, C. Patten, D. H. Kothari, and F. E. Zajac, "Gait differences between individuals with post-stroke hemiparesis and non-disabled controls at matched speeds," *Gait Posture,* vol. 22, pp. 51-6, Aug 2005.

[66] A. Mahboobin, "An automated iterative method for adjusting virtual model markers in an OpenSim model," presented at the 37th annual meeting of the American Society of Biomechanics, Omaha, Nebraska, 2013.

[67] T. Marasović, M. Cecić, and V. Zanchi, "Analysis and interpretation of ground reaction forces in normal gait," *WSEAS transactions on systems,* vol. 8, p. 9, 2009.

[68] H. Sadeghi, "Local or global asymmetry in gait of people without impairments," *Gait & Posture,* vol. 17, pp. 197-204, 6// 2003.

[69] A. Silva, A. S. Sousa, J. M. Tavares, A. Tinoco, R. Santos, and F. Sousa, "Ankle dynamic in stroke patients: agonist vs. antagonist muscle relations," *Somatosens Mot Res,* vol. 29, pp. 111-6, 2012.

[70] B. A. Knarr, D. S. Reisman, S. A. Binder-Macleod, and J. S. Higginson, "Understanding compensatory strategies for muscle weakness during gait by simulating activation deficits seen post-stroke," *Gait & posture,* vol. 38, pp. 270-275, 2013.

Annex

Annex 1 - Experimental body markers

Table 6.1 Correspondence between the marker set used in the gait trial performed in the LABIOMEP and the default marker set used in OpenSim. The X indicates that a marker is not included in the respective configuration.

RIGHT BODY		LEFT BODY		HEAD AND TORSO	
LABIOMEP	**OPENSIM**	**LABIOMEP**	**OPENSIM**	**LABIOMEP**	**OPENSIM**
RAC	R.Acromium	LAC	L.Acromium	**X**	**Top.Head**
RASIS	R.ASIS	LASIS		C7	X
RPSIS	X	LPSIS	X	STERN	Sternum
X	R.Thigh.Upper	X	L.Thigh.Upper	X	V.Sacral
X	R. Thigh.Front	X	L. Thigh.Front		
X	R. Thigh.Rear	X	L. Thigh.Rear		
RLK	R.Knee.Lat	LLK	L.Knee.Lat		
RMK	R.Knee.Med	LMK	L.Knee.Med		
X	R.Shank.Upper	X	L.Shank.Upper		
X	R.Shank.Front	X	L.Shank.Front		
X	R.Shank.Rear	X	L.Shank.Rear		
RLA	R.Ankle.Lat	LLA	L.Ankle.Lat		
RMA	R.Ankle.Med	LMA	L.Ankle.Med		
RFOOT1	X	LFOOT1	X		
RFOOT4	X	LFOOT4	X		
X	R.Midfoot.Sup	X	L.Midfoot.Sup		
X	R.Midfoot.Lat	X	L.Midfoot.Lat		
X	R.Toe.Lat	X	L.Toe.Lat		
X	R.Toe.Med	X	L.Toe.Med		
X	R.Toe.Tip	X	L.Toe.Tip		
RBACKFOOT	R.Heel	LBACKFOOT	L.Heel		

Annex 2 - Ground reaction moments

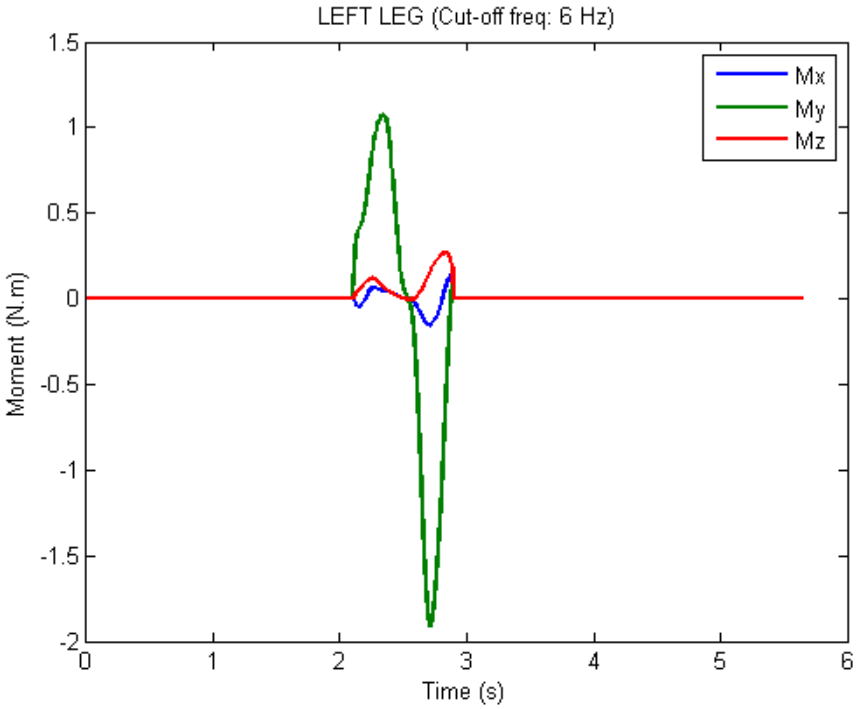

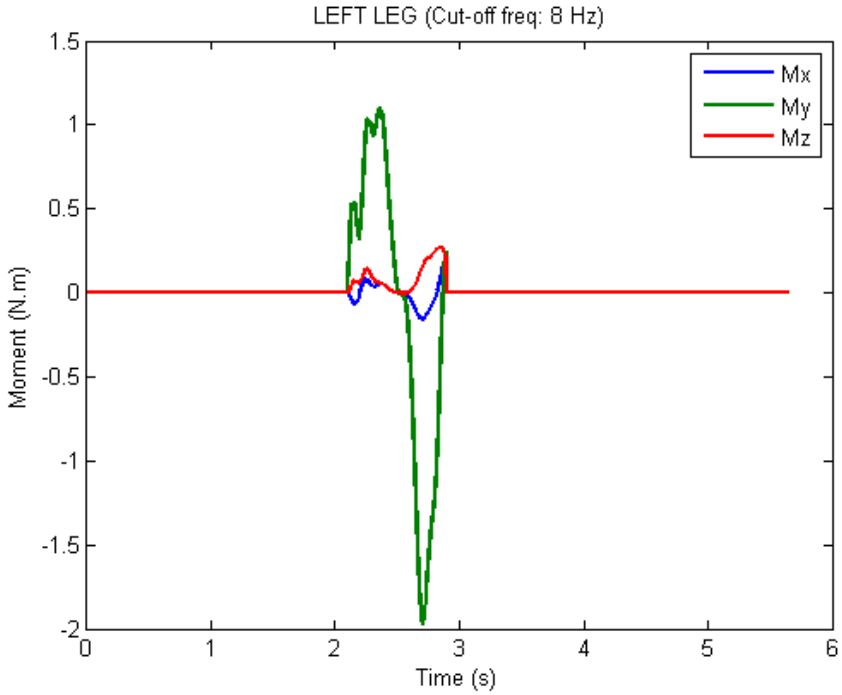

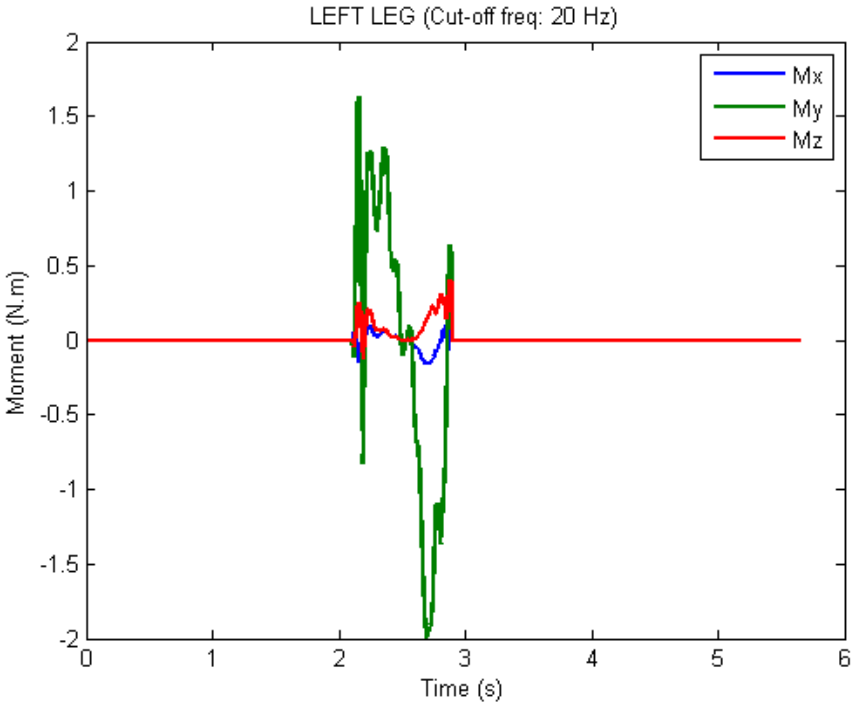

Figure 6. 1 Ground reaction moments acting on the left leg, after filtering using a 4th order low-pass Butterworth filter zero-lag, with cut-off frequencies of 6Hz, 8Hz and 20 Hz.

Annex 3 - Marker weights used in the scaling of musculoskeletal model

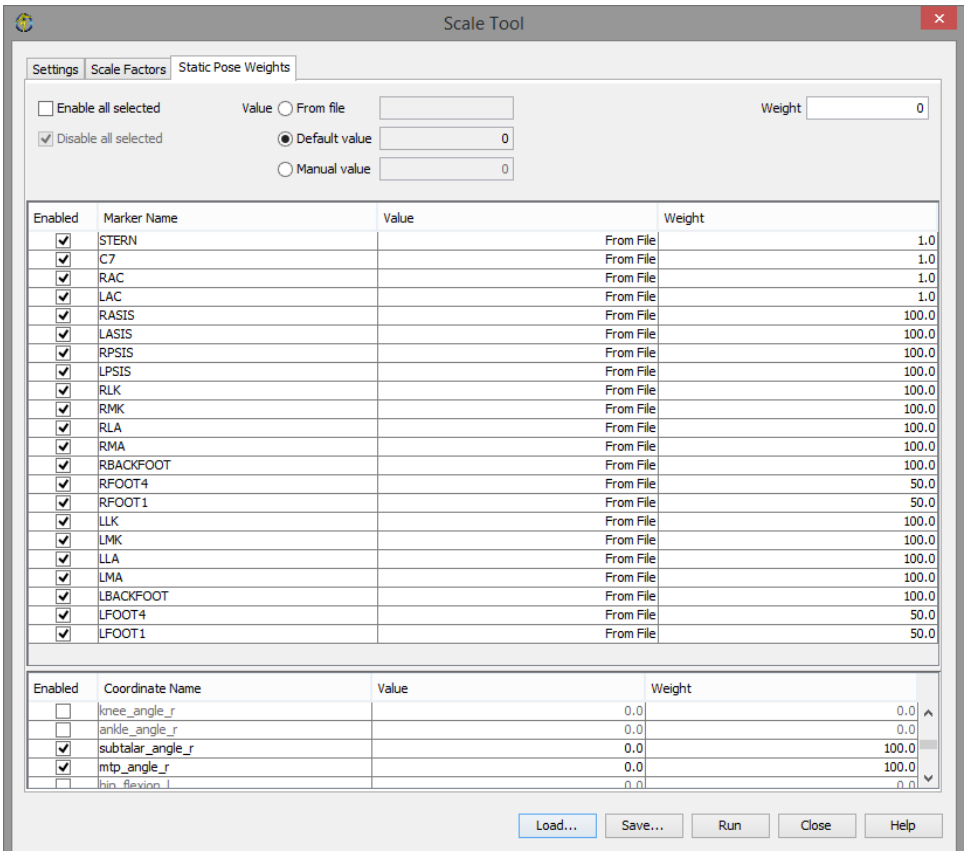

Figure 6.2 Scale Tool window showing the weights and the values attributed to each marker for the scaling step of the Study 2. In the lower part it is shown an example of the locked joints (value = 0) and the respective weight.

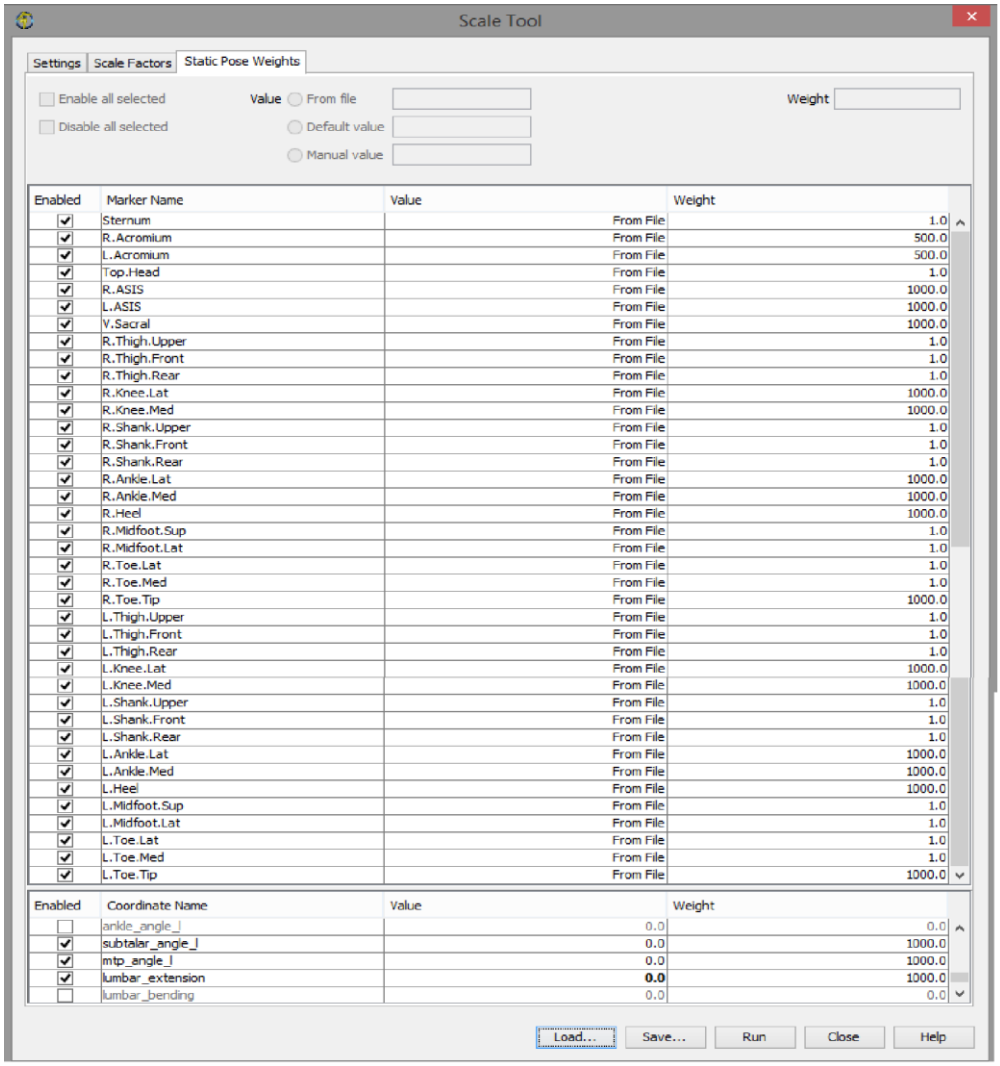

Figure 6.3 Scale Tool window showing the weights and the values attributed to each marker for the scaling step of the Study 1. In the lower part it is shown an example of the locked joints (value = 0) and the respective weight.

Annex 4 - Marker weights used in the IK

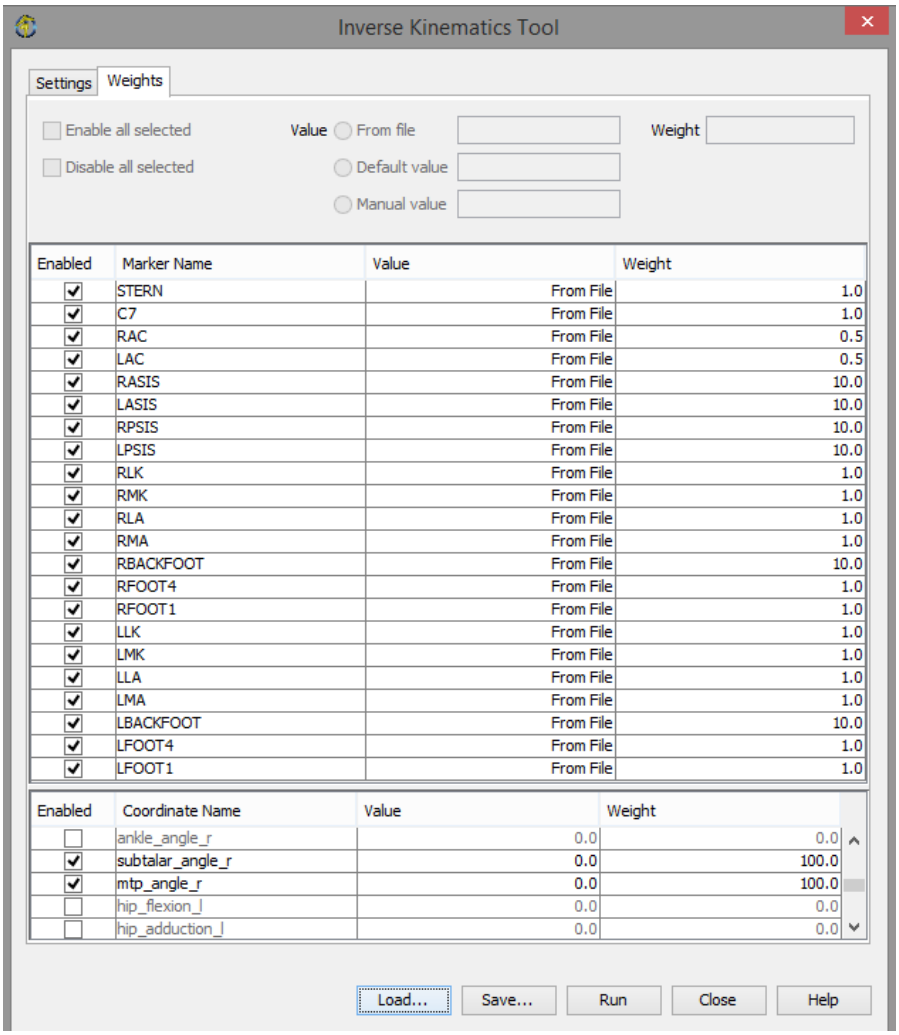

Figure 6.4 Inverse kinematics Tool window showing the weights and the values attributed to each marker for the inverse kinematics step of the Study 2. In the lower part it is shown an example of the locked joints (value = 0) and the respective weight.

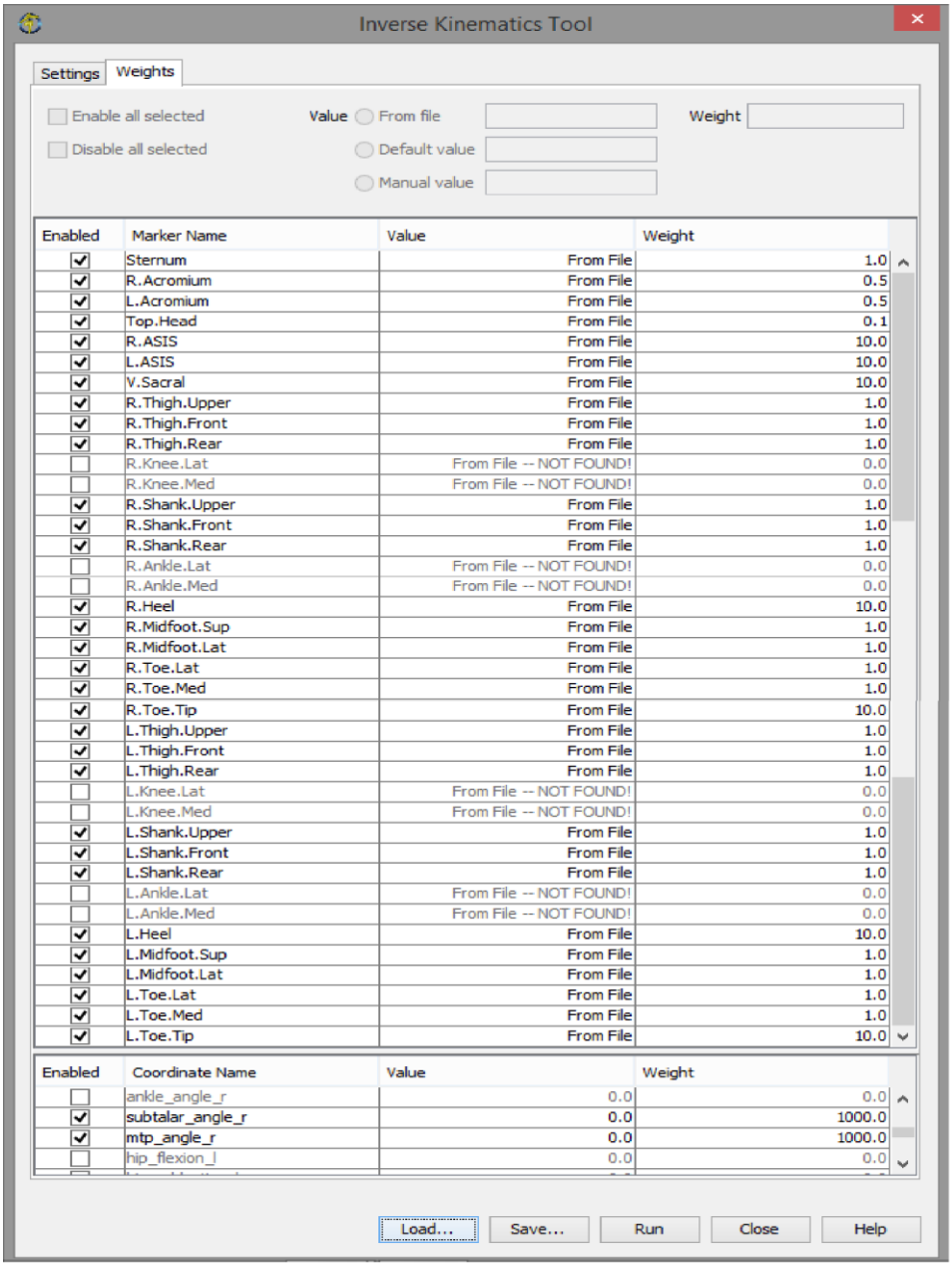

Figure 6.5. Inverse kinematics Tool window showing the weights and the values attributed to each marker for the inverse kinematics step of the Study 1. In the lower part it is shown an example of the locked joints (value = 0) and the respective weight.